C/EBPBETA3 (LIP) INDUCES CELL DEATH IN BREAST CANCER CELLS

By

Maria M. Abreu

Dissertation

Submitted to the Faculty of the

Graduate School of Vanderbilt University

in partial fulfillment of the requirements

for the degree of

DOCTOR IN PHILOSOPHY

in

Cancer Biology

May, 2012

Nashville, Tennessee

Approved:

Professor Vito Quaranta

Professor Barbara Fingleton

Professor Andries Zijlstra

Professor Linda Sealy

Para mi madre- Lourdes Abreu, gracias por todo tu apoyo.

To my mentor- Linda Sealy, thank you for believing in me.

To all the women that continue the battle and those that have lost their battle to breast cancer.

ACKNOWLEDGEMENTS

I would like to begin by thanking my mentor, role model, and friend Linda Sealy. Words cannot express how grateful I am to have the opportunity to learn from such a brilliant scientist, teacher, and woman. This work could not have been accomplished without her creativity, guidance, support, and relentless enthusiasm for science. It would be impossible to list the many things Linda has taught me regarding life and science. Still, one of the main things I have learned from Linda is the importance of "thinking outside of the box". I sincerely appreciate all the time Linda has spent mentoring and preparing me for a successful career in science. I am also indebted to Roger Chalkley for his guidance and support throughout my graduate school years. I would like to thank my lab mates and friends Allison Atwood, Linda Bundy, Rachel Jerrell, and Alisha Russell. I would especially like to thank Allison, my lab partner, for her continuous support with science and life matters as well as Rachel, my work wife, for all her mathematic and technical skills. You four have helped me at different stages throughout this process, thank you for all the wonderful memories.

I would like to express my gratitude to my committee members Andries Zijlstra (chair), Vito Quaranta, Barbara Fingleton, and Mike Thomson - for their help with reagents, suggestions, and questions that have strengthened my project. Thank you as well to Cathy Alford of the VA flow cytometry core for her technical support, as well as the Vanderbilt University cores. I would like to thank the staff of the Department of Cancer Biology, especially Tracy Tveit. Thank you to the staff members of the BRET/IGP office and Vanderbilt University.

I was honored and very grateful for the various sources of funding I have been awarded throughout my graduate studies. The Virus, Nucleic Acid, and Cancer (VNAC) training grant at Vanderbilt University funded my first two years. The NIH Ruth L. Kirschstein National Research Service Award GM089106 has funded the remaining years of my graduate studies. We are very grateful to the Vanderbilt Ingram Cancer Center (VICC) for core scholarship funds and the Vanderbilt Institute for Clinical and Translational Research award that also funded some of this study.

I am very fortunate to have a long list of friends that have made this an amazing experience. Some have been with me from the start of IGP (Mohammed Aiyegbo, Mike Lindquist, Veronica Placencio, Thomas Tomasiak), while others have been placed in my path along the way (Freddie Pruitt, Lisa McCorvey, Maggie Manning). I would like to thank my entire Nashville family for all their support, encouragement, patience, and willingness to listen to all of my life and science problems. Thank you for being there through thick and thin. I would also like to thank my long-time college friend Christina Stujenske, without her I would not have applied to Vanderbilt University. My sincerest thanks to my best friend, Trenis Palmer, for all his support, patience, and love throughout this entire graduate school process. I will always cherish the many memories we have shared in Nashville.

Finally, I would like to thank my family- Lourdes, Jorge, Frank, and Mario for all their unconditional love and support, as well as my extended family. Muchas gracias a mi familia tan hermosa. My mother is an incredible and

intelligent woman, who has worked hard to make sure that I succeed in life. She has instilled in me some of the most important things required to succeed as a scientist: hard-work, optimism, and perseverance.

TABLE OF CONTENTS

LIST OF FIGURES

LIST OF TABLES

LIST OF ABBREVIATIONS

ACS-American Cancer Society

Ad- adenoviral

AGP/EBP- alpha 1-acid glycoprotein enhancer-binding protein

ATCC- American Type Culture Collection

ATP-adenosine triphosphate

ATG- *autophagy-related* genes

AV-autophagic acidic vesicles

BECN1- Beclin 1

BME- 2-mercaptoethanol

BRCA1- breast cancer susceptibility gene 1

BRCA2- breast cancer susceptibility gene 2

BSA- bovine serum albumin

C-terminal- carboxyl-terminal

CDK- cyclin-dependent kinase

C/EBPbeta- CCAAT/enhancer-binding protein beta

COX-2- cyclooxygenase-2

CRT- calreticulin

CUGBP1- CUG triplet repeat binding protein

DAPK- death-associated protein kinase-1

DMEM- Dulbecco's Modified Eagles's medium

DOR- diabetes- and obesity-regulated

DRAM- damage-regulated autophagy modulator

E2F1- E2 factor 1

EDTA- ethylenediaminetetraacetic acid

EGF- epidermal growth factor

EGFR- epidermal growth factor receptor

eIF- eukaryotic translation initiation factor

EM- electron microscope

EMT- epithelial-to-mesenchymal transition

ER-endoplasmic reticulum

FACS- fluorescence-activated cell sorting

FBS- fetal bovine serum

FOXO- forkhead box O

GFP-green fluorescent protein

HER2/Erb2- human epidermal growth factor receptor 2

HIV- human immunodeficiency virus

HMGB1- high mobility group box 1

HR- homologous recombination

HRP- horse radish peroxidase

IGF-IR- insulin-like growth factor I receptor

IL- interleukin

IL6/DBP- IL-6 DNA binding protein

JNK- c-Jun N-terminal kinase

kD- kilodalton

LAP- liver-enriched activator protein

LIP- liver-enriched inhibitory protein

LC3- microtuble-associated protein light chain 3

mTOR- mammalian target of rapamycin

MEC- mammary epithelial cells

MMTV/c-neu- mouse mammary tumor virus/ c-neu

MOI- multiplicity of infection

mRNA- messenger RNA

MTS- 3-(4,5-dimethylthiazol-2-yl)-5-(3-carboxymethoxyphenyl)-2-(4 sulfophenyl)-2H-tetrazolium

NFDM- nonfat dried milk

NF-IL6- nuclear factor-interleukin 6

NF-κB- nuclear factor kappa B

N-terminal- amino-terminal

NK- natural killer cells

Nec-1- necrostatin-1

NV- no virus

OsO_4- osmium tetroxide

PBS- phosphate-buffered saline

PCD- programmed cell death

PAGE- polyacrylamide gel electrophoresis

PE- phosphatidylethanolamine

PEPCK- gluconeogenic phosphoenolpyruvate carboxykinase

PI3K- class I phosphatidylinositol 3-kinase

PKB- protein kinase B

PLAC1- placenta specific 1

PMS- phenazine methosulfate

PtdSer- phosphatidylserine

PTEN- phosphatase and tensin homolog

RANKL- receptor activator of nuclear factor kappa B ligand

RIP-1- receptor-interacting protein kinase-1

ROCK- Rho-associated protein kinase

ROS- reactive oxygen species

SD- standard deviation

SDS- sodium dodecyl sulfate

SL- stem-loop

SUMO- sumoylation

TBS-T- Tris Buffered Saline + Tween-20

TEM- transmission electron microscopy

THR-Thyroid hormone receptor

TLR- Toll-like receptors

TNFR1- tumor necrosis factor receptor 1

TOR- target of rapamycin

TRAIL-R- TNF-related apoptosis-inducing ligand receptor

TSC- tuberous sclerosis

uORF- upstream open reading frame

UTP- uridine triphosphate

v/v- volume/volume

WAP- whey acidic promoter

WHO- World Health Organization

w/v- weight/volume

CHAPTER I

Introduction

Breast cancer overview

Cancer remains a leading cause of death worldwide. According to the latest reports from the World Health Organization (WHO) in 2008, cancer accounted for 7.6 million deaths worldwide. About 70% of all cancer deaths occurred in low- and middle- income countries. Deaths from cancer worldwide are projected to continue to rise to over 13 million in 2030 (Siegel *et al*., 2011).

In the United States, the American Cancer Society (ACS) estimates approximately 1.7 million new cancer cases to be diagnosed in 2012. Invasive breast cancers diagnosed in women will account for about 226,870 of these new cases (Siegel *et al*., 2011). Breast cancer is still the most common cancer among American women, with the exception of skin cancers (Siegel *et al*., 2011). In fact breast cancer remains the second leading cause of cancer-related death in women. The ACS estimates about 39,510 women will tragically lose their battle against breast cancer in 2012. Women diagnosed with aggressive and/or more advanced forms of breast cancer have a meager 26% five-year survival rate. While the battle against cancer continues, the ACS reports that earlier detection through screening and increased awareness, as well as advances in improved treatment options have significantly improved patient outcomes and survival. Death rates from breast cancer have been declining since about 1990, with larger decreases in women younger than 50. This decline is likely due to

increases in the prevalence of mammography screening and also decreased use of menopausal hormones following the publication of the Women's Health Initiative randomized trial results (Ravdin *et al*., 2007 and Coombs *et al*., 2010). Currently, there are more than 2.6 million breast cancer survivors in the United States (Siegel *et al*., 2011). Despite significant advances in diagnosing and treating breast cancer, several major unresolved clinical and scientific problems remain. Hence, the search for more effective preventative strategies and improved treatments for cancer patients continue to drive those involved in cancer research.

While the exact etiology of breast cancer is unknown, there are a number of important risk factors that have been identified. The use of hormone therapy following menopause, obesity, and alcohol consumption have all been shown to increase risk in women (Coombs *et al*., 2010; La Vecchia *et al*., 2011; Pelucchi *et al*., 2011). Other factors that increase risk include a long menstrual history, use of oral contraceptives, never having children, age at first full-term pregnancy, exposure to radiation and breast density (Madigan *et al*., 1995; McCormack and dos Santos, 2006). Although most women with breast cancer do not have a family history of the disease, it is one of the strongest determinants of risk, suggesting hereditary factors such as germline mutations in breast cancer susceptibility gene 1 (*BRCA1*) and breast cancer susceptibility gene 2 (*BRCA2*) increase risk (Miki *et al*., 1994; Roy *et al*., 2011). BRCA1 has been implicated in controlling the cell cycle by its ability to interact with various cyclins and cyclin-dependent kinases (CDKs) (Yoshida and Miki, 2004). Also, BRCA1 is known to

induce the activity/expression of the negative cell cycle regulators, CDK inhibitor p21 and the p53 tumor suppressor gene. Both of these breast cancer susceptibility genes also play a key role during homologous recombination (HR), a vital process employed during repair of DNA double strand breaks and stalled DNA replication (Moynahan *et al*., 1999). Therefore the loss of BRCA1 or BRCA2 may lead to impairment of HR providing an enhanced opportunity for a cell to become transformed. Notably, inherited mutations in breast cancer susceptibility genes account for approximately 5%-10% of all female and male breast cancer cases (Brody and Biesecker, 1998; Ellisen and Haber, 1998).

Like many other types of cancer, breast cancer is not a single disease but it is highly heterogeneous at both the molecular and clinical level. The natural course of breast tumorigenesis involves a multistep process through defined pathological and clinical stages, starting with ductal hyperproliferation, with subsequent evolution into in situ and invasive carcinomas, and finally into metastatic disease (Sakorafas and Tsiotou, 2000). These steps reflect genetic alterations that propel the progressive transformation of normal mammary epithelial cells (MEC) into highly malignant derivatives. During tumorigenesis there are a variety of biological capabilities acquired by tumor cells, recognized as the hallmarks of cancer (Hanahan and Weinberg, 2000). Included in these hallmarks of cancer is the ability of tumor cells to resist cell death. Over several decades, it has become evident that cell death serves as a natural barrier to tumorigenesis.

Different types of programmed cell death

Programmed cell death (PCD) plays a vital role during animal development and tissue homeostasis (Fuchs and Steller, 2011). Abnormal regulation of this process is associated with a wide variety of human diseases, including neurodegeneration, immunological and developmental disorders, as well as cancer (Thompson, 1995; Fuchs and Steller, 2011). Studies of normal and cancerous cells led to the definition of three main forms of cell death. It is generally understood that apoptotic (type I) cell death requires two cells: the dying cell and the phagocyte that digests the dead cell with the help of the phagocyte lysosome (Savill and Fadok, 2000). Autophagic (type II) cell death depends on the dying cells' own lysosomes and a self-cannibalization process known as autophagy (Klionsky and Emr, 2000). Nonlysosomal (type III) cell death, also known as necrosis, is associated with membrane leakage and inflammation without any role for the lysosome (Proskuryakov *et al*., 2003). It should also be noted that a single stimulus often triggers several distinct death programs concurrently. Normally, only the fastest and most effective death pathway is evident, but one cell may also display characteristics of several death programs simultaneously (Hirsch *et al*., 1997; Zeiss, 2003; Elmore, 2007).

Apoptosis

Kerr and his colleagues coined the expression “apoptosis” when describing specific morphological features of dying cells. Their ultrastructure studies revealed rounding-up of the dying cell (shrinking) while organelles and

plasma membrane retained their integrity (Kerr *et al*., 1972). In addition, they proposed this process reflects the operation of an active, intracellular death program that can be activated or inhibited by a variety of physiological or pathological environmental stimuli. It wasn't until two decades later that our understanding of apoptosis progressed when Horvitz and colleagues performed screens to identify genes that are required for programmed cell death in the worm *Caenorhabditis elegans* (Horvitz, 1999). These studies provided many important advances in our understanding of apoptosis.

The apoptosis cascade can be initiated via two major pathways, involving either activation of death receptors in response to ligand binding (extrinsic or death receptor pathway) or the release of proapoptotic proteins, such as cytochrome c, from mitochondria to cytosol (intrinsic or mitochondrial pathway) (Elmore, 2007). However, evidence now suggests that both pathways are linked and that molecules in one pathway can influence the other (Igney and Krammer, 2002). The central players in both pathways are the caspases (the cysteine dependent, aspartate specific family of proteases), which function as the main executors of apoptotic cell death (Cohen, 1997). Regulated at the post-translational level, caspases are synthesized and exist within the cell as inactive pro-caspases or zymogens. Under stimulation of pro-apoptotic signals, pro-caspases are cleaved by proteases to become active caspases (Yuan *et al*., 1993; Miura *et al*., 1993; Cohen, 1997).

Fragmentation of internucleosomal DNA (karyorrhexis) is a feature of apoptosis (Elmore, 2007). Lamins are intra-nuclear proteins that maintain the

shape of the nucleus and mediate interactions between the nuclear membrane and chromatin. Degradation of lamins by caspases results in chromatin condensation (pyknosis) and nuclear fragmentation (Elmore, 2007). Retraction of pseudopods, blebbing of the plasma membrane along with formation of apoptotic bodies that contain nuclear or cytoplasmic material are also changes that occur before plasma membrane integrity is lost and the cell dies through apoptosis (Elmore, 2007).

Various techniques are commonly used to detect these apoptotic features such as caspase activation assays, DNA laddering assays, as well as measuring cellular DNA content by flow cytometry (Muppidi *et al*., 2004). When measuring cellular DNA content cells are permeabilized. During this procedure fragmented DNA multimers leak out of the cell. The result is a population of cells with reduced DNA content. If the cells are then stained with a DNA intercalating dye (e.g., propidium iodide) then a DNA profile representing cells in G_1, S-phase, and G_2M will be observed with apoptotic cells being represented by a sub G_0/G_1 population (Muppidi *et al*., 2004).

In addition to these biochemical features, changes in several cell surface molecules are also observed. The presence of cell surface molecules ensures that apoptotic cells are immediately recognized and phagocytized by neighboring cells in tissues, resulting in many cells being removed from tissues relatively quickly (Bratton *et al*., 1997). The clearance of such dying cells is mediated either by phagocytes that are professional engulfers: macrophages and immature dendritic cells (Aderem and Underhill, 1999; Sauter *et al*., 2000; Fadok *et al*.,

1992; 2001) or neighboring cells: fibroblasts and epithelial cells (Monks *et al*., 2008). Elimination of dying cells through apoptosis prevents an inflammatory response (Savill and Fadok, 2000; Kurosaka *et al*., 2003).

The multi-step process involved in the clearance of dying cells is a complex one. One of the first steps is the "find-me" signals (such as low levels of nucleotides adenosine triphosphate (ATP) and uridine triphosphate (UTP)) released by apoptotic cells (Lauber *et al*., 2004). The find-me signal helps attract motile phagocytes to the proximity of the cell undergoing apoptosis (Lauber *et al*., 2004). Although find-me signals can guide phagocytes to the proximity of apoptotic cells within a tissue, the specific recognition of the dying cell among the neighboring live cells depends on eat-me signals exposed by the apoptotic cells (Lauber *et al*., 2004; Gardai *et al*., 2006). To date, multiple eat-me signals have been identified (Gardai *et al*., 2006). Among these is exposure of phosphatidylserine (PtdSer) on the outer leaflet of the plasma membrane. This is the most universally seen alteration on the surface of apoptotic cells (Fadok *et al*., 1992, 2001). In fact, PtdSer exposure is the best studied and the most accepted definition for calling a cell apoptotic.

Autophagic cell death

Apoptotic cell death continues to be the most studied and best characterized cell death mechanism at both genetic and biochemical levels. However, there is evidence that other PCD mechanisms exist. Autophagic (Type-II) PCD occurs in the absence of chromatin condensation but is

accompanied by massive autophagic vacuolization of the cytoplasm (Gozuacik and Kimchi, 2004). The existence of autophagic cell death continues to be a topic of debate and more recent evidence indicates that cell death is not executed by autophagy, but that autophagic cell death simply describes cell death with autophagy (Levine and Yuan, 2005).

The catabolic process of autophagy is an evolutionarily conserved cellular process and responsible for self-cannibalization through a lysosomal degradation pathway (Levine and Klionsky, 2004). It is a multi-step process that is characterized by the formation of double-membrane vesicles called autophagosomes. These autophagosomes engulf bulk cytoplasm, which leads to the degradation of long-lived or damaged proteins and the turnover of various cytoplasmic organelles such as mitochondria, endoplasmic reticulum (ER), and Golgi (Levine and Klionsky, 2004; Meijer and Codogno, 2004). Eventually, the outer membrane of autophagosomes fuse with lysosomes generating autolysosomes, where acidic lysosomal hydrolases degrade the cytoplasm-derived contents of the autophagosome together with its inner membrane (Levine and Klionsky, 2004). This process takes place in cells at a basal level where it plays a pivotal role in housekeeping or disposal of assorted cytoplasmic components comprising of damaged organelles and of toxic, aggregation-prone proteins. The individual components are then used as renewable resources to provide components and energy for cell survival (Meijer and Codogno, 2004; Wang and Klionsky, 2003). In addition, autophagy is essential for maintaining cell survival following a variety of extracellular and intracellular stimuli including

ER stress, oxidative stress, nutrient-starvation, and growth factor deprivation (Levine and Klionsky, 2004). Amino acids, fatty acids, and nucleic acids generated by this process can be used for protein synthesis, or can be oxidized by the mitochondrial electron transport chain to produce ATP for cell survival under harsh conditions. Yet, this mechanism of cell autonomous survival is inevitably self-limited and the ultimate consequence is autophagy-mediated cell death if the stress imposed on the cell is sustained (Gozuacik and Kimchi, 2004).

Autophagy was first detected by electron microscopy (Klionsky, 2007). Degradation of cytoplasmic areas sequestered by the phagophore, which matures into the prelysosomal autophagosome remains the hallmark of autophagy (Klionsky, 2007). The functional significance of this process was unknown until the 1990s when *autophagy-related genes (ATG)* in the yeast Saccharomyces cerevisiae were discovered in response to starvation. These genes are highly conserved among eukaryotes (Nakatogawa *et al*., 2009). To date, over 30 ATG genes have been identified in yeast and at least 11 (ATG1, 3, 4, 5, 6, 7, 8, 9, 10, 12 and 16) have orthologs in mammals (Krick *et al*., 2011). ATG6 is also known as Beclin 1 (BECN1) and ATG8 is referred to as microtuble-associated protein light chain 3 (LC3) in mammals (Klionsky, 2007).

LC3 is the first mammalian protein known to specifically associate with autophagosomes (Kabeya *et al*., 2000). LC3 is synthesized as proLC3, which is cleaved by Atg4B to form LC3-I, with the carboxyl terminal glycine exposed (Figure 1). LC3-I binds the elongating preautophagosomal membrane after activation by Atg7. LC3-I is then transferred to Atg3, and finally conjugated to

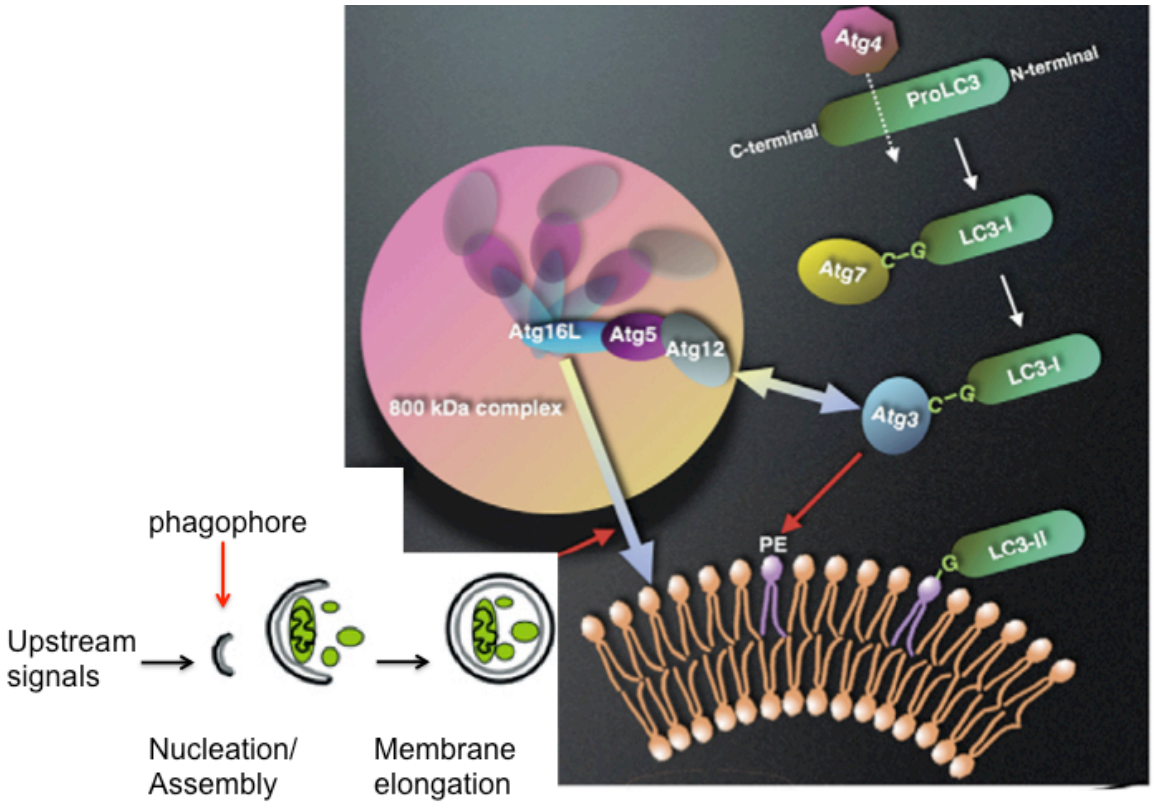

Figure 1. Model of autophagosome formation. Atg5-Atg12 conjugate and Atg16L localize to the isolation membrane (phagophore) during the elongation process. ProLC3 is processed for recruitment to the membrane in an Atg5-dependent manner. Atg12-Atg5 and Atg16L dissociate from the membrane upon completion of autophagosome formation, while LC3-II remains on the autophagosome membrane. Modified from Gozuacik and Kimchi, 2004 and Yoshimori and Noda, 2008.

phosphatidylethanolamine (PE) (Kabeya *et al*., 2000; Geng and Klionsky, 2008). The LC3-PE conjugate is referred to as LC3-II (Kabeya *et al*., 2000). The proteolytic cleavage converts LC3 from an 18kD (LC3-I) to a 16kD (LC3-II) protein. The conversion of soluble or cytosolic form of LC3 (LC3-I) to the autophagosome-associated form (LC3-II) is a well-accepted autophagosomal marker (Klionsky *et al*., 2007). LC3-II on the cytoplasmic surface of autophagosomes is delipidated by Atg4B to recycle LC3-I for further autophagosome formation.

To date, ultrastructural analysis of autophagosome formation using electron microscopy together with the detection of processed LC3 by western blot or fluorescence studies have been the conventional methods for autophagy detection (Klionsky *et al*., 2007). Mitochondrial dilation, extensive intracellular membrane remodeling, and the generation of other autophagic acidic vesicles (AV) are also characteristics of autophagy. There is a long list of guidelines for monitoring and interpreting the results of autophagy assays (Klionsky *et al*., 2008). As with any experimental methods, each has its strengths and limitations.

Necrosis

Necrotic (type III) cell death or necrosis is morphologically distinguishable by a gain in cell volume (oncosis), swelling of organelles, plasma membrane rupture and subsequent loss of intracellular contents (Elmore, 2007). Necrosis is caused by factors external to the cell or tissue, such as infection, toxins, or trauma. One major difference between type I-II cell death and type III necrotic

cell death is that necrosis can lead to local inflammation, presumably through the liberation of factors from dead cells that alert the innate immune system (Kanduc *et al*., 2002). As necrotic cells swell, they are internalized by a macropinocytotic mechanism, with the implication that phagocytes take up only parts of the cell. As research in this area has progressed, sequences of biochemical events that define necrosis have been described. Production of reactive oxygen species (ROS) by mitochondria and swelling of mitochondria, ATP depletion, failure of calcium homeostasis, perinuclear clustering of organelles, activation of a few non-caspase proteases, specifically cathepsins and calpains, lysosomal rupture, and ultimately plasma membrane rupture occur in necrotic cells (Golstein and Kroemer, 2007).

While necrosis has been traditionally seen as a passive and uncontrolled form of cell death, proteins that finely regulate this process have been identified recently (Barros *et al*., 2001). Necrosis is activated by death domain receptors [e.g. tumor necrosis factor receptor 1 (TNFR1), Fas/CD95, and TNF-related apoptosis-inducing ligand receptor (TRAIL-R)] and Toll-like receptors (e.g. TLR3 and TLR4), in particular in the presence of caspase inhibitors (Festjens *et al*., 2006). This necrotic cell death seemingly depends on the serine/threonine kinase receptor-interacting protein kinase-1 (RIP-1); this has been demonstrated by its knockout/knockdown and chemical inhibition by a small molecule inhibitor necrostatin-1 (Nec-1) (Christofferson and Yuan, 2010). This form of cell death is termed ‘‘necroptosis” (Christofferson and Yuan, 2010; Yuan and Kroemer, 2010). This area is relatively new and further studies are required to fully comprehend

the similarities and differences involved between necrosis and necroptosis.

Besides the conventional three types of PCD, other pathways have been discovered. These pathways are called "nonapoptotic programmed cell death" or "caspase-independent programmed cell death". These alternative routes to death are as efficient as apoptosis and can occur concomitantly with apoptosis or function as an alternative cell death mechanism when apoptosis is impaired. Increasing evidence indicates that nonapoptotic cell death mechanisms mediate such important developmental processes as interdigital cell death and hollowing of the mammary ducts during puberty (Chautan *et al*., 1999; Debnath *et al*., 2005; Degterev *et al*., 2005; Mailleux *et al*., 2007). One specific mechanism of cell death that has recently received much attention is the cell internalization process termed entosis (Overholtzer *et al*., 2007).

Entosis and Cell engulfment

Entosis is described as a nonapoptotic cell death mechanism that occurs in matrix-detached cells, where viable target cells invade into viable host cells, forming cell-in-cell structures (Overholtzer *et al*., 2007). While apoptosis can also result in the internalization of one cell inside of another, the mechanisms responsible for entosis are substantially distinct. The fate of entotic cells varies. Internalized cells can be released; but the most common fate of internalized cells is cell death (Overholtzer *et al*., 2007). Entotic cells are targeted to lysosomal compartments where they are degraded. In trying to decipher a mechanism for entotic cell death, Florey et al. show a role for autophagy in entosis. During

entosis, the entotic vacuole membrane encircling internalized cells recruits the autophagy protein LC3 (Florey *et al*., 2011). This was shown to be independent of autophagosome formation, yet dependent on ATG5, ATG7, and VPS34, which are all part of autophagy machinery (Florey *et al*., 2011). LC3-targeted entotic vacuoles recruit lysosomes, resulting in the degradation of internalized cells, which are killed by their hosts. Autophagy protein inhibitors can significantly increase the level of transformed growth of cells undergoing high rates of entosis. These data suggest that entosis may suppress transformed growth by inducing cell death, using proteins important in the autophagy process (Florey *et al*., 2011).

Interestingly, entosis is not the first description of a process that leads to cell-in-cell structures. Reports of cell-in-cell structures date back to the mid 1800's (Overholtzer and Brugge, 2008). Many terms have been used in the literature to describe cell-in-cell structures including entosis, emperipolesis, cytophagocytosis, and cannibalism (xeno-cannibalism). Humble et al. were the first to introduce the term emperipolesis in the 1950's to refer to a heterogeneous cell-in-cell phenomenon in which viable lymphocytes move into malignant cells (Humble *et al*., 1956). During cell cannibalism, the cannibalistic (host) cell comes in contact with the target cell. The next step is the gradual engulfment of the cell cytoplasm of the target cell. The nucleus of the target cell appears unaltered; yet the nucleus of the host cell is pressed to one side, changing into a crescent or semilunar shape (Humble *et al*., 1956; Sharma and Dey, 2011). Finally the target cell completely dies off and its nucleus disintegrates. There is some

evidence implying the lack of nutrients as the cause of death of target cells.

It has been proposed that emperipolesis denotes the process of cells entering, moving within, as well as exiting the cell, whereas cytophagocytosis, cannibalism, and entosis describe the specific mechanism of cell-in-cell formation (Overholtzer and Brugge, 2008). While there are some overlapping similarities among the various mechanisms, entosis is a mechanism whereby target cells invade the host cell (Overholtzer *et al*., 2007). Conversely, in cell cannibalism a host cell actively engulfs the target cell. The ability of cannibal tumor cells to engulf other tumor cells resembles autophagic digestion of cellular organelles.

Cell cannibalism has been frequently detected in highly malignant or metastatic tumors and has been correlated with poor prognosis (Sharma and Dey, 2011). This could possibly be due to the tumor cell's ability to ingest immune cells such as lymphocytes and neutrophils for immune evasion (Overholtzer and Brugge, 2008; Sharma and Dey, 2011). In contrast, natural killer (NK) cell internalization has been shown to precede target tumor cell death and NK cell self-destruction, suggesting that this cell-in-cell pathway is a mechanism to kill tumor cells (Xia *et al*., 2008). This potential tumor suppressive function is similar to that observed in soft agar assays during entosis (Overholtzer *et al*., 2007). Nevertheless, the significance of cell-in-cell structures and the underlying mechanism(s) of their formation remain unknown. Information on factors that stimulate or regulate cell engulfment is almost nonexistent. One such protein that may play a role in stimulating engulfment of

cells is the transcription factor CCAAT/enhancer-binding protein beta (C/EBPbeta).

CCAAT/enhancer-binding protein family

C/EBPbeta is one of the members of the CCAAT/enhancer-binding protein family. These DNA binding transcription factors belong to the basic leucine zipper superfamily of transcription factors (Tsukada *et al*., 2011). The following six genes encode the C/EBP family including: C/EBPalpha, C/EBPbeta, C/EBPgamma, C/EBPdelta, C/EBPepsilon, and C/EBPzeta (Lekstrom-Himes and Xanthopoulos, 1998; Ramji and Foka, 2002). Members of this superfamily are characterized by a leucine zipper motif, which allows them to homodimerize or heterodimerize with other members of the family (Tsukada *et al*, 2011). Upon dimerization, the C/EBPs exploit their basic domain to bind to the specific consensus sequence: TTnnG(C/T)AAT in the promoters of countless genes (Tsukada *et al*., 2011). The carboxyl (C)-terminal region contains both the DNA binding in addition to the dimerization motifs. It is this C-terminal region that is highly conserved within the family. The members of the C/EBPs are divergent in their amino (N)-terminal region containing regulatory and transactivation domains that interact with transcriptional coactivators, corepressors, and the basal transcription machinery (Tsukada *et al*., 2011). Although these family members can bind the same target sequences in gene promoters, it is the interaction with the numerous binding partners that successfully determines specificity. Overall, C/EBPs have been shown to play important roles in growth control and the induction of differentiation (Tsukada *et al*., 2011).

The C/EBPs are a fascinating and complex family of transcription factors. C/EBPgamma, C/EBPdelta, and C/EBPzeta exist as single polypeptides, whereas multiple polypeptides are generated through alternative splicing and regulated translation initiation from the genes encoding C/EBPalpha, C/EBPbeta, and C/EBPepsilon (Ramji and Foka, 2002). C/EBPalpha is the founding member of the C/EBP family and was first identified as a liver-enriched DNA binding protein (Johnson and McKnight, 1989). Genetic deletion studies of individual C/EBPs in mice revealed information regarding expression patterns as well as their ability to cooperate in essential roles in the development and function of various tissue types (Lekstrom-Himes and Xanthopoulos, 1998; Ramji and Foka, 2002). Some of the members (e.g. C/EBPPbeta, C/EBPgamma, and C/EBPzeta) are ubiquitously expressed; most of the C/EBPs are expressed and involved in tissue-specific gene expression in the liver, lung, intestine, bone, adipose tissue, immune cells, ovary and breast (Ramji and Foka, 2002).

C/EBPbeta

In the early 1990's C/EBPbeta was independently identified by separate groups of investigators working on different model systems. Shiazu Akira and colleagues identified the factor then cloned the protein from a human glioblastoma cell line and referred to it as nuclear factor-interleukin 6 (NF-IL6). This was due to the fact that it is a nuclear factor and it can activate the interleukin-6 promoter (Akira *et al*., 1990). In regards to the rat and mouse proteins, Patrick Descombes and Ueli Schibler identified the protein from rat liver

extracts and named the larger, activator isoforms liver-enriched activator protein (LAP) and the smaller, inhibitory isoform liver-enriched inhibitory protein (LIP) (Descombes *et al*., 1990). AGP/EBP, IL6-DBP, CRP2, and NF-M (chicken protein) are terms scarcely used in the literature since it was later realized that these proteins displayed homology to the recently identified CCAAT/enhancer binging protein (now referred to as C/EBPalpha) cloned in the laboratory of Steve McKnight (Landschulz *et al*., 1988; Ramji and Foka, 2002).

C/EBPbeta is transcribed from an intronless gene that gives rise to three protein isoforms from a single messenger RNA (mRNA) (Figure 2). This is due to alternative translation initiation at three in-frame methionine initiator codons or regulated proteolysis (Descombes *et al*., 1991; Ramji and Foka, 2002). In humans, full-length C/EBPbeta1 is 346 amino acids long (Akira *et al*., 1990) (297 in rat and mouse (Cao *et al*., 1991; Descombes *et al*., 1990) and has an apparent molecular weight of 55 kilodalton (kD). C/EBPbeta2 begins at the second in-frame methionine located 23 amino acid downstream from the first. C/EBPbeta2 appears as a doublet on immunoblots with an apparent molecular weight of 45kD and 42kD. The smallest isoform, C/EBPbeta3, begins at the final in-frame methionine at position 198 in the human protein and has an apparent molecular weight of 20kD (Descombes and Schibler, 1991). The structure of C/EBPbeta is such that the transactivation domain resides in the N-terminal region and the protein dimerization (leucine zipper) and DNA binding domains (basic region) reside in the C-terminal end. Unlike the first two transcription activator isoforms,

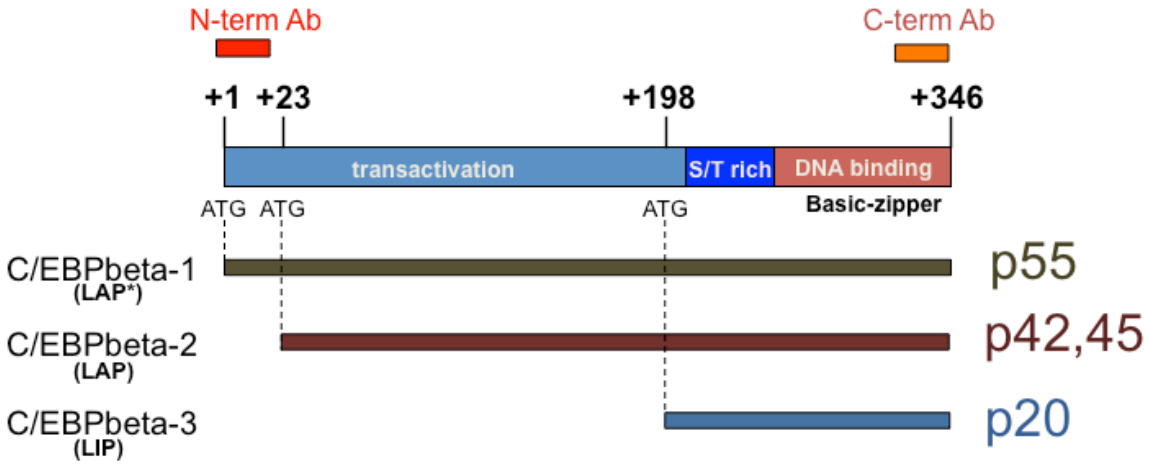

Figure 2. Schematic representation of C/EBPbeta. Three proteins isoforms are generated from a single mRNA by alternative translation. The positions of the three ATG start codons and the relative sizes of each isoform are shown. The positions of epitopes recognized by two antibodies are also depicted.

C/EBPbeta1 and C/EBPbeta2 (termed LAP* and LAP in rodents), the third isoform, C/EBPbeta3 (termed LIP in rodents) lacks the entire N-terminal activation domain, while retaining the DNA binding/protein dimerization domain (Descombes and Schibler, 1991). Therefore, this protein acts as a transcriptional repressor since it can occupy the C/EBPbeta consensus DNA elements within promoters of target genes.

Isoform specific C/EBPbeta expression

Several mechanisms by which a cell regulates the production of a specific C/EBPbeta isoform have been proposed. One of the earliest explanations is that the three isoforms arise by a "leaky" ribosome scanning mechanism (Descombes and Schibler, 1991). Since then, there has been more complex mechanisms proposed; some that specifically lead to increases in C/EBPbeta3 (hereafter referred to as LIP) protein expression.

Mammalian target of rapamycin (mTOR) and additional signal transduction pathways that regulate the function of the translation initiation factors such as eukaryotic translation initiation factor (eIF2) alpha and eIF-4E have been shown to determine the ratio of C/EBP isoforms (Raught *et al*., 1996) Calkhoven and colleagues showed that high eIF2alpha activity leads to increased LIP production. Alternative translation initiation involves a highly conserved small upstream open reading frame (uORF) at the 5' region of C/EBPbeta mRNA (Lincoln *et al*., 1998; Calkhoven *et al*., 2000; Wethmar *et al*., 2010). Studies of molecular mechanisms that control the initiation of translation

on the uORF-specific AUG codon suggested that certain RNA-binding proteins might regulate this process by interacting with the uORF region of C/EBPbeta mRNA. Two RNA-binding proteins, CUG triplet repeat binding protein (CUGBP1) and calreticulin (CRT), which specifically bind to the uORF were identified to be important players in regulating LIP translation (Timchenko *et al*., 1999; 2002; 2006). Although CUGBP1 and CRT interact with the same sequence of the 5′ region of C/EBPbeta mRNA, the consequences of these interactions are different. CRT binds to the 5′ region of C/EBPbeta mRNA and stabilizes a stem-loop (SL) structure, leading to the inhibition of translation of C/EBPbeta. On the contrary, the interaction of CUGBP1 with the 5′ region of C/EBPbeta mRNA increases translation of C/EBPbeta (Timchenko *et al*., 1999; 2002; 2006). It is not surprising that cells have highly regulated mechanisms to control translation initiation of the C/EBPbeta isoforms, since each have been linked to specific biological processes.

The second proposed mechanism to generate LIP is through specific proteolysis of the larger C/EBPbeta isoforms. *In vivo* studies have shown specific cleavage of the larger isoforms results in an increase in LIP protein levels (Welm *et al*., 2000; Baer and Johnson, 2000). This was shown to occur in the liver and depend on C/EBPalpha; it is likely that this occurs in other tissues as well (Welm *et al*., 2000). It is of great importance to note that *in vitro* cleavage of the larger C/EBPbeta isoforms can also occur (Baer and Johnson, 2000). LIP can be generated through artifactual proteolysis depending on the method used during sample preparation. Hence, there are discrepancies in the literature

regarding the production of LIP in cells.

Most of the research on C/EBPbeta has focused on the C/EBPbeta2 (LAP) and C/EBPbeta3 (LIP) isoforms. Until recently, many investigators failed to acknowledge the existence of C/EBPbeta1 (LAP*), due to its low expression levels in cultured cells. Historically there was this notion that C/EBPbeta1 and C/EBPbeta2 were functionally redundant, since they only differ by a 23 N-terminal amino acid truncation and both are transcriptional activators. However, mounting evidence by our lab and others demonstrate that the three C/EBPbeta isoforms have very different and unique roles in cells. C/EBPbeta1 plays important functions in differentiation and senescence (Kowenz-Leutz and Leutz, 1999; Eaton, *et al*., 2001; Eaton and Sealy, 2003; Atwood and Sealy, 2010), while C/EBPbeta2 participates in more proliferative roles in cells (Bundy and Sealy, 2003). This is evident in the ability of C/EBPbeta1, not C/EBPbeta2, to synergistically collaborate with c-Myb in co-expression assays to turn on differentiation genes in myeloid cells. Unlike C/EBPbeta2, C/EBPbeta1 was able to activate differentiation genes by interacting with and recruiting the SWI/SNF chromatin-remodeling complex (Kowenz-Leutz and Leutz, 1999). This recruitment was dependent on the N-terminal amino acids present in C/EBPbeta1, but not C/EBPbeta2. In addition, the N-terminal amino acids unique to C/EBPbeta1 are necessary for efficient sumoylation (SUMO) (Eaton and Sealy, 2003). Briefly, sumoylation is a post-translational modification that has been shown to regulate the function of various proteins (Geiss-Friedlander and Melchior, 2007). Specifically, sumoylation of transcription factors leads to

transcriptional repression by altering binding partners. C/EBPbeta1 is the only transactivator isoform that is sumoylated in COS cells even though both C/EBPbeta1 and C/EBPbeta2 contain a SUMO consensus sequence around lysine 173 (Eaton and Sealy, 2003). More recently, our lab found that C/EBPbeta1 more efficiently induces senescence than C/EBPbeta2 (Atwood and Sealy, 2010). This is likely due to the ability of C/EBPbeta1 to induce interleukin-6 (IL-6) expression (Atwood and Sealy, 2010). Interestingly, expression of sumo-C/EBPbeta1 fusion protein does not induce IL-6 in comparison to expression of wild-type C/EBPbeta1, indicating that sumoylation of C/EBPbeta1 does lead to transcriptional repression (Atwood and Sealy, 2011).

Differences in protein expression have also been observed in mammary epithelial cells. C/EBPbeta1 is found in normal mammary epithelial cells from reduction mammoplasties, whereas C/EBPbeta2 is undetectable (Eaton *et al*., 2001). Interestingly, in human breast tumors, where cancer cells are actively proliferating, there is a significant gain of C/EBPbeta2 protein levels (Eaton *et al*., 2001). In fact, C/EBPbeta 2 but not C/EBPbeta1, was observed to transactivate the promoters of *cyclin D1* (Eaton *et al*., 2001) and *placenta specific 1* (*PLAC1*) genes (Koslowski, *et al*., 2009), which promote proliferation and are frequently upregulated in breast tumors. Moreover, overexpression of C/EBPbeta2 in the MCF10A mammary epithelial cell line leads to cell transformation (Bundy and Sealy, 2003). C/EBPbeta2-expressing MCF10A cells form foci, gain anchorage independence, express markers associated with having undergone an epithelial-to-mesenchymal transition (EMT), and acquire an

invasive phenotype (Bundy and Sealy, 2003). The role of LIP in cells continues to be a topic of debate and will be discussed further in greater detail in the next chapters.

Role of C/EBPbeta in the mammary gland

Genetic deletion of C/EBPbeta in mice revealed the importance of this transcription factor in a number of physiological processes. The C/EBPbeta null mice exhibit a number of dramatic phenotypes including impaired liver regeneration, increased sensitivity to infections, sterility, and defects in mammary gland development (Greenbaum *et al*., 1998; Sterneck *et al*., 1997; Robinson *et al*., 1998; Seagroves *et al*., 1998). The mammary gland is a dynamic organ, which undergoes growth and extraordinary remodeling in response to hormonal signals at puberty, pregnancy and continues through weaning of the offspring (Figure 3A). During embryonic development, a rudimentary epithelial ductal tree is formed which remains mostly unchanged until puberty. During puberty, estrogen stimulates the expansion and development of the ductal tree and lobuloalveolar structures at the ends of the ducts. During gestation, estrogen and progesterone stimulate additional proliferation and further development of the ducts and lobuloalveoli. Following parturition, epithelial cells differentiate into secretory epithelial cells for milk production and secretion. After lactation, the mammary epithelial ductal tree regresses to a quiescent state through the process of involution (Sternlicht *et al*., 2006). The involution process encompasses several changes including the reabsorption of residual milk, loss of

the epithelium by programmed cell death, clearance of these dying cells, and regrowth of the interstitial adipose cells. This regressed state has mistakenly been thought to be the same as the gland in the nulliparous state, before the first pregnancy and lactation. However, D'Cruz et al. have described a host of gene-expression changes of the mammary gland following pregnancy and lactation, (D'Cruz *et al*., 2002) and distinct genetic signatures have been reported for the parous and nulliparous human breast (Balogh *et al*., 2006). During the involution process, many secretory and epithelial cells undergo massive cell death; this has been shown to involve several forms of cell death including apoptosis, autophagy, and cell engulfment (Zarzynska and Motyl, 2008; Monks *et al*., 2008). This process of epithelial cell growth, differentiation, and involution of the mammary gland occurs with each pregnancy.

In wild type mice extensive mammary gland development occurs around three weeks of age during puberty (Figure 3B). This fascinating process of developing normal mammary glands is well orchestrated and arises from an epithelial cell bud proximal to the nipple. At puberty, the epithelial cells divide and migrate to penetrate the mammary fat pad, forming the ductal tree. Secondary and tertiary branching ducts stem from the primary ducts. These secondary and tertiary branching ducts also penetrate the fat pad. One way to measure the development of the mammary gland in mice is to monitor the position of the epithelial tree in relation to the distal lymph node in the inguinal mammary gland.

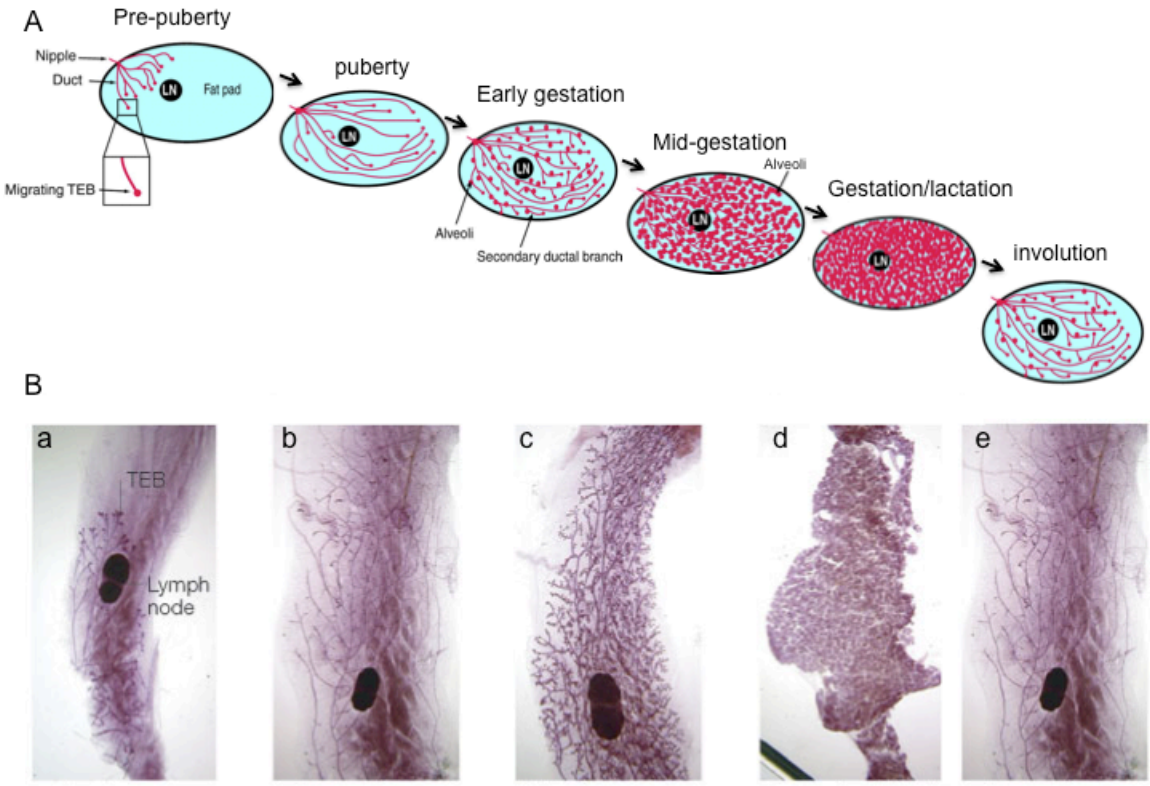

Figure 3. Mouse mammary gland development. **A,** schematic representation of the stages of mammary gland development in the adult mouse, from pre-puberty to gestation, lactation and involution. **B**, whole mount images of the different stages a, puberty; b, mature virgin; c, pregnancy; d, lactation; e, post-involution. LN, lymph node; TEB, terminal end bud. Modified from Watson and Khaled, 2008; Hennighausen and Robinson, 2005.

In 1998, studies were published describing the mammary gland deficiencies of two independently created C/EBPbeta knockout mice. Studies by Jeff Rosen and colleagues as well as Peter Johnson and colleagues reveal that C/EBPbeta is essential for proliferation of lobuloalveolar secretory units and ductal morphogenesis (Robinson *et al*., 1998; Seagroves *et al*., 1998). C/EBPbeta null mice have obvious defects in epithelial cell penetration into the mammary fat pad. In contrast to extensive lobuloalveolar development observed in C/EBPbeta heterozygous mammary glands, large areas of ductal epithelium of the C/EBPbeta null glands do not contain secondary/tertiary side branches or alveoli (Figure 4). Ducts that do form appear enlarged and produce distended ends. Both beta-casein and whey acidic protein expression are inhibited or absent in C/EBPbeta null mice (Grimm and Rosen, 2003). These data provide evidence for the essential role of C/EBPbeta in mammary epithelial proliferation in response to hormonal stimulation at puberty or gestation. Furthermore, the studies depict the importance of C/EBPbeta in functional differentiation of secretory epithelium in the mammary gland. Taken together, C/EBPbeta is a crucial component in both proliferation and differentiation in mammary epithelial cells. The mechanism by which C/EBPbeta is directing these antagonistic processes is likely due to the distinct functional properties of the three C/EBPbeta isoforms.

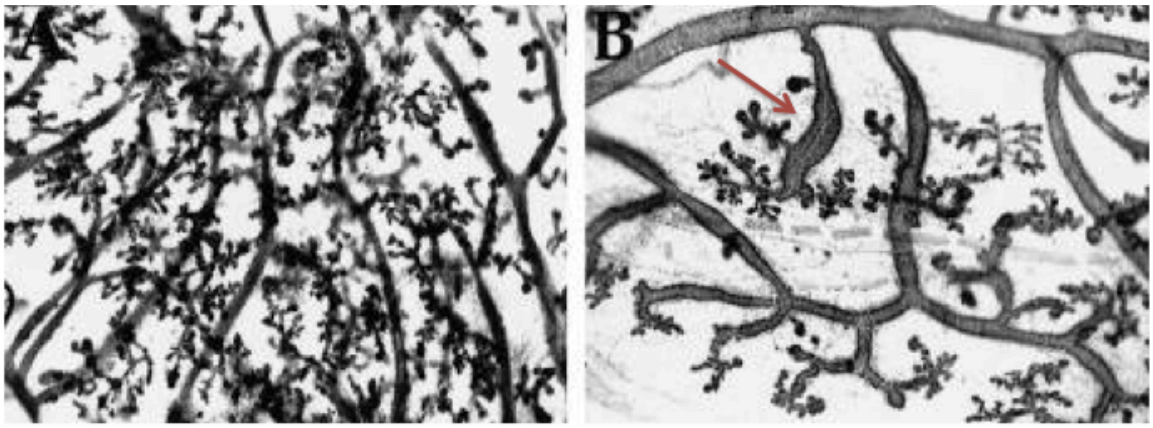

Figure 4. Lobuloalveolar development is compromised in the C/EBPbeta null mice upon stimulation of pregnancy with estrogen and progesterone. Since C/EBPbeta null females are sterile, pregnancy in these studies was simulated by treatment with estrogen and progesterone. Following treatment, thoracic mammary glands are isolated from C/EBPbeta+/- and C/EBPbeta-/- mice treated with estrogen and progesterone. The glands were fixed and stained with hematoxylin for whole mount preparation. In contrast to extensive lobuloalveolar development observed in **A**, the C/EBPbeta+/− glands, large areas of ductal epithelium in **B**, the C/EBPbeta−/− glands did not contain either secondary/tertiary side branches or alveoli. Also, ducts that form appear enlarged as indicated by the red arrow. (Modified from Seagroves *et al*., 1998)

C/EBPbeta in Breast cancer

With the establishment that C/EBPbeta is an important player in proliferation during mammary gland development, many investigators focused their attention on the role of this protein in cancer. Increased C/EBPbeta expression has been detected in ovarian tumors, colorectal tumors, and breast tumors (Sundfeldt *et al*., 1999; Rask *et al*., 2000; Staiger *et al*., 2009; Grimm and Rosen, 2003; Bundy and Sealy, 2003). Increases in C/EBPbeta mRNA have been detected in 18 of 18 MMTV/c-neu mammary tumors, approximately 2-5 fold over levels expressed during lactation or involution (Dearth *et al*., 2001). However, this does not provide information on which isoform is being upregulated. Some studies have described elevated levels of LIP in both murine mammary hyperplasia and in human breast cancers (Zahnow *et al*., 1997; Zahnow *et al*., 2001). It has been argued that the transcriptional inhibitor LIP isoform is predominantly expressed during proliferative cellular responses and is associated with aggressive tumors (Zahnow *et al*., 1997). It has also been reported that expression of LIP under the control of the whey acidic promoter (WAP) in the mouse mammary gland results in the formation of hyperplastic tissue, and more infrequently, carcinomas (Zahnow *et al*., 2001). However, because the LIP transgene was not epitope-tagged in these mice it is not possible to ascertain transgene expression from any endogenous LIP expression. Moreover, the level of LIP expression (transgene or endogenous) in the mammary tumors was not actually examined. Zahnow et al. have stated that LIP is overexpressed in 23% of infiltrating ductal carcinomas specimens. Yet,

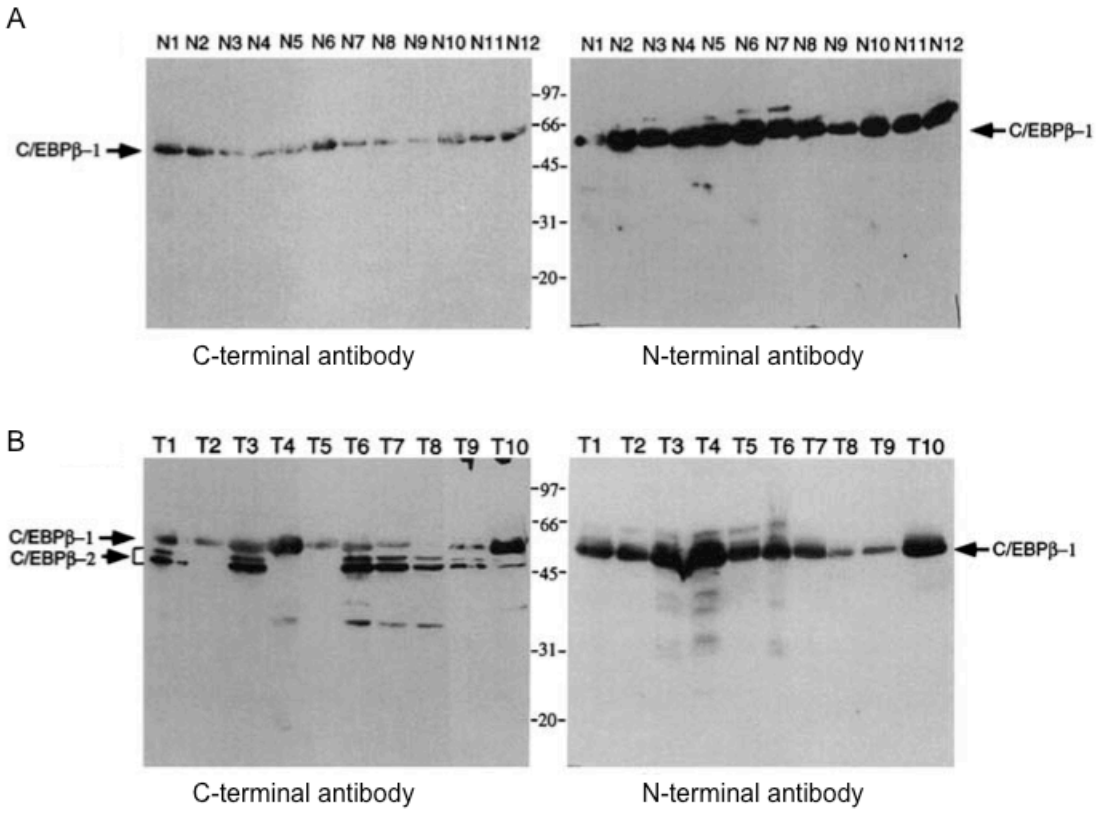

Figure 5. C/EBPbeta isoform expression in mammary samples. Whole cell extracts were prepared from **A,** normal breast tissue from reductive mammoplasty or **B**, breast tumors obtained from the Tissue Procurement Core at Vanderbilt University. Immunoblot analysis was performed using either the C-terminal or N-terminal C/EBPbeta antibody as indicated. Modified from Eaton, *et al*., 2001.

our own study on primary breast tumor samples found that high grade, invasive mammary carcinomas showed significant C/EBPbeta2 expression, but no LIP protein was detected in any of the samples (Figure 5) (Eaton *et al*., 2001). LIP is known to be easily generated by artifactual proteolysis of the larger isoforms, which could explain this discrepancy (Baer and Johnson, 2000).

We wanted to address this issue by overexpressing each C/EBPbeta isoform individually in a normal MEC line model. Overexpression of C/EBPbeta2 (but not C/EBPbeta1 or LIP) results in a variety of cancer phenotypes. In previous studies by our lab, we asked whether LIP could confer epidermal growth factor (EGF)-independent growth of MCF10A cells (Bundy *et al*., 2005). In contrast to C/EBPbeta2, a high level of LIP expression is incompatible with continued proliferation. In fact, our data reveals a remarkable increase in cell death of LIP-expressing cells, even in the presence of EGF (Bundy *et al*., 2005).

Purpose of this Study

In recent years, huge strides have been made in pursuing transcription factors as anticancer targets (Karamouzis *et al*., 2002; Frank, 2009). Therapeutics directed at C/EBPbeta are promising, not only for cancer, but for many other diseases. C/EBPbeta is known to play key roles in diverse pathological conditions such as human immunodeficiency virus (HIV), diabetes, as well as various inflammatory diseases. Nevertheless, it is essential to find ways to target a specific isoform, since the three are functionally distinct. Recent findings in our laboratory corroborate the importance of C/EBPbeta, specifically

C/EBPbeta1, in oncogene-induced senescence (Atwood and Sealy, 2010). Also, we found C/EBPbeta1 to be negatively regulated during transformation. We previously demonstrated a role for C/EBPbeta2 in promoting tumor cell proliferation and transformation (Bundy and Sealy, 2003). On the other hand, overexpression of C/EBPbeta1 or LIP does not promote tumor cell proliferation. Yet, the exact role of LIP in cancer is unclear. The main objective of this work is to examine the role of LIP in breast cancer in order to gain a better understanding of whether LIP is a tumor-promoter, tumor-suppressor, or both.

These studies demonstrate high levels of LIP stimulate cell death in breast cancer cell lines. Moreover, my work shows that LIP leads to a nonapoptotic cell death process in breast cancer cell lines involving cell engulfment and autophagy. The central hypothesis to be tested is that as a transcriptional repressor, LIP stimulates cell death in breast cancer cells by altering the cellular transcriptional program.

Significance

The apoptotic cell death pathway has been one of the major emphases in anticancer therapeutics. However, a critical step in tumor formation and progression is the ability of tumor cells to evade apoptosis, resulting in malignant cells that will not die (Hanahan and Weinberg, 2000). Apoptosis is complex mechanism and encompasses many pathways. Errors can transpire at any point along these pathways, leading to not only malignant transformation of the affected cells, but many times to tumor cell metastasis and resistance to

anticancer therapies.

Several alternative cell death pathways have been recently described. The aims of this work focus on characterizing the induction of autophagy as well as describing the ability to engulf neighboring cells which ultimately leads to cell death upon LIP expression in breast cancer cell lines. It is clear that knowledge of mechanisms and identification of new agents capable of inducing alternative cell death pathways has vast potential to improve cancer therapeutics.

CHAPTER II

C/EBPbeta3 (LIP) and autophagy

Introduction

Autophagy is a process involving the bulk degradation of cellular components in the cytoplasm via the lysosomal degradation pathway (Levine and Klionsky, 2004). Autophagy manifests a protective role in stressful conditions such as nutrient or growth factor depletion; however, extensive degradation of regulatory molecules or organelles essential for survival can lead to the demise of the cell, or autophagy-mediated cell death (Gozuacik and Kimchi, 2004). The role of autophagy in cancer is complex with roles in both tumor suppression and tumor promotion proposed (Hippert *et al*., 2006).

Activation of autophagy may lead to different outcomes depending on the cell genetic background as well as the duration and strength of the stress-inducing stimulus. It has been suggested that in early stages of tumor formation, a defective autophagic system leads to the accumulation of damaged proteins and organelles. This increase in genotoxic substances may lead to both failure to constrain cell growth and mutations. Yet, at later stages of tumorigenesis, autophagy may be a means by which tumor cells survive under oxygen and nutrient limiting conditions, providing extra time for adaptation via the induction of angiogenesis and/or motility and invasion (Hippert *et al*., 2006). The mechanisms by which autophagy may be regulated to provide complete cellular destruction or a survival advantage remain unknown.

One mechanism by which autophagy is regulated is through transcriptional control. This area has become more intricate with recent studies focusing on the roles of different transcription factors and their ability to induce or regulate autophagy in a cell context and stimulus specific manner. An example of this is the activation of E2 factor 1 (E2F1), which upregulates the expression of autophagy genes: LC3, autophagy related 1 (ATG1), and damage-regulated autophagy modulator (DRAM) by directly binding to their promoters (Polager *et al*., 2008). Other findings indicate dual roles for the transcription factor p53 in autophagy. Tasdemir et al. reports cytoplasmic p53 negatively regulates autophagosome formation (Tasdemir *et al*., 2008). Others have shown that nuclear p53 directly induces DRAM and autophagy (Crighton *et al*., 2006). The transcription factor nuclear factor kappa B (NF-κB) controls the expression of Beclin 1 by interacting with the BECN1 promoter (Copetti *et al*., 2009). Also, c-Jun N-terminal kinase (JNK) has been shown to control the expression of Beclin 1 through c-Jun. JNK controls autophagy by both cytoplasmic and nuclear effects (Li *et al*., 2009). Recent studies implicate forkhead box O (FoxO) transcription factors in promoting autophagy (Sengupta *et al*., 2009). Taken together, we hypothesize that the C/EBPbeta isoform, LIP, is another member of the group of transcription factors, including E2F1, NF-kB, and p53, which are capable of playing a role in autophagy.

In this study, I show that LIP stimulates autophagy and induces cell death in human breast cancer cells. Overexpression of LIP is incompatible with cell proliferation and when cell cycle analysis was performed, a DNA profile of cells

undergoing apoptosis was not observed. Instead, LIP expressing cells appeared to have large autophagic vesicles when examined via electron microscopy. Autophagy was further assessed in LIP expressing cells by monitoring the development of acidic vesicular organelles and conversion of LC3 from the cytoplasmic form to the membrane-bound form. Although the mechanism by which LIP induces autophagy remains unknown, preliminary data suggest that the nuclear cofactor, diabetes- and obesity- related gene (DOR), may be involved.

Materials and Methods

Adenoviral Constructs and Cell lines

The adenoviral (Ad) constructs used in these experiments were previously constructed and described (Duong *et al*., 2002). The human breast cancer cell lines MDA-MB-231, MDA-MB-468, and MCF-7 were obtained from the American Type Culture Collection (ATCC) (Manassas, VA). MDA-MB-231 cells and MDA-MB-468 cells were maintained in Iscove's Modified Eagle media supplemented with 10% (v/v) fetal bovine serum (FBS) from HyClone Laboratories (Logan, UT, USA), 10 µg/ml bovine insulin, 100 U/ml penicillin, and 100 µg/ml streptomycin (Life Technologies, Inc., Carlsbad, CA). MCF-7 cells were grown and maintained in Dulbecco's Modified Eagles's medium (DMEM) (Invitrogen, Burlington, ON, Canda) supplemented with 10 µg/ml bovine insulin, 100 U/ml penicillin, 100 µg/ml streptomycin (Life Technologies, Inc., Carlsbad, CA) and 10% (v/v) heat inactivated FBS. All cells were grown at 37°C in a humidified atmosphere

containing 5% CO_2.

Cell proliferation assays

MDA-MB-231, MCF-7, or MDA-MB-468 cells were grown to subconfluency (60–70%) on 100mm dishes. Cells were either uninfected (NV: no virus) or adenovirally (Ad) infected with Ad-green fluorescent protein (GFP) or Ad-LIP at a multiplicity of infection (MOI): 5–10. After 24hrs, cells were trypsinized and collected in normal growth media. Cells were counted with a hemocytometer and plated at a density of 1×10^5 cells/mL for the MDA-MB-231 cell line or 2×10^5 cells/mL for the MDA-MB-468 cell line. Cells were counted every day for seven to nine days. Cells were replenished with normal growth media every third day. Some assays were performed by plating 1×10^6 cells/mL and cells were counted every other day.

The (3-(4,5-dimethylthiazol-2-yl)-5-(3-carboxymethoxyphenyl)-2-(4 sulfophenyl)-2H-tetrazolium) (MTS) assay was used to monitor cell proliferation. Control (NV and GFP) MDA-MB-468 cells and LIP-expressing MDA-MB-468 cells were plated 24hrs post-infection in a 96-well plate at a density of 4×10^3 cells per well. Assays were performed at 2–5 days post-infection by adding a small amount of the CellTiter 96® AQueous One Solution Reagent (Promega, Madison, WI) directly to culture wells as recommended by manufacturer. This reagent contains an electron coupling reagent phenazine methosulfate (PMS) and a tetrazolium compound (inner salt, MTS). Dehydrogenase enzymes, found in metabolically active cells, convert MTS into a purple insoluble formazan product. After a 4hr incubation period, absorbance at

490nm was measured with a 96-well plate reader. The quantity of formazan product as measured by the amount of 490nm absorbance is directly proportional to the number of living cells in culture.

Colony formation assays

Control (NV or GFP) and LIP-expressing cells were plated 24hrs post-infection. Cells were seeded at different densities (800, 1600, and 3200 cells per 100mm tissue culture dish) for each condition. Cells were grown in normal growth media and replenished every three days. After 12–20 days in culture, plates were rinsed with phosphate-buffered saline (PBS), fixed with 95% (v/v) ethanol for 15 minutes at room temperature. After removing the ethanol, plates were stained with Gill No. 3 hematoxylin solution for approximately 1 hour at room temperature (Cat. # GHS332-1L; Sigma Chemical Co., St. Louis, MO). Plates were then repeatedly rinsed and colonies counted by visual inspection for each condition.

Cell Cycle Analysis

DNA cell cycle profiles of sub-confluent (60–70%) cultures were determined by flow cytometry using a BD FACScan (Becton Dickinson, San Jose, CA). All cultures were harvested at 24, 72, and 96hrs post-infection by trypsinization and pelleting in the presence of 20% (v/v) FBS at 500 × g for 7 minutes. Cells were then counted using a hemocytometer. Approximately 2×10^6 cells were washed twice in cold PBS and fixed in ice-cold 70% ethanol overnight. The samples were pelleted at 500 × g for 7 minutes and washed twice with ice-cold PBS. Lastly, the cells were incubated in a staining solution containing 2.5 mg/ml

RnaseA, 2.0 mg/ml propidium iodide, 0.1% (v/v) Triton X-100, 1 μM ethylenediaminetetraacetic acid (EDTA) in 1 × PBS for 30–60 minutes at 4°C in the dark. Data was collected using BD Cellquest software (BD Biosciences Immunocytometry Systems, San Jose, CA), and cell cycle modeling was performed using Modfit software (Verity Software House, Topsham, ME). The cell cycle profile of each population was generated from DNA content data collected from between 15,000 to 25,000 separate events.

Electron Microscopy

Control MDA-MB-231 cells or MDA-MB-231 cells infected with Ad-GFP or Ad-LIP were fixed with a solution containing 3% (v/v) glutaraldehyde plus 2% (v/v) paraformaldehyde in 0.1 M cacodylate buffer (pH 7.3) for 1 hour. The samples were then post-fixed in 1% osmium tetroxide (OsO_4) in the same buffer for 1 hour. Samples were then dehydrated in a graded alcohol series and embedded in epoxy resin. Representative areas were chosen for thin sectioning and viewed with an electron microscope (JEM 1010 transmission electron microscope; JEOL, Peabody, MA).

Whole cell lysates, cell fractionation, and immunoblot analysis

Whole cell lysates were prepared from 100mm dishes of 50–90% confluent MDA-MB-231 or MDA-MB-468 cells by scraping the cells at 4°C into (100 mM sodium chloride (NaCl), 10 mM Tris pH 8, 1 mM EDTA) (STE) in the presence of the following protease/phosphatase inhibitors: (10 μM Na vanadate, 10 mM Na molybdate, 10 mM beta-glycerolphosphate, 1 μg/ml aprotinin, 1 μg/ml leupeptin, 1 μg/ml pepstatin, and 1 mM phenylmethylsulfonyl fluoride). Nuclear and

cytoplasmic extracts were prepared in Buffer A. An equal volume of 2x sodium dodecyl sulfate (SDS) sample buffer and 2-mercaptoethanol (BME) was added and samples were boiled for 5 minutes. Relative protein concentrations were determined using Protein Assay Reagent (BioRad Laboratories, Hercules, CA, USA) as per manufacturer's instructions. Equal amounts of protein were loaded onto a 10% or an 18% SDS – polyacrylamide gel electrophoresis (PAGE) and separated by electrophoresis. The 18% SDS-PAGE running gel is prepared using 24mL of 30%(v/v) acrylamide and 0.15%(v/v) Bis N,N'-methylethylene-bis acrylamide, 10mL of 3M Tris pH 8.8, 0.4mL of 10% (v/v) SDS and 0.4ml of 10% (w/v) ammonium persulfate in a final volume of 40mL. The stacker gel is prepared using 6mL of 10% (v/v) acrylamide and 0.15% (v/v) N,N'-methylethylene-bis acrylamide, 5mL of 1M Tris pH 6.8, 0.2mL of 10% (v/v) SDS and 0.2mL of 10% (v/v) ammonium persulfate in a final volume of 20mL. The proteins were transferred to an Immobilon®-P or Immobilon®-FL filter (EMD Millipore, Billerica, MA) and the blots were processed as described previously (Eaton *et al*., 2001). Briefly, the nonspecific binding sites were blocked with 5% (w/v) nonfat dried milk (NFDM) in Tris Buffered Saline (TBS-T: 100 mM Tris pH 7.5, 150 mM NaCl, and 0.05% Tween-20). Then blots were incubated with primary antibodies: MAP1-LC3 at a 1:1,000 dilution overnight (Cat. # PD012, MBL, Woburn, MA), Caspase-3 at a 1:1,000 dilution overnight (sc-9662 Cell Signaling, Boston, MA), TP53INP2/DOR at a 1:1,000 dilution overnight (cat. # T1879, Epitomics, Burlingame, CA) T7-tag at a 1:20,000 dilution (EMD Bioscience, San Diego, CA) in TBS-T containing 0.5% (w/v) NFDM for 1 hour at

room temperature with gentle agitation. The blots were detected with a horse radish peroxidase (HRP)-conjugated goat anti-mouse or anti-rabbit antibody (Cell Signaling, Boston, MA). Signal was detected by chemiluminescence using SuperSignal West Pico reagent (Pierce, Rockford, IL, USA). Alternatively, the LI-COR ODYSSEY infrared imaging system (Lincoln, Nebraska) was used for immunoblot analysis and quantitation as per manufacturer's instruction.

Indirect immunostaining and image acquisition

Endogenous high mobility group box 1 (HMG1) and LC3 were detected in control (NV, GFP) and LIP-expressing MDA-MB-468 cells. All MDA-MB-468 cell cultures were grown in 35mm dishes fitted with collagen-coated glass coverslips (MatTek Corp, Ashland, MA, USA). Cultures were washed three times in PBS, fixed in 3.7% (v/v) formalin in PBS for 30 minutes at room temperature, washed an additional three times, and processed for indirect immunofluorescence. The cells were washed at least three times in PBS after each treatment. First, the cells were permeabilized in PBS containing 0.1% (v/v) Triton X-100 for 20 minutes at room temperature. The cells were washed and nonspecific binding sites were blocked in PBS containing 5% (w/v) bovine serum albumin (BSA) (Fraction V, Sigma Chemical Co., St. Louis, MO) at 4°C for 24hrs. Immediately following aspiration of the blocking solution, the cells were incubated with HMG1 polyclonal antibody (Cat. # 10829-1-AP, Proteintech Group, Chicago, IL) at a dilution of 1:75 or LC3B polyclonal antibody (Cat. # NB600-1384, Novus Biologicals, Littleton, CO) at a dilution of 1:150 in PBS containing 2% (w/v) BSA and 0.1% (v/v) Triton X-100 for 2hrs at room temperature. The cells were

washed as described above. Cells were then incubated for an additional hour at room temperature in the dark with fluorescent-conjugated Alexa 594 goat-anti-rabbit secondary antibody diluted to a final concentration of 2 μg/ml in PBS containing 2% (w/v) BSA and 0.1% (v/v) Triton X-100. The cells were then washed three times in PBS containing 0.1% (v/v) Triton X-100 and a few final rinses with double-distilled water. In some cases, Hoechst 33342 (Sigma-Aldrich Co., St. Louis, MO) was used to label the nucleus. The cells were visualized on a Leica DM IRB inverted fluorescence microscope equipped with a Nikon DMX 1200C digital camera.

Quantification of Acidic Vesicles by Acridine Orange using Flow Cytometry

Control (NV, Ad-GFP) MDA-MB-231 cells and Ad-LIP MDA-MB-231 cells were stained with acridine orange 96hrs post-infection. Cells were trypsinized and prepared from 100mm dishes. Acridine orange (Polyscience, Warrington, PA) was added at a final concentration of 1μg/mL for a period of 15 minutes at room temperature. Cells were washed and collected in 1x PBS. Following quantification on a hemocytometer, approximately 1×10^6 cells were stained and then analyzed by flow cytometry. Data was collected using BD Cellquest software (BD Biosciences Immunocytometry Systems, San Jose, CA). Red (>650nm) fluorescence emission from 10^6 cells illuminated with blue (488nm) excitation light was measured with a BD FACScan (Becton Dickinson, San Jose, CA). Winlist software (Verity Software House, Topsham, ME) was used to determine the fluorescence means and make the overlays. The profile of each population was generated from data collected from a representative sample of

25,000 events. Five separate experiments were performed.

Statistical analysis

Quantitative data are expressed as means ± standard deviation (SD). For comparisons between multiple groups, ANOVA followed by the Student-Newman-Keuls multiple comparisons test was used. Prism 5.0 (GraphPad, La Jolla, CA) was used for all analyses.

Results

LIP expression attenuates proliferation of the MDA-MB-468 breast cancer cell line

We have previously demonstrated that overexpression of LIP in the MCF10A cell line is incompatible with cell proliferation (Bundy *et al*., 2005). When attempting to generate a population of LIP-expressing cells by infection with the chimeric retrovirus, LZRS-HisLIP-IRES-GFP, followed by cell sorting, we found we could not establish a cell population stably expressing elevated LIP. We reasoned adenovirally infecting the cells would eliminate the problematic expansion of sorted cells when LIP is growth inhibitory. To analyze the effect of LIP expression, we used an adenoviral vector to transduce the breast cancer cell line, MDA-MB-468, with the truncated C/EBPbeta gene comprising the C-terminal half encoding a T7-epitope tagged 20kDa LIP protein. The adenoviral vector also encodes a GFP marker protein so that infected cells are easily detected by their green fluorescence; as such control adenoviral vector

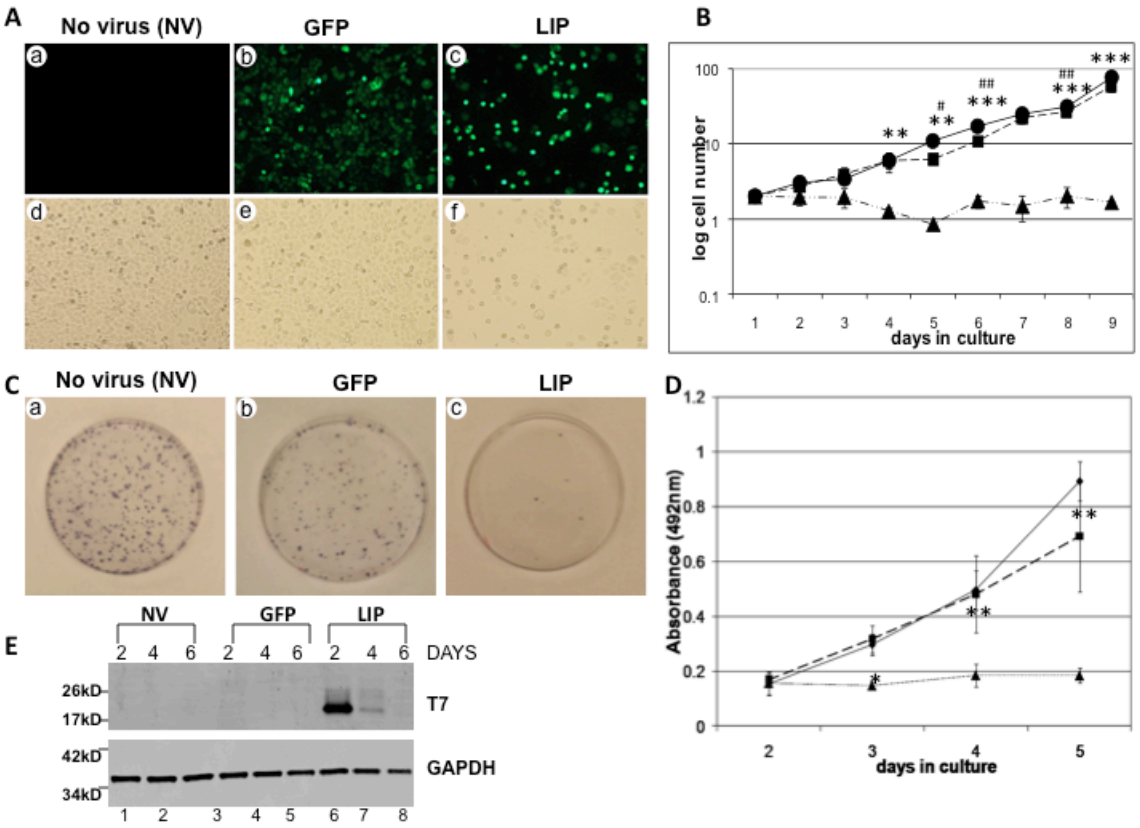

Figure 6. LIP expression attenuates proliferation of the MDA-MB-468 breast cancer cell line. **A**, Fluorescent micrographs are shown for **a**, NV; **b**, GFP; and **c**, LIP cells. Corresponding brightfield micrographs of control **d**, NV or **e**, GFP cells are shown. Brightfield micrographs of LIP cells are shown in panel **f**. Cells were plated on day 1 post-infection at the same density (2×10^6 per 100 mm dish); images were taken 3 days post-infection. **B**, MDA-MB-468 cells infected with Ad-LIP (▲) or Ad-GFP (■) and compared to NV (●) control cells. Cells were plated on day 1 post infection at 200,000 cells per 100 mm dish and counted every day. Results are shown as the mean of three experiments. Error bars represent the standard deviation (SD). *p<0.05; **p<0.01; ***p<0.001 comparing the Ad-LIP to the control (NV and Ad-GFP) MDA-MB-468 cells. #p<0.05; #p<0.01 comparing the controls (NV and Ad-GFP) MDA-MB-468 cells. **C**, Representative plates with visible colonies from colony formation assays of control (NV, GFP) and LIP MDA-MB-468 cells. **D**, The proliferative activity of MDA-MB-468 cells infected with LIP (▲), GFP (■), and NV (●) control cells was assessed by the MTS assay. Cells were plated on day 1 post infection at 4×10^3 cells per well. Data are the mean ± SD of three separate experiments. *p<0.05; **p<0.01 comparing the LIP to the control (NV and GFP) MDA-MB-468 cells. **E**, Cell extracts were prepared from MDA-MB-468 NV cells (lanes 1–3), Ad-GFP cells (lanes 4–6), and Ad-LIP cells (lanes 7–9) at days 2, 4, and 6 post-infection. Expression of T7-tagged LIP was determined by immunoblot analysis using anti-T7 epitope tag antibody. GAPDH is shown as a loading control.

expressing GFP only was also used. Cells were plated at the same density and adenovirally infected with control Ad-GFP or Ad-LIP on day 0. Uninfected or no virus (NV) control cells are used in our experiments to compare to adenoviral infected cells. Adenoviral infection efficiency was approximately 90% for the GFP only infected cells and >95% for the LIP-GFP infected cells (Fig. 6A panels a–c). Photomicrographs of the MDA-MB-468 cells in culture three days post-infection are shown in Figure 6A. The NV MDA-MB-468 cells and Ad-GFP MDA-MB-468 cells continue to proliferate (Note the control cell cultures are >90% confluent three days after plating). LIP-expressing cells, however, are unable to proliferate in culture leading to a decrease in cell density in comparison to the control cells (Fig. 6A, panel c and f).

To quantitate and monitor the decrease in cell density, cell counts were performed daily for 9 days post-infection. LIP expression in MDA-MB-468 cells leads to a decrease in cell number (Fig. 6B) after several days post-infection, demonstrating that LIP overexpression results in cell death. Next, I performed colony formation assays with MDA-MB-468 cells. These assays are based on the principle that stable expression of certain proteins cause either cell cycle arrest or cell death, thus there is a reduction in colony number. Control MDA-MB-468 cells (NV and Ad-GFP) were able to produce significantly more colonies than the LIP-expressing MDA-MB-468 cells (Fig. 6C). I further examined the proliferation of control (NV, Ad-GFP) and (Ad-LIP) MDA-MB-468 cells by performing MTS assays. LIP expression results in inhibition of the proliferative activity of MDA-MB-468 cells to 20–40% of control cells at days 4 and 5 post-

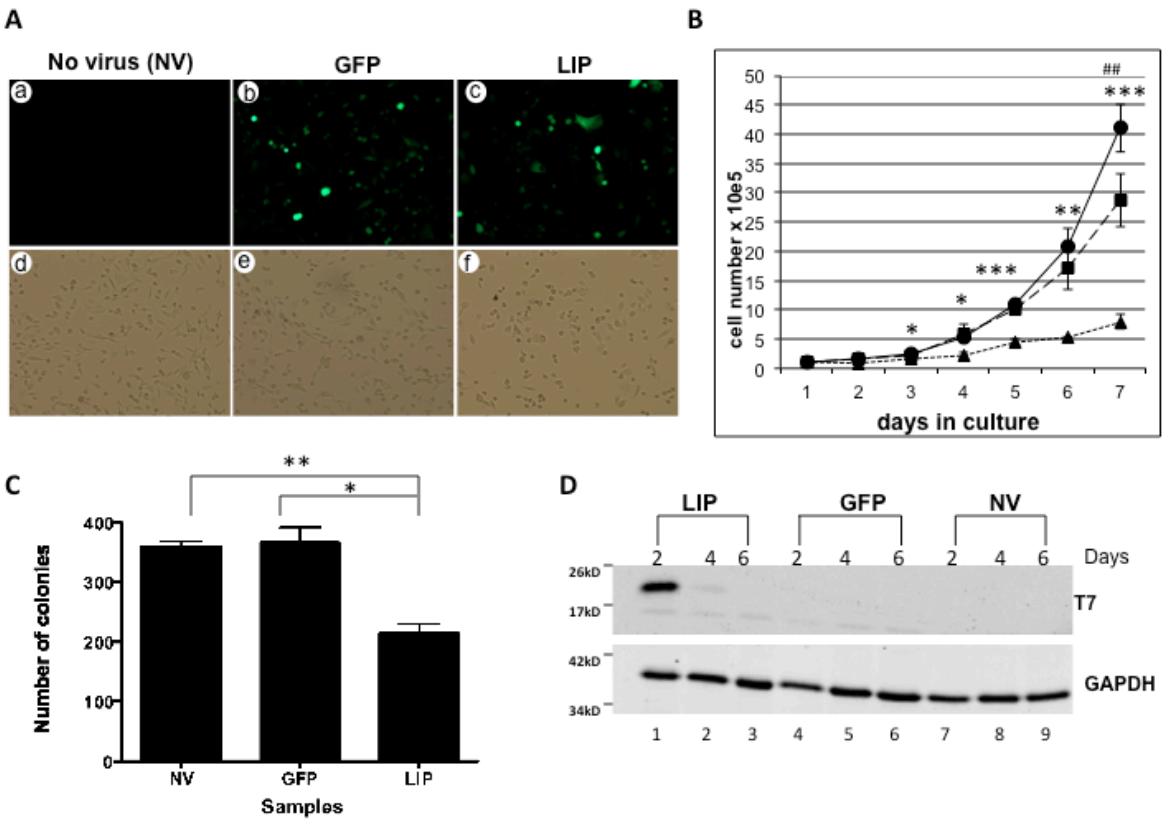

Figure 7. LIP expression attenuates proliferation of the MDA-MB-231 breast cancer cell line. **A**, Fluorescent micrographs are shown for control **a**, uninfected (NV); **b**, Ad-GFP; and **c**, Ad-LIP cells. Corresponding brightfield micrographs of NV cells or Ad-GFP cells and Ad-LIP cells are shown in panels d-f, respectively. MDA-MB-231 cells were adenovirally infected at an MOI of 10. Cells were plated on day 1 post-infection at the same density (1 x 10^6 per 100 mm dish) and images were taken three days post-infection. **B**, MDA-MB-231 cells were infected with Ad-LIP (▲) or Ad-GFP (■) and compared to NV (●) control cells. Cells were plated on day 1 post-infection at 100,000 cells per 100 mm dish and counted every day. Results are shown as the mean of three experiments. Error bars represent the standard deviation (SD). *p<0.05; **p<0.01; ***p<0.001 comparing the Ad-LIP to the control (NV and Ad-GFP) MDA-MB-231 cells. #p<0.05; #p<0.01 comparing the controls (NV and Ad-GFP) MDA-MB-231 cells. **C**, MDA-MB-231 cells (NV, Ad-GFP, or Ad-LIP) were plated into 100mm dishes at a density of 3200 cells per dish. Colonies were scored by counting visible colonies after 12 days and are presented as the mean value ± standard deviation from three individual experiments. *p<0.05; **p<0.01 comparing Ad-LIP to the control (NV and Ad-GFP) MDA-MB-231 cells. **D**, Cell extracts were prepared from MDA-MB-231 Ad-LIP cells (lanes 1-3), Ad-GFP cells (lanes 4-6), and NV cells (lanes 7-9) at days 2, 4, and 6 post-infection. Expression of T7-tagged LIP was determined by immunoblot analysis using anti-T7 epitope tag antibody. GAPDH is shown as a loading control.

infection (Fig. 6D). To confirm LIP expression, I conducted immunoblot analysis of whole cell lysates using anti-T7 antibody. As shown in Figure 6E, we initially detect a high level of the T7-tagged 20kD LIP protein at day 2 post-infection in LIP expressing cells that remain attached to the plate. However, LIP levels decline at day 4 post-infection and are undetectable by immunoblot analysis at six days post-infection. These results show that cells expressing LIP do not proliferate and are lost from the population.

LIP expression attenuates proliferation of the MDA-MB-231 breast cancer cell line

To extend our findings in other breast cancer cell lines, LIP was introduced into MDA-MB-231 and MCF-7 cells and cell proliferation was monitored. Photomicrographs of the MDA-MB-231 cells in culture three days post-infection are shown in Figure 7A. In the same way, the Ad-LIP MDA-MB-231 cells are dying or unable to proliferate in culture leading to a decrease in cell density in

comparison to the control cells (Fig. 7A, panel c and f). Cell density was monitored by plating cells at the same density post-infection and counted every day (MDA-MB-231) or every other day (MCF-7 cells). LIP expression inhibited cell proliferation in MDA-MB-231 (Fig. 7B) and MCF-7 cells (Figure 8).

Colony formation assays were also performed with the MDA-MB-231 cells. Likewise, the LIP-expressing MDA-MB-231 cells formed fewer colonies than the control (NV and Ad-GFP) MDA-MB-231 cells (Fig. 7C). LIP expression in the MDA-MB-231 was confirmed by immunoblot analysis using the anti-T7 antibody.

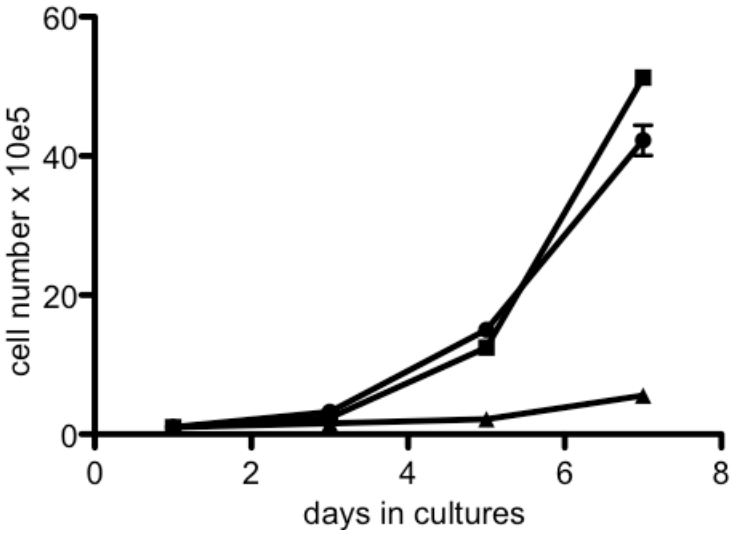

Figure 8. LIP expression attenuates proliferation of MCF-7 breast cancer cell line. MCF-7 cells were adenovirally infected with Ad-LIP (▲) or Ad-GFP (●) and compared to NV (■) control cells. Cells were plated on day 1 post-infection at the same density (1 x 10^6 per 100 mm dish) and counted every other day. Results are shown as the mean of three experiments. Error bars represent the standard error (SE).

We detect LIP expression at day 2 post-infection; however, LIP levels rapidly decline and are undetectable after four days post-infection (Fig. 7D). Interestingly, at day 6 this cell population is beginning to recover, coinciding with the loss of overexpressed LIP protein.

LIP does not block cell cycle progression or induces apoptosis

We considered that LIP expression might inhibit proliferation by blocking the cell cycle or by inducing apoptosis, since we observe a decrease in cell number in the LIP-expressing cell population and lower to almost no colony formation. To address these possibilities, cell cycle analysis and caspase-3 activation assays were performed on the MDA-MB-231 cell line. Fluorescence-activated cell sorting (FACS) analysis was performed at various time points (days 1, 3, and 6 post-infection) and revealed no significant differences in the cell cycle phases (Fig. 9A and B). Ad-LIP infected cells did not show a G_1 phase arrest and LIP-expressing cells are present in the G_2/M phase as well as the S-phase (Fig. 9A panel c). We can conclude that Ad-LIP does not block cell cycle progress. Interestingly, a sub-G_1 phase (arrow in Fig. 9A panel a–c), a characteristic of apoptosis, was not detected in Ad-LIP infected cells. To confirm the absence of apoptosis, I examined caspase-3 activation in the Ad-LIP infected cells. Activation of caspase-3 is key in mediating apoptosis (Cohen, 1997). Activation requires proteolytic processing of its inactive zymogen into activated p17 and p12 fragments (Cohen, 1997). Caspase-3 activation was screened in MDA-MB-231 cells by western blotting (Fig. 9C). LIP-expressing cells did not activate caspase-3 at a low or higher MOI as indicated by the absence of the

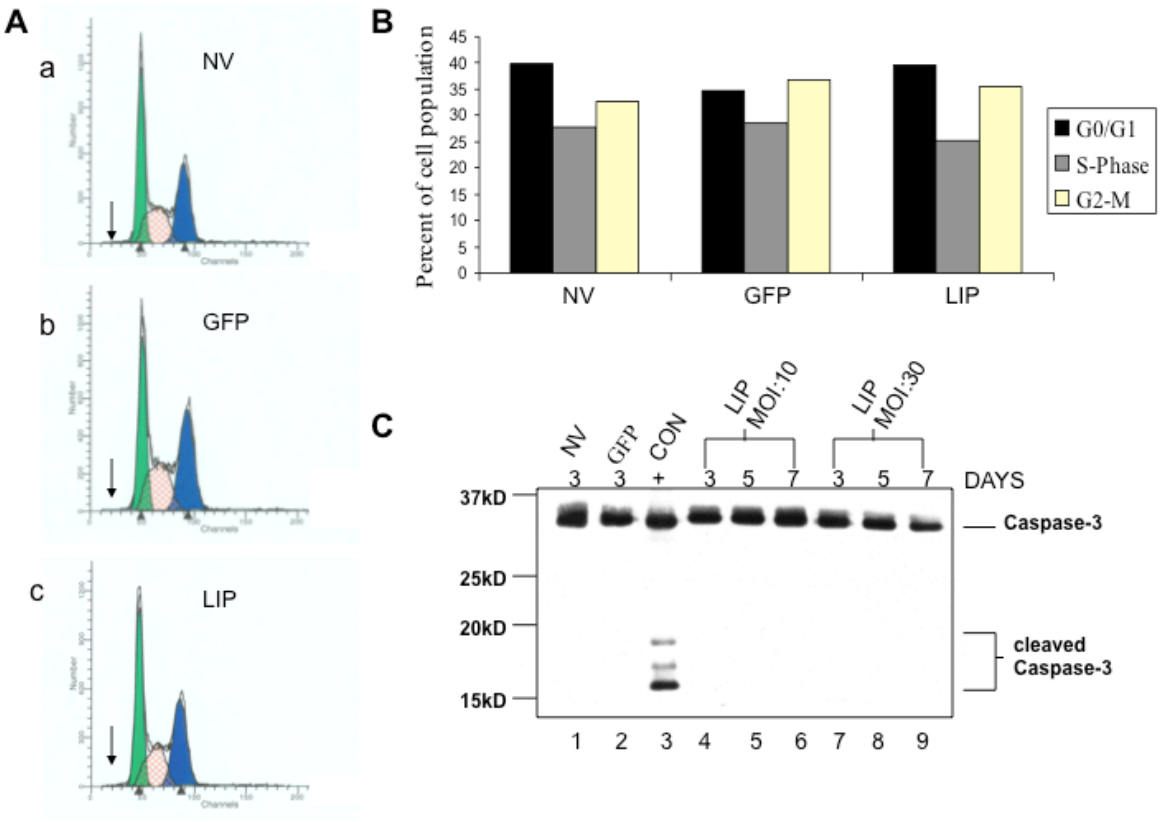

Figure 9. LIP does not block cell cycle progression or induce apoptosis. A, Cell cycle profiles of **a**, uninfected NV MDA-MB-231 cells, **b**, Ad-GFP cells, and **c**, Ad-LIP cells. Results from a representative experiment are shown. **B**, Quantification of cell cycle analysis of MDA-MB-231 cells at day 6 post-infection. Solid black bars indicate the percentage of cells in G0/G1, gray-filled bars the percentage in S-phase, and yellow-filled bars the percentage in G2-M. **C**, Whole cell lysates were prepared from control NV (lane 1) and Ad-GFP MDA-MB-231 cells (lane 2) at day 3 post-infection. Whole cell lysates were also prepared from MDA-MB-231 cells infected with Ad-LIP at a MOI of 10 or 30 (lanes 4-9) at different time points (days 3, 5, and 7) post-infection. RKO colon cancer cell line treated with 5-fluorouracil (lane 3) is included as a positive control. Samples were analyzed by 12% SDS-PAGE and immunoblot analysis for caspase-3 activation was performed. Equal amounts of total protein were loaded in each lane as determined by Ponceau S staining.

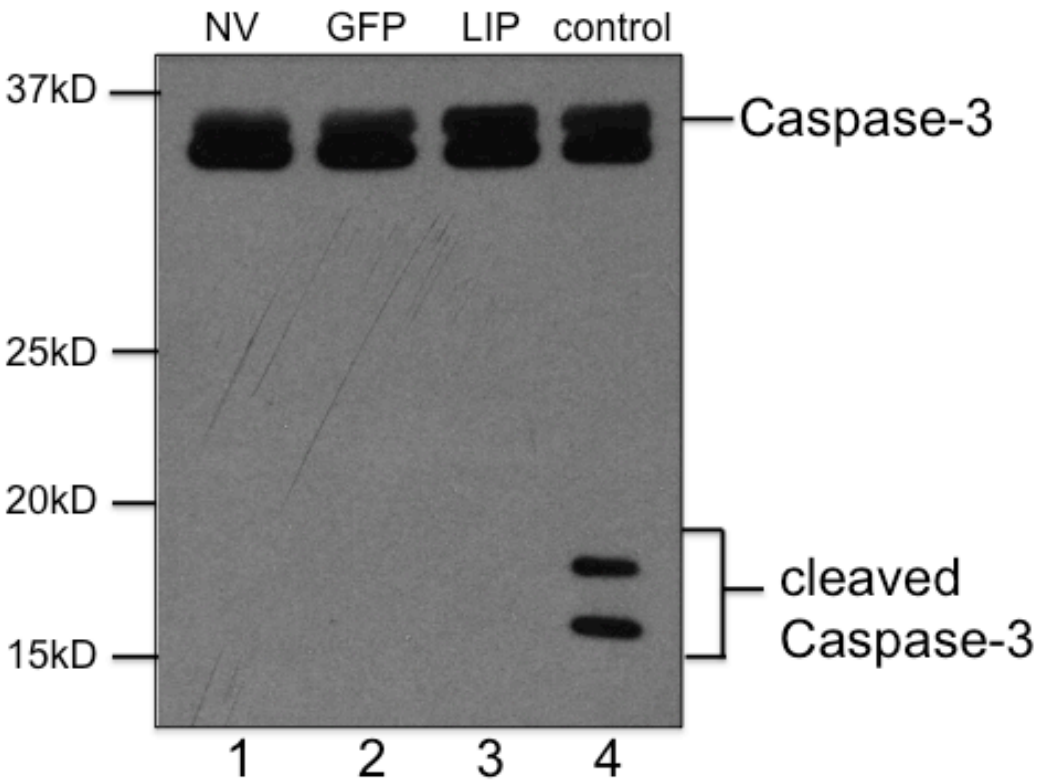

Figure 10. LIP expression does not induce caspase-3 activation. Whole cell lysates were prepared from control NV (lane 1), Ad-GFP MDA-MB-468 cells (lane 2), Ad-LIP MDA-MB-468 cells (lane 3) infected at a MOI of 10. Lane 4 is a positive control for caspase-3 activation. Lysates were prepared at day 3 post-infection. Samples were analyzed by 12% SDS-PAGE and immunoblot analysis for caspase-3 activation was performed. Equal amounts of total protein were loaded in each lane as determined by Ponceau S staining.

cleaved caspase fragments (Fig. 9C lanes 4–9) that are present in the positive control (Fig. 9C Lane 3). Activation of caspase-3 was also screened in MDA-MB-468 cells (Figure 10) and caspase-3 activation was not detected. Furthermore, chromatin condensation and nuclear breakdown was not observed in the ultrastructural analysis of these cells as illustrated in Figure 12. Collectively, these results indicate that Ad-LIP does not induce apoptosis.

LIP does not induce necrosis

In contrast to apoptosis, necrotic cell death is not a developmentally programmed type of cell death. Necrosis takes place when cells are exposed to extreme stress conditions, which leads to a deregulation of normal cellular activities. High mobility group box 1 (HMG1) is a non-histone nuclear protein participating in chromatin architecture and transcriptional regulation (Degryse *et al*., 2001). However, it is also secreted from damaged or necrotic cells (Degryse *et al*., 2001). In order to test whether LIP expression was inducing necrotic cell death, I assayed the intracellular localization of HMG1 in the MDA-MB-468 cells by immunostaining. MDA-MB-468 cells were forced into necrosis by treatment with deoxyglucose and azide. HMG1 is no longer localized to the nucleus of these cells as shown in Figure 11 (left panel). Under normal conditions, HMG1 is localized to the nucleus as seen in control (NV and Ad-GFP) MDA-MB-468 cells. More importantly, LIP expression does not lead to secretion of HMG1. We detect HMG1 in the nucleus of the LIP-expressing MDA-MB-468 cells. I repeated these experiments at days 3, 4, and 6 post-infection and did not detect any changes in the HMG1 localization.

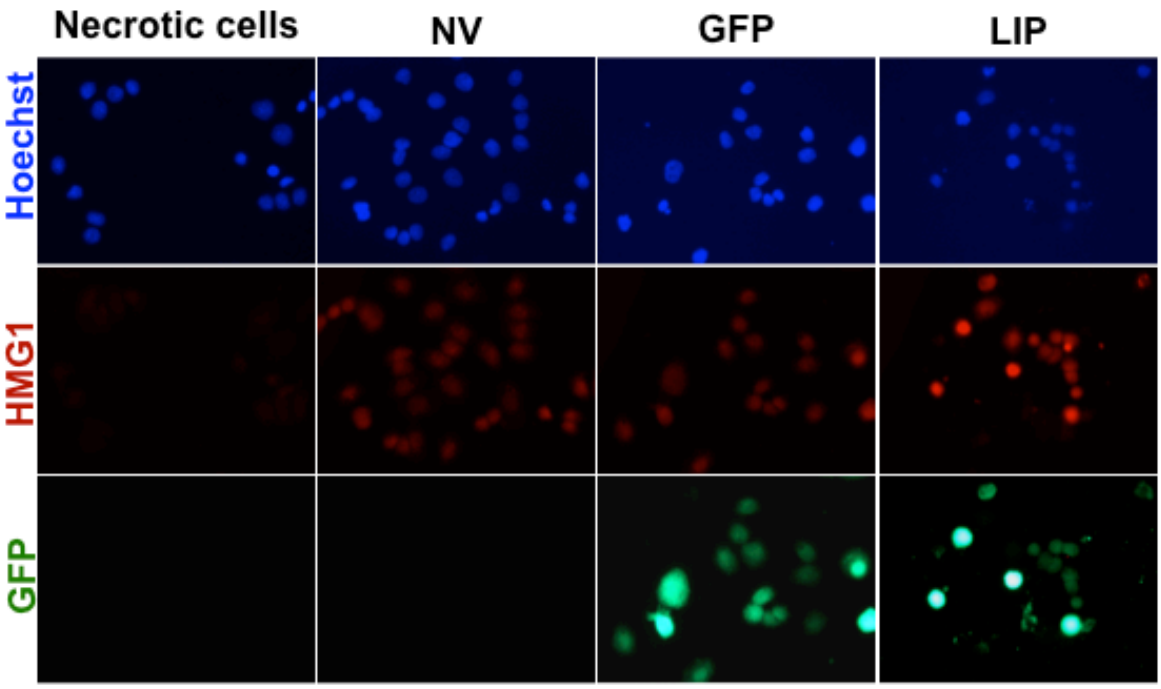

Figure 11. LIP does not induce necrosis. MDA-MB-468 cells were induced into necrosis by adding 6mM deoxyglucose plus 10mM sodium azide for 18hrs and used as a positive control. Immunofluorescence studies were performed on MDA-MB-468 cells (NV, Ad-GFP, or Ad-LIP) at day 4 post-infection. Cells were fixed and stained for DNA (Hoechst top panel) and HMG1 (middle panel). GFP positive cells are shown (bottom panel).

Ultrastructure of autophagic vesicles (AV) formed during LIP-induced autophagy

Interestingly, when examining the LIP-expressing cells under the light microscope, the dying/dead cells exhibited a change in cell morphology with increased intracellular vacuoles. Given the vacuolated appearance of the MDA-MB-231 cells infected with Ad-LIP, we wanted to confirm if autophagy was occuring using electron microscopy. Autophagy can be observed through ultrastructural analysis using transmission electron microscopy (TEM) (Klionsky *et al*., 2007). This method is one of the most indispensable methods to detect autophagic compartments in mammalian cells (Klionsky *et al*., 2007). LIP-expressing MDA-MB-231 cells, displayed in Figure 12A (panel c), show a dramatic amount of autophagic vesicles (AV) not seen in the control (NV and Ad-GFP) MDA-MB-231 cells (Fig. 12A panel a and b, respectively). The magnified images illustrate autophagosomes with characteristic double or multiple membranes (Fig. 12B panel a, b). These autophagosomes contain engulfed materials, including degraded cytoplasmic areas, as well as organelles. In addition, there are many multi-lamellar structures observed (Fig. 12B panel b). Empty vacuoles were also identified (Fig. 12B panel c) that are not likely to be autophagic, although their significance is unknown. In addition, electron microscope (EM) micrographs reveal “myelin” bodies (Fig 12B, panel d), which is the end result of extensive autophagy. These EM micrographs provide strong evidence that LIP induces autophagy in MDA-MB-231 cells.

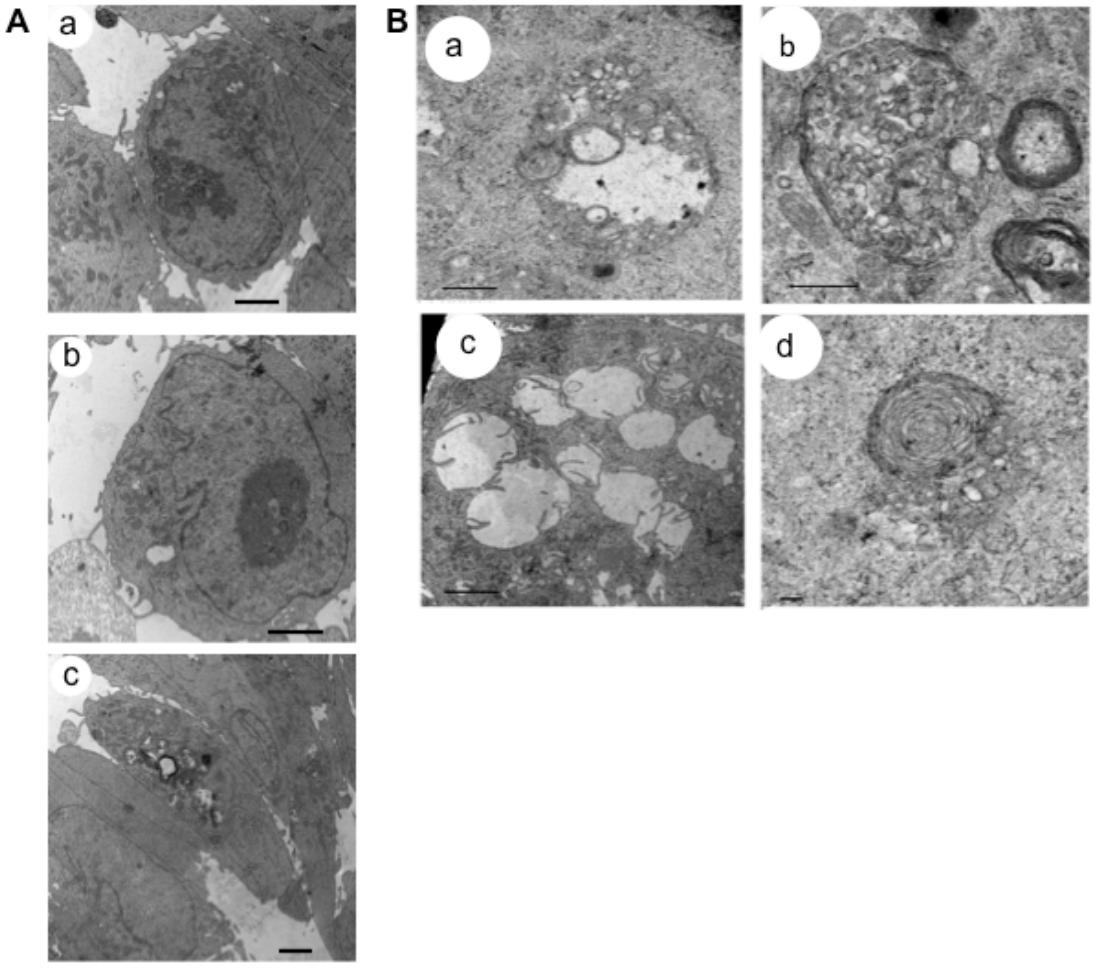

Figure 12. Ultrastructure of autophagic vacuoles (AV) formed during LIP-induced autophagy. **A**, Representative electron micrographs shown of **a**, uninfected NV MDA-MB-231 cells; **b**, Ad-GFP MDA-MB-231 cells; and **c**, Ad-LIP MDA-MB 231 cells 2 days post-infection. **B**, Electron micrographs of LIP-expressing MDA-MB-231 cells at later stages (six days post-infection) of autophagic process. Scale bar: **A**, 2 micron (a–c); **B**, 500nm (a,b); 2 micron (c); 100nm (d).

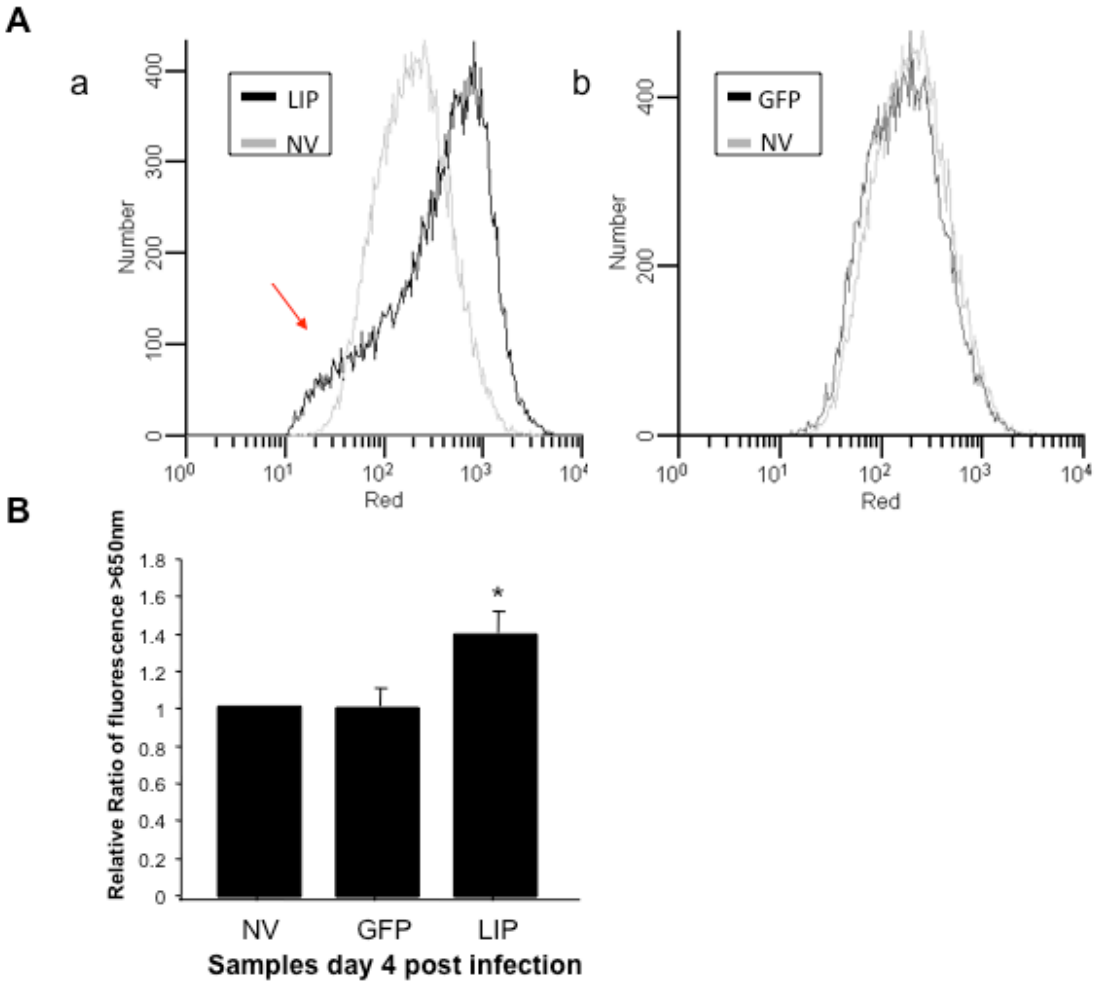

Figure 13. LIP overexpression leads to increase of autophagic vacuoles (AV). LIP-induced appearance of AV was detected by staining with the lysosomotropic agent, acridine orange. Cells were stained and processed for flow cytometric analysis. Mean red fluorescence was determined as described in "Materials and Methods". **A**, Panel a shows an overlay comparing the control NV and Ad-LIP MDA-MB 231 cells. Panel b shows an overlay comparing the control NV and Ad-GFP MDA-MB-231 cells. **B**, Quantitation of red fluorescence (>650nm) for control NV, Ad-GFP, or Ad-LIP MDA-MB-231 cells four days post-infection. Results are shown as the mean of 5 separate experiments. Error bars indicate ± standard error of the mean (SEM). (*p-value<0.01).

LIP overexpression leads to increase acidic vesicles

Autophagy can also be monitored by the development of acidic vesicular organelles (Klionsky *et al*., 2007). Acidification of autophagic vesicles is mediated by the vacuolar H^+-ATPase in yeast or lysosomal hydrolases in mammalian cells. The lysosomotropic agent acridine orange is a weak base that moves freely across biological membranes when uncharged. Its protonated form accumulates in acidic compartments (Paglin *et al*., 2001). Therefore, it can be used to quantify acidic AV accumulation. When compared to control uninfected MDA-MB-231 cells, the Ad-LIP cells show a shift or increase in the red fluorescence. Interestingly, we also detect a side plateau indicative of dying cells (arrow in Fig. 13A panel a). There are no changes detected in the control (NV and Ad-GFP) MDA-MB-231 cells (Fig. 13A panel b). The results of five separate experiments were quantitated as shown in Figure 13B. In comparison to the controls, NV and Ad-GFP MDA-MB-231 cell populations, LIP-expressing cells were determined to have a statistically significant ($p<0.01$) increase in acidic vesicles (Fig. 13B). There was no statistical difference between the NV and Ad-GFP MDA-MB-231 cells. After performing these experiments at various time points, we detect the greatest changes in acridine orange staining four days post-infection.

LIP-induced activation of LC3

Induction of autophagy by LIP was also confirmed by LC3 activation. LC3 is the first mammalian protein known to specifically associate with the autophagosomes (Kabeya *et al*., 2000). LC3 binds the elongating

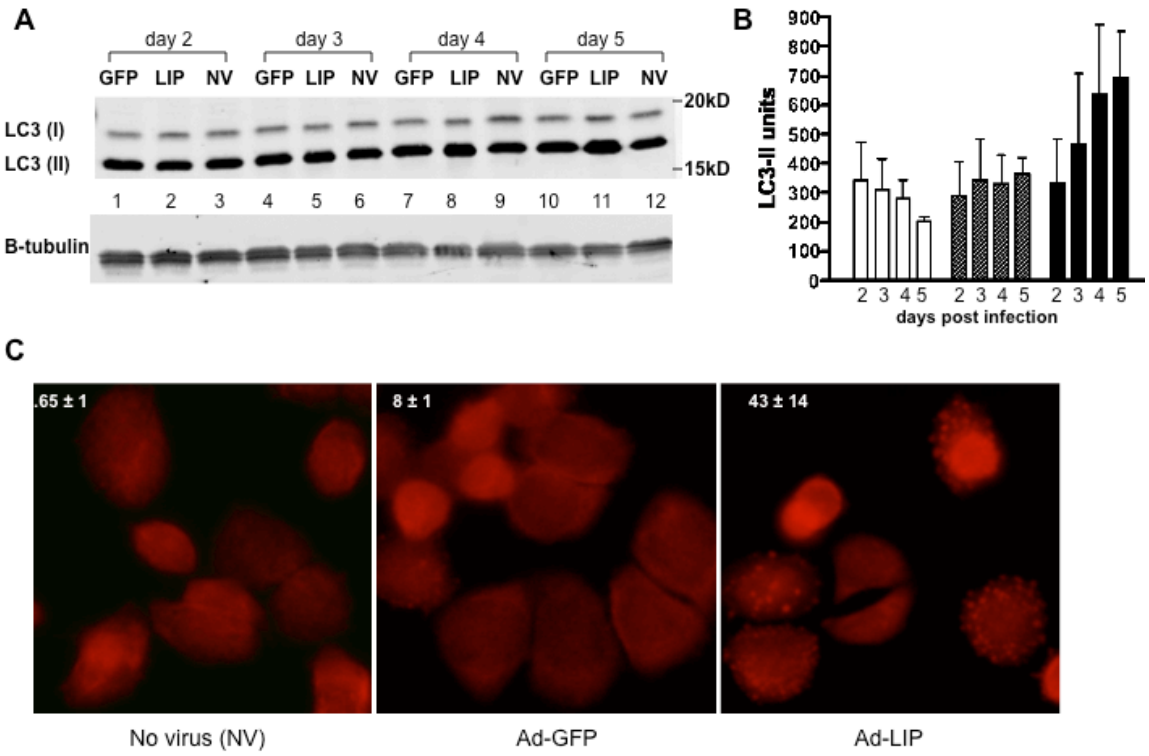

Figure 14. LIP-induced activation of LC3. **A**, Whole cell lysates were prepared from control uninfected NV MDA-MB-468 cells (lanes 3,6,9, and 12), Ad-GFP MDA-MB-468 cells (lanes 1,4,7, and 10), and Ad-LIP MDA-MB-468 cells (lanes 2,5,8, and 11) at different time points (days 2–5) post-infection and analyzed by 18% SDS-PAGE. Immunoblot analysis with anti-LC3 antibody and a B-tubulin antibody (used as a loading control) is shown. LC3-I, soluble form of LC3; LC3-II, membrane-bound form of LC3. **B**, Densitometric analysis of LC3-II in MDA-MB-468 cells using the ODYSSEY infrared imaging system. Data shown represents the mean ± SEM. White-filled bars represent the uninfected NV MDA-MB-468 cells, shaded bars the Ad-GFP MDA-MB-468 cells, and the solid black bars the Ad-LIP MDA-MB-468 cells. **C**, LC3 immunostaining (red) of control NV, Ad-GFP, or Ad-LIP MDA-MB-468 cells are shown. The percentage of cells with LC3 punctate staining relative to the total cell number at day 4 post-infection is shown in the corner of each panel (mean ± SD).

preautophagosomal membrane after activation by proteolytic cleavage and conjugation of a phosphatidylethanolamine molecule to the exposed C-terminus (Kabeya *et al*., 2000; Geng and Klionsky, 2008). The proteolytic cleavage converts LC3 from an 18kD (LC3-I) to a 16kD (LC3-II) protein (Kabeya *et al*., 2000). The conversion of soluble form of LC3 (LC3-I) to the autophagosome-associated (LC3-II) is a well-accepted method for monitoring the onset of autophagy (Klionsky *et al*., 2007). To improve separation of these two small proteins I performed immunoblotting after analyzing protein extracts on an 18% non-Laemmli acrylamide gel. We detect an increase in the membrane-bound form (LC3-II) in LIP-expressing MDA-MB-468 cells beginning at day 3 post-infection (Figure 14A lane 5). LC3-II levels greatly increase at days 4 and 5 post-infection in LIP-expressing cells (Figure 14A lanes 8 and 11) in comparison to the control (NV and GFP) MDA-MB-468 cells (Figure 14B).

In addition to immunoblot analysis, I assayed the intracellular localization of endogenous LC3 in MDA-MB-468 cells using indirect immunostaining and fluorescence microscopy. LC3 has been reported to localize to punctate-structures when the process of autophagy is occurring. The NV and Ad-GFP MDA-MB-468 cells show dispersed LC3 staining (Figure 14C). Even under nutrient-rich conditions, we detect punctate LC3 staining in 43% of LIP-expressing cells (Figure 14C). Our results indicate that LIP expression leads to an increase in endogenous LC3-II levels and an increase in punctate LC3 staining reflective of an increase in autophagosomes or autolysosomes.

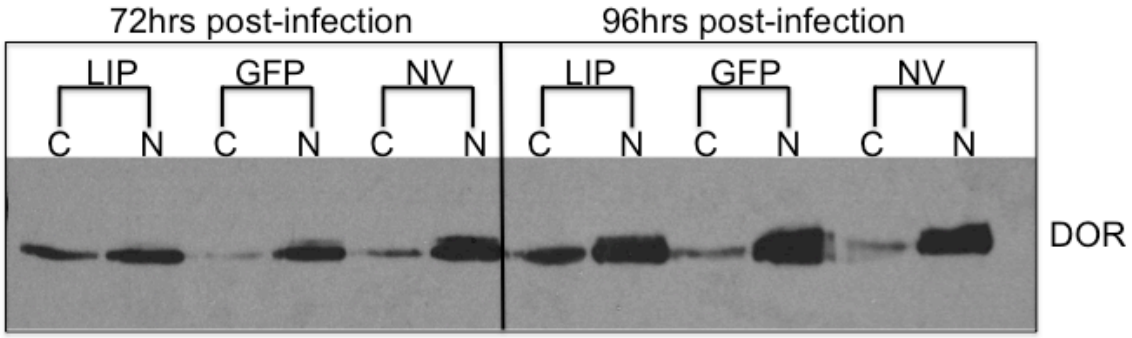

Figure 15. LIP-induced DOR nuclear to cytoplasmic translocation. Nuclear and cytoplasmic fractions were prepared from control uninfected LIP MDA-MB-468 cells, Ad-GFP MDA-MB-468 cells, and uninfected NV MDA-MB-468 cells at 72hrs and 96hrs post-infection and analyzed by 12% SDS-PAGE. Immunoblot analysis was performed with anti-DOR antibody. Equal amounts of total protein were loaded in each lane as determined by Ponceau S staining.

LIP expression leads to diabetes- and obesity related (DOR) protein translocation

The diabetes- and obesity- regulated protein (DOR), a nuclear cofactor of thyroid hormone receptors (THR), is expressed abundantly in metabolically active tissues (Baumgartner *et al*., 2007). Mauvezin *et al* recently reported a role for DOR in regulating autophagy. This work showed that DOR shuttles between the nucleus and the cytoplasm, depending on cellular stress conditions, and re-localizes to autophagosomes upon autophagy activation (Mauvezin *et al*., 2010). I examined DOR localization by immunoblot analysis (Figure 15). I was able to demonstrate elevated levels of DOR in the cytoplasm of LIP-expressing cells beginning at 72hrs post-infection, with a substantial increase at 96hrs post-infection. These results suggest that at least the stimulation of autophagy by LIP may involve alterations in DOR localization.

Discussion

The exact mechanisms controlling induction of autophagy in eukaryotic cells are not clearly understood but it appears that induction of autophagy involves both transcriptional and post-transcriptional steps. In this study, I set out to demonstrate a role for LIP in stimulating autophagy and inducing cell death in breast cancer cell lines. We had previously found that exogenous LIP expression is incompatible with MCF10A cell proliferation, since the initially LIP-expressing, GFP positive cells rapidly disappear from a mixed population of LIP-expressing and non-expressing cells (Bundy *et al*., 2005). Cell cycle profiling,

ultrastructural analysis, and caspase-3 immunoblot analysis performed here reveal that LIP expression did not lead to a cell cycle block and apoptotic cells are not observed (Figure 9, 10). I examined whether LIP expression leads to necrotic cell death and determined this is not the case (Figure 11). In contrast, ultrastructural analysis using electron microscopy showed a marked induction of autophagy in LIP-expressing cells with the accumulation of autophagic vesicles (Figure 12). The induction of autophagy was also confirmed by quantification of lysosomal induction as well as the analysis of endogenous LC3 by Western blotting and immunofluorescence (Figure 13 and 14). Finally, I was able to demonstrate that stimulation of autophagy by LIP leads to elevated levels of DOR in the cytoplasm (Figure 15). Overall, the data presented provide strong evidence that expression of the transcription factor, LIP, leads to the induction of autophagy and cell death.

C/EBP transcription factors are involved in a variety of physiological processes, such as metabolic regulation, cellular differentiation, and stress responses. The expression of the C/EBP beta gene has been shown to increase during endoplasmic reticulum (ER) stress. In recent years, emerging data indicate that ER stress is a strong inducer of autophagy (Høyer-Hansen M and Jäättelä, 2007). Interestingly, Li et al. describe increased LIP levels during the late phase of ER stress (Li *et al*., 2008). Recently, Meir et al. examined the distinct roles that LAP and LIP isoforms play in ER stress (Meir *et al*., 2010). They find that LIP augments ER stress-induced cell death in mouse B16 melanoma cells. In addition, LIP inhibited B16 melanoma tumor progression

(Meir *et al*., 2010). Although both of these studies did not examine any markers of autophagy, elevated LIP may be one way of linking ER stress and the induction of autophagy. It is interesting that LC3-II levels are highest at 4–5 days post-infection with Ad-LIP while the highest levels of LIP are present at 2–3 days post-infection. It is possible that LIP is repressing or downregulating genes whose products inhibit autophagy. Thus, the half-life of such proteins will determine the kinetics of when elevated LC3-II is observed.

As mentioned above, DOR was identified as a nuclear cofactor of thyroid hormone receptors (Baumgartner *et al*., 2007). It is well known that thyroid hormones (TH) influence various physiological processes including development, cell cycle progression, as well as maintaining metabolic homeostasis (Baumgartner *et al*., 2007). Using various cancer cell line models (e.g., breast, pancreas, thyroid), TH has been shown to induce proliferation (Glinskii *et al*., 2009; Verga Falzacappa *et al*., 2007; Lin *et al*., 2007; 2009;). Notably, DOR has been shown to enhance the transcriptional activity of thyroid hormone receptor alpha 1 TR (alpha1) (Baumgartner *et al*., 2007). Additionally, DOR was shown to regulate autophagy in mammalian cells by shuttling between the nucleus and the cytoplasm and localizing to autophagosomes upon autophagy activation (Mauvezin *et al*., 2010). Our studies show a substantial increase in cytoplasmic DOR protein levels in LIP-expressing cells (Figure 15). We know LIP localizes to the nucleus; therefore, one possible mechanism for autophagy stimulation by LIP expression may involve DOR displacement from the nucleus to the cytoplasm. Following LIP expression, DOR shuttles to the cytoplasm where it may interact

with autophagic proteins and regulate autophagosome formation. In addition, when DOR localizes to the cytoplasm it can no longer function as a THR cofactor and enhance THR transcriptional activity. This may result in a decrease in cell proliferation similar to what we observe upon LIP expression (Figures 6-8).

Our finding that LIP expression induces autophagy may help to resolve the paradox over whether LIP is pro- or anti- tumorigenic. This is because autophagy is generally thought to play dual roles in cancer development. For instance, allelic loss of beclin1, an essential autophagy gene, is found with high frequency in human ovarian, prostate, and breast cancers (Liang *et al*., 1999; Qu *et al*., 2003). BECN +/- mice develop spontaneous tumors including lymphomas, hepatocellular carcinomas, lung carcinomas, as well as precancerous lesions in the mouse mammary glands. In addition, autophagy-related 4C (Atg4C)-deficient mice have an increase in tumor incidence (Qu *et al*., 2003; Mariño *et al*., 2007). Also, tumor suppressor gene products such as p53, phosphatase and tensin homolog (PTEN), death-associated protein kinase-1 (DAPK) and tuberous sclerosis (TSC1/TSC2) exert a stimulatory effect on autophagy. Moreover, the products of common oncogenes, such as B cell lymphoma-2 (Bcl-2), class I phosphatidylinositol 3-kinase (PI3K), protein kinase B (PKB), and target of rapamycin (TOR) act as autophagy repressors. Autophagy plays an important role in sustaining organelle and protein quality control, working alongside with the ubiquitin degradation pathway to prevent the accumulation of polyubiquinated and aggregated proteins (Williams *et al*., 2006). By doing so, it limits the accumulation of genome damage and suppresses the mutation rate of

tumor cells in which the cell-cycle checkpoints have been inactivated (Mathew *et al*., 2007). Recent studies support that autophagy defends the cell in a bimodal fashion by directly eliminating invading pathogens and simultaneously assisting the immune system of the host organism to mount a specialized immune response against the invader by processing pathogenic antigens for presentation to T cells. These studies all provide a strong case for autophagy as a tumor suppressor. Yet at later stages of tumor development, studies have shown that this catabolic process may be a means by which tumor cells survive in response to metabolic stress and in hypoxic tumor regions, providing extra time for the recruitment of a blood supply via induction of angiogenesis and/or motility and invasion (Degenhardt *et al*., 2006). Thus, it is possible that some expression of LIP could promote cancer by increasing survival of certain cells under stress, explaining the slightly increased incidence (9%) of tumors observed in WAP-LIP transgenic mice (Zahnow *et al*., 2001).

Although it may be difficult to define the physiological role of LIP's ability to induce autophagy, further understanding of the mechanism(s) by which LIP expression stimulates autophagy and leads to cell death may provide new avenues for inducing this alternative death pathway, especially in tumor cells that are resistant to apoptosis.

CHAPTER III

C/EBPbeta3 (LIP) and cell engulfment

Introduction

There is little doubt that autophagy is a regulated cellular process of self-cannibalization through the lysosomal degradation pathway (Meijer and Codogno, 2004). There are, however, many questions regarding autophagy as a nonapoptotic cell death mechanism (Levine and Yuan, 2005). Does prolonged autophagy play a causal role in cell death or does autophagy merely accompany cell death induced by other causes? Numerous studies report the presence of autophagosomes as well as other autophagy markers in dying cells. Additional evidence comes from *in vitro* experiments where genetic or pharmacologic inhibition of autophagy prevented cell death. These and other studies have been the main force behind the idea that autophagy is a nonapoptotic form of programmed cell death.

Alternatively, many argue that autophagy is a cell survival defense mechanism that simply fails in its mission. Others argue that the autophagic pathway is simply a garbage disposal mechanism that cleans up remnants of a cell that is already committed to die. While there is evidence that autophagy can act as a cell death mechanism especially in cells whose apoptotic machinery is impaired, most agree that autophagy is actually a bystander that accompanies cell death.

In the previous chapter, I demonstrate a role for LIP in stimulating

autophagy in breast cancer cell lines. In addition, I show that exogenous expression of LIP leads to cell death in different breast cancer cell lines. Considering that autophagy may be only a bystander, we wanted to understand the mechanism(s) by which LIP overexpression causes cell death in breast cancer cells. In examining all the various cell death processes described in the literature to date, we came across the phenomenon of live cell engulfment or cell-in-cell structures (Overholtzer and Brugge, 2008). One of the most common and well-documented methods that results in the transient appearance of cell-in-cell structures is the engulfment of apoptotic cells by phagocytosis. Phagocytosis targets dying or dead cells for engulfment, and is propelled by cytoskeletal rearrangements of the engulfing cell in response to signals from the internalized cell (Overholtzer and Brugge, 2008). However, there are other processes that were introduced in Chapter 1, such as entosis, emperipolesis, and xeno-cannibalism that also lead to cell-in-cell structures. These other processes describe the formation of cell-in-cell structures via engulfment of another cell or through invasion of one cell into another. Notably, these processes are distinct from phagocytosis in that target cells are viable, with some cells even undergoing cell division, and some occasionally escaping from internalization altogether (Overholtzer *et al*., 2007). Nevertheless, the fate of most engulfed cells is cell death.

In this chapter, I show that autophagy appears to accompany or possibly follow the engulfment of neighboring cells by the LIP-expressing cells. In 2-3 days up to 30-40% of LIP-expressing MDA-MB-468 cells have engulfed live cells,

leading to extensive cell death. This study demonstrates that expression of a specific transcription factor can mediate cell engulfment.

Materials and Methods

Cell Culture and adenoviral constructs

The human breast cancer cell line MDA-MB-468 was obtained from the ATCC (Manassas, VA). MDA-MB-468 cells were maintained in Iscove's Modified Eagle media supplemented with 10% (v/v) FBS from HyClone Laboratories (Logan, UT, USA), 100 U/ml penicillin, 100 µg/ml streptomycin (Life Technologies, Inc., Carlsbad, CA), and 10 µg/ml bovine insulin. Cells were grown at 37°C in a humidified atmosphere containing 5% CO_2. The adenoviral constructs used in these experiments were discussed in the previous chapter. MDA-MB-468 cells were grown to subconfluency (60–70%) on 100mm dishes. Cells were either uninfected or adenovirally infected with Ad-GFP or Ad-LIP at a MOI: 5–10 for all experiments.

Cell cycle analysis

DNA cell cycle profiles of sub-confluent (60–70%) cultures were determined by flow cytometry using a BD FACScan (Becton Dickinson, San Jose, CA). Cultures were harvested at 72hrs post-infection by trypsinization and pelleting in the presence of 20% (v/v) FBS at 500 x g for 7 minutes. Cells were then counted using a hemocytometer. Approximately 2×10^6 cells were washed twice in cold PBS and fixed in ice-cold 70% ethanol overnight. The samples were pelleted at 500 x g for 7 minutes and washed twice with ice-cold PBS.

Lastly, the cells were incubated in a staining solution containing 2.5 mg/ml RnaseA, 2.0 mg/ml propidium iodide, 0.1% (v/v) Triton X-100, 1 μM EDTA in 1×PBS for 30–60 minutes at 4°C in the dark. Data were collected using BD Cellquest software (BD Biosciences Immunocytometry Systems, San Jose, CA), and cell cycle modeling was performed using Modfit software (Verity Software House, Topsham, ME). The cell cycle profile of each population was generated from DNA content data collected from between 20,000 to 30,000 separate events.

Cell Internalization Assays

MDA-MB-468 cells were grown to subconfluency (60–70%) on 100mm dishes. Cells were either uninfected or adenovirally infected with Ad-GFP or Ad-LIP. After 24hrs, the uninfected monolayer cultures were stained with fluorescent orange or violet CellTracker dyes (SKU# C2927 or C10094, Invitrogen, Grand Island, NY) for 1hr at 37°C in serum-free media. After 1hr, cells were replenished with normal growth media for 2-3 hrs. Stained cells were then washed three times with PBS and trypsinized to a single cell suspension in normal growth media. MDA-MB-468 Ad-GFP and Ad-LIP cells were also trypsinized to a single cell suspension and collected in normal growth media. Each population was counted with a hemocytometer and mixed in 1:3 (LIP or GFP: stained NV cells) ratio. Cells were either plated on 60mm dishes for FACS analysis or when acquiring images cells were plated on 35mm dishes fitted with collagen-coated glass coverslips (MatTek Corp, Ashland, MA, USA). In some cases, Hoechst 33342 (Sigma-Aldrich Co., St. Louis, MO) was used to stain DNA. Images

presented in Figure 17 were acquired using a Leica DM IRB inverted microscope equipped with a Nikon DXM1200C camera and Metamorph software.

Electron microscopy

Control uninfected, Ad-GFP, and Ad-LIP MDA-MB-468 cells were fixed at 48 and 72hrs post-infection with a solution containing 2.5% (v/v) glutaraldehyde in 0.1 M cacodylate buffer (pH 7.3) for 1hr at room temperature. Samples were then refrigerated overnight. Postfix, staining, sectioning, and TEM were performed as described above. Representative areas were chosen for thin sectioning and viewed with an electron microscope (Philips CM-12 transmission electron microscope).

Quantitative cell engulfment assay using flow cytometry

In these assays, cells were stained and mixed in a ratio of 1:3 as described above. At 24-48hrs post-mixing, cells were trypsinized and collected in phenol-red free Iscove's media. Cells were collected for flow cytometry analysis using a 3-laser FACSCanto II instrument, (Becton-Dickinson, San Jose, CA) equipped with standard 5-2-2 filter configuration. FACSDiVa Software was used for data acquisition and analysis. Inhibition of Rho-associated protein kinase (ROCK) was performed with 20-40μM of Y-27632 (EMD, Calbiochem, product number 688000) for 36-48hrs post-mix until cell populations were prepared for FACS analysis.

Phospatidylserine exposure

Control uninfected MDA-MB-468 cells and Ad-GFP or Ad-LIP infected cells were washed twice with cold PBS and then resuspended in 1X Binding Buffer at a concentration of ~1 x 10^6 cells/ml. Initially, 10X Binding Buffer was prepared which consists of 0.1 M HEPES, pH 7.4; 1.4 M NaCl; 25 mM CaCl 2; it was diluted to 1X for the experiments. Briefly, 100 µl of the solution (~1 x 105 cells) was transferred to a 5 ml culture tube. Cells were stained with Annexin V (Molecular Probes, Life Technologies, Grand Island, NY) and/or the vital dye, 7-aminoactinomycin D (7-AAD). MDA-MB-468 cells treated with 10 µmol/L cisplatin (Sigma-Aldrich, St. Louis, MO) were used as a positive control. Tubes were mixed and incubated for 15 minutes at room temperature in the dark. An additional 400 µl of 1X Binding Buffer was added to each tube following staining procedure. Samples were analyzed by flow cytometry.

Transfections

2 x 10^5 MDA-MB-468 cells were plated in 35mm dishes fitted with collagen-coated glass coverslips (MatTek Corp, Ashland, MA, USA) and transfected in complete Iscove's growth medium with *Trans*IT-LT1 transfection reagent (Mirus Bio LLC, Madison, WI) using 5µg of pLZRS-IRES-GFP DNA or 4µg pLZRS-IRES-GFP DNA and 1µg of pcDNA3.1hisLIP at a 1:1 ratio of *Trans*IT-LT1 reagent:DNA according to manufacturer's instructions. Cells were imaged at 4 or 6 days post-transfection.

Indirect immunostaining and image acquisition

Transfected cells were prepared for immunofluorescence studies as described in the previous chapter. Briefly, MDA-MB-468 cell cultures were washed three times in PBS, fixed in 3.7% (v/v) formalin in PBS for 30 min at room temperature, washed an additional three times, and processed for indirect immunofluorescence. Cells were permeabilized in PBS containing 0.1% (v/v) Triton X-100 for 20 minutes at room temperature. The cells were washed and nonspecific binding sites were blocked in PBS containing 5% (w/v) BSA (Fraction V, Sigma) at 4°C for 24 hrs. Immediately following aspiration of the blocking solution, the cells were incubated with beta-catenin polyclonal antibody (Sigma, C2206) at a dilution of 1:1,000 in PBS containing 2% (w/v) BSA and 0.1% (v/v) Triton X-100 for 2hrs at room temperature. The cells were washed as described above. Cells were then incubated for an additional hour at room temperature in the dark with fluorescent-conjugated Alexa 594 goat-anti-rabbit secondary antibody diluted to a final concentration of 2 μg/ml in PBS containing 2% (w/v) BSA and 0.1% (v/v) Triton X-100. The cells were then washed three times in PBS containing 0.1% (v/v) Triton X-100 and a few final rinses with double-distilled water. The DNA stain, Hoechst 33342 (Sigma-Aldrich Co., St. Louis, MO), was used to label the nucleus. Images were acquired with an Eclipse TE2000-E wide-field fluorescent microscope (Nikon) equipped with a 60x, 1.4NA, oil immersion lens and a cooled charge-coupled device (CCD) camera by the use of Metamorph software.

Time-Lapse Microscopy

Cells were mixed and plated on coverglass bottom dishes (MatTek, Ashland, MA) as described above. At 36hrs post-mix images were acquired automatically at multiple locations on the coverslip using a Zeiss LSM 510 inverted confocal microscope fitted with a 20x objective. The microscope was housed in a custom-designed 37°C chamber with a secondary internal chamber that delivered humidified 5% CO_2. For Supplemental movies 1 and 2, fluorescence images were obtained every 4 minutes for a period of 12-14hrs using Zeiss image processing software (LSM 5; Carl Zeiss). Imaging conditions did not adversely affect cell proliferation or viability. Supplemental movies 3 and 4 were imaged using an Olympus BX61WI upright microscope fitted with a 40x objective. The microscope was housed in a custom-designed 37°C chamber and Volocity (Perkin Elmer) software was used for image acquisition.

Confocal Microscopy

To confirm if target cells were completely internalized by host LIP-expressing cells, cells were imaged using a confocal laser-scanning microscope (model LSM 510; Carl Zeiss, Inc.), using a 63x objective. Optical section series were collected with a spacing of 0.4 μm in the z-axis through ~3-μm thickness of the cell-in-cell complex. The images from triple labeling were simultaneously collected using a dichroic filter set with Zeiss image processing software (LSM 5; Carl Zeiss). Digital data were exported into Adobe Photoshop for presentation and as quick-time movie.

Immunoblot analysis of mouse mammary glands

Mouse mammary gland samples were generously provided by Dr. Fiona Yull's laboratory. Mouse mammary glands were isolated and prepared as previously described (Connelly et al., 2007). Relative protein concentrations were determined using Protein Assay Reagent (BioRad Laboratories, Hercules, CA, USA) as per manufacturer's instructions. Equal amounts of protein were loaded onto a 10% SDS-PAGE gel and immunoblot analysis was performed with an anti-C/EBPbeta antibody (cat. # sc-150, Santa Cruz, CA) as described above.

Statistical analysis

Quantitative data are expressed as means. For comparisons between two groups paired t-test and Wilcoxon matched pairs test was used. In order to compare multiple groups, ANOVA followed by the Student-Newman-Keuls multiple comparisons test was used. Prism 5.0 (GraphPad, La Jolla, CA) was used for all analyses.

Results

Cell disintegration following exogenous expression of LIP

In the previous chapter I present a role for LIP in stimulating autophagy and causing cell death in breast cancer cell lines. I evaluated the role of LIP overexpression in proliferation, necrosis, and LC3 protein turnover of MDA-MB-468 cells in particular. Exogenous expression of LIP in MDA-MB-468 cells leads to attenuation of cell proliferation as determined by cell proliferation assays. Colony formation assays show a dramatic reduction in colonies formed

by LIP-expressing MDA-MB-468 cells. This suggests overexpression of LIP causes cell death. In order to further characterize the mechanism of cell death due to LIP overexpression, I used an adenoviral vector, Ad-LIP, to transduce the breast cancer cell line, MDA-MB-468, as previously described. Photomicrograph of MDA-MB-468 cells in culture 3 days post-infection are shown in Figure 16. Images were taken at the same time point for all control Ad-GFP and Ad-LIP cells. A representative image of the control Ad-GFP MDA-MB-468 cells is shown in Figure 16, panel a. The remaining panels (b-i) capture the heterogeneity we observe among Ad-LIP infected cells. Some cells appear intact (Figure 16, panel b), while others appear very vacuolated (Figure 16, panel c). In addition, we observe a high percent of LIP-expressing cells breaking down into a number of smaller vesicles (Figure 16, panels d-i). Some of the vesicles appear to be held together by a network of fibers (Figure 16, panel f, g). These LIP-expressing cells will continue to disintegrate until eventually there is only cell debris in the culture medium.

DNA content of LIP-expressing MDA-MB-468 cells

We had observed that the extent of cell death was most severe in the MDA-MB-468 breast cancer cell line in comparison to other breast cancer cell lines tested. To assess whether the dying cells were undergoing apoptosis I performed cell cycle profiling on the MDA-MB-468 cells expressing LIP. A sub-G_1 phase characteristic of apoptotic cell death was not detected; even though I show in Figure 16 that cells are disintegrating and there is a clear breakdown into vesicles. Instead, we were surprised to find that LIP-expressing cells (Figure

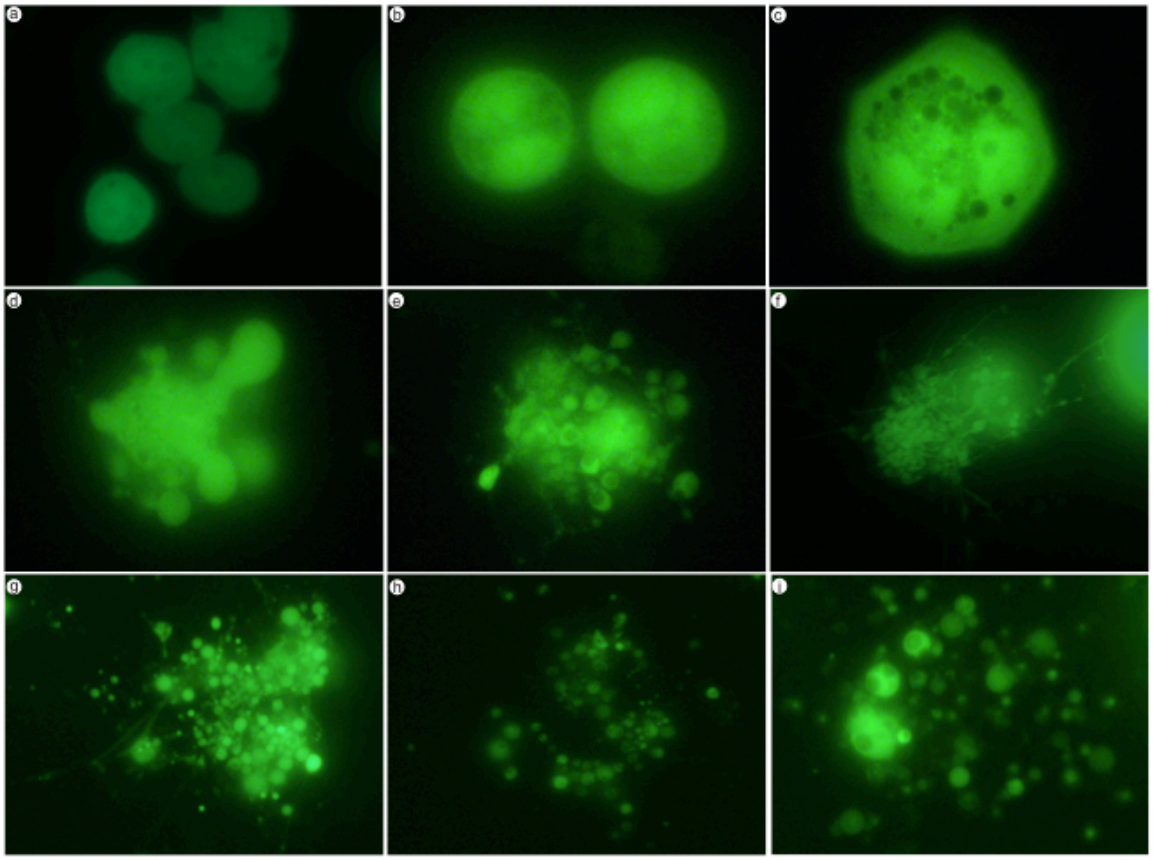

Figure 16. Cell disintegration following exogenous expression of LIP. Microscopic examination of cell breakdown. Equal numbers of MDA-MB-468 cells were plated for adenoviral infection with either control Ad-GFP or Ad-LIP. Representative fluorescent photomicrographs of cells imaged at 72hrs post-infection are shown. Panel a represents Ad-GFP MDA-MB-468 cells. Panels b-i represent Ad-LIP MDA-MB-468 cells.

17A panel c) have a significantly greater DNA content than the control uninfected and Ad-GFP MDA-MB-468 cells (Figure 17A panel a and b, respectively). Significant portions (>40%) of the LIP-expressing MDA-MB-468 cells have more than 2n DNA content at 72hrs post-infection (Figure 17B).

LIP-expressing MDA-MB-468 cells engulf neighboring cells

Over several days of examining LIP-expressing cells via microscopy, we noticed cells that appeared to be multinucleated as well as cells residing in large vacuoles. Taking this data together with the increase in DNA content, we reasoned it was possible for LIP overexpression to stimulate engulfment of neighboring cells. To further investigate this possibility, I took GFP positive LIP-expressing MDA-MB-468 cells and mixed them with a population of control uninfected MDA-MB-468 cells that were labeled with fluorescent CellTracker orange dye. After mixing the populations in a 1:3 ratio, cells were plated and observed for 24-48hrs. Engulfment of neighboring cells was evident beginning at 36hrs post-mixing. I acquired fluorescent images of LIP-expressing cells (green) that had engulfed anywhere from one to three orange-labeled cells (Figure 18). DNA staining shows the appearance of multinucleated cells. Similar experiments were performed with control Ad-GFP MDA-MB-468 cells and this engulfment process was rare and occurred at a very low frequency.

To study engulfment in real time, GFP positive LIP-expressing MDA-MB-468 cells mixed with uninfected CellTracker-labeled MDA-MB-468 cells were analyzed by time-lapse microscopy over a 6 to 14hr period. In work published by Overholtzer et al. they describe the entosis process to involve the active invasion

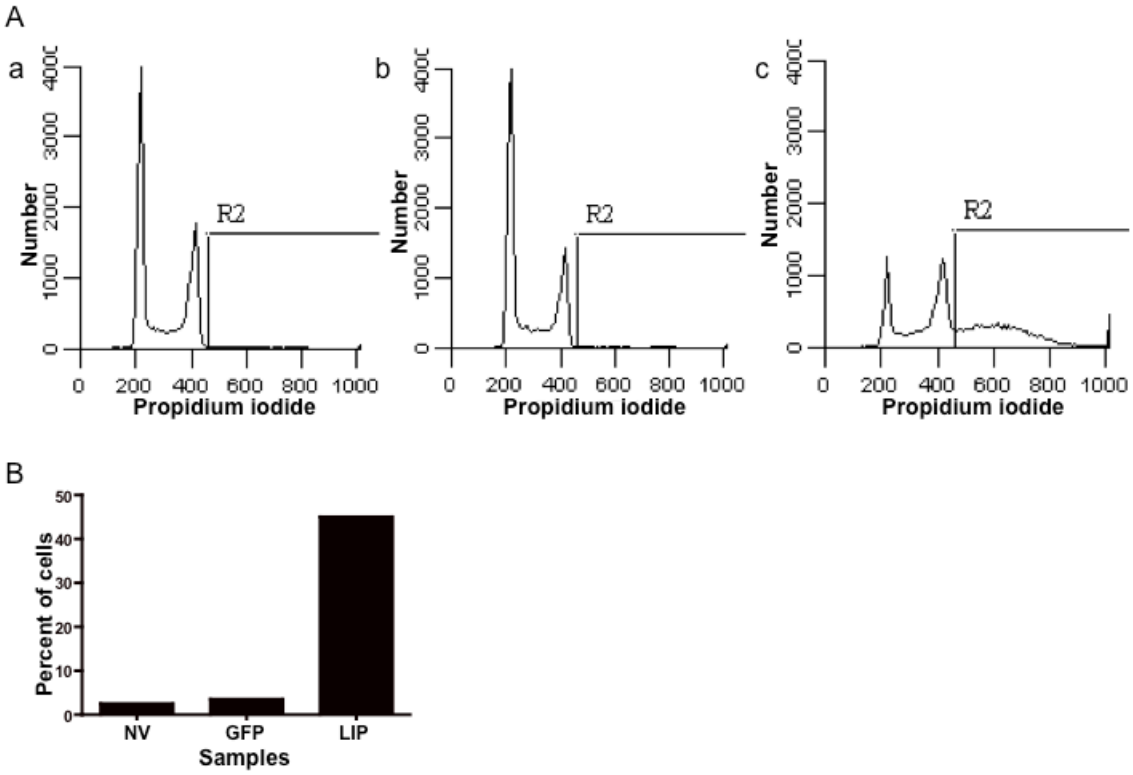

Figure 17. DNA content of LIP-expressing MDA-MB-468 cells. **A**, Representative cell cycle profiles of control uninfected: no virus (NV) (panel a), Ad-GFP (panel b), and Ad-LIP (panel c) MDA-MB-468 cells are shown. The experiment was performed at least two separate times. **B**, Quantification of the percent of cells with greater than 2n DNA content as measured by the area marked as R2 in the graphs is presented.

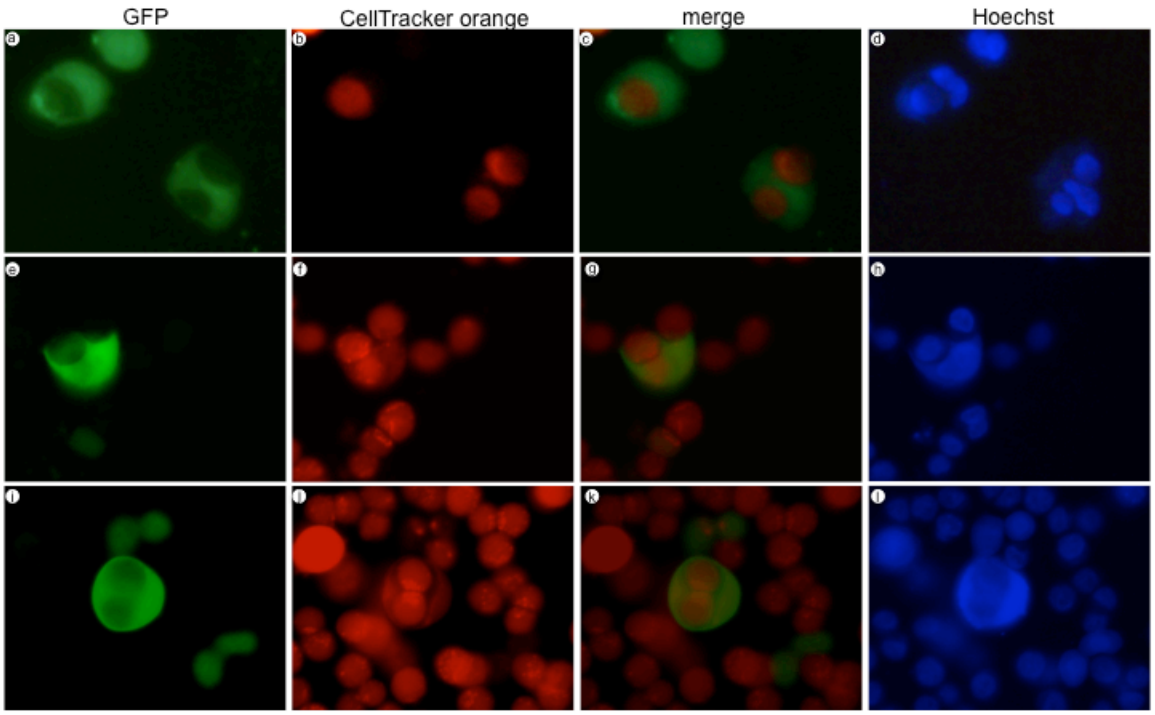

Figure 18. LIP-expressing MDA-MB-468 cells engulf neighboring cells.
GFP positive LIP-expressing MDA-MB-468 cells were mixed with uninfected CellTracker orange labeled MDA-MB-468 cells. Hoechst dye was used to stain DNA. Cells were imaged at 36-48hrs post-mix.

of one cell into another (Overholtzer *et al*., 2007). As presented in movie 1, we see the GFP positive LIP-expressing MDA-MB-468 cell extending its cell membrane and wrapping around the orange-labeled cell. These cells seem to battle for quite some time, with the orange cell trying to come out of the GFP positive LIP-expressing cell. However, the orange cell is not able to escape, at least within the time course of this movie (approximately 12hrs). In movie 2, there are a few green cells in the field that have orange-labeled cells inside. The GFP positive LIP-expressing cells are very active making contacts with neighboring cells and forming smaller vesicle-like structures. During this process, a group of GFP positive LIP-expressing cells come into view that have internalized orange-labeled cells. After some time, one of these cells begins to disintegrate into smaller vesicles until it eventually fades from the field. Interestingly, we were also able to capture a GFP positive LIP-expressing cell releasing an internalized orange-labeled cell. This is clearly seen in movie 3 as the GFP positive LIP-expressing cell opens and the orange-labeled cell escapes or is expelled. It is difficult to conclude the fate of both of these cells, because they appear to detach and disappear from the plane of focus. In movie 4, the GFP positive LIP-expressing cell clearly has engulfed more than one orange-labeled cell. One of the labeled cells is able to escape; however after the LIP-expressing cell rearranges, we see the LIP-expressing cell begin to breakdown and take the innermost-labeled cell with it. Both appear to disintegrate and again detach from the plane of focus.

It should be noted that GFP positive LIP-expressing cells will also engulf

other GFP positive LIP-expressing cells as well. While we focus on the green cells engulfing the orange-labeled cells, this is not meant to imply that there is any preference for engulfing labeled orange cells; it is just easier to observe this photographically. Interestingly, we have not observed any GFP positive LIP-expressing cells inside of control uninfected orange-labeled cells. The GFP positive LIP-expressing cells do not invade the orange-labeled cells, as would be expected if the LIP-expressing cells were undergoing entosis.

Ultrastructure analysis of LIP-mediated cell engulfment

To gain further confirmation of cell engulfment, TEM analysis was performed at 48 and 72hrs post-infection of MDA-MB-468 cells with Ad-LIP. At 48hrs we detect LIP-expressing cells extending their membranes and wrapping around the edges of neighboring cells (Figure 19 panels a-c). These engulfing intermediate cells appear to be vacuolated and forming cell contacts with the neighboring cells. It is unclear whether adherens junctions are being formed; yet fibers and secreted basement membrane can be detected (Figure 19 panels 1-2). Remarkably, the engulfing cell's nucleus begins to change into a more crescent-like shape, characteristic of cannibalistic cells (Sharma and Dey, 2011). Figure 19 panels d and e are examples of LIP-expressing cells that present with immense vacuoles. A captured cell that was able to escape may have previously occupied these large vacuoles, possibly leaving traces behind, or they could represent intake of extracellular fluid. In Figure 19 panels f-h, it is evident that a target cell has been internalized and resides in the large vacuole of the host cell. In these images we are able to detect more than one nucleus (Figure 19 panel f).

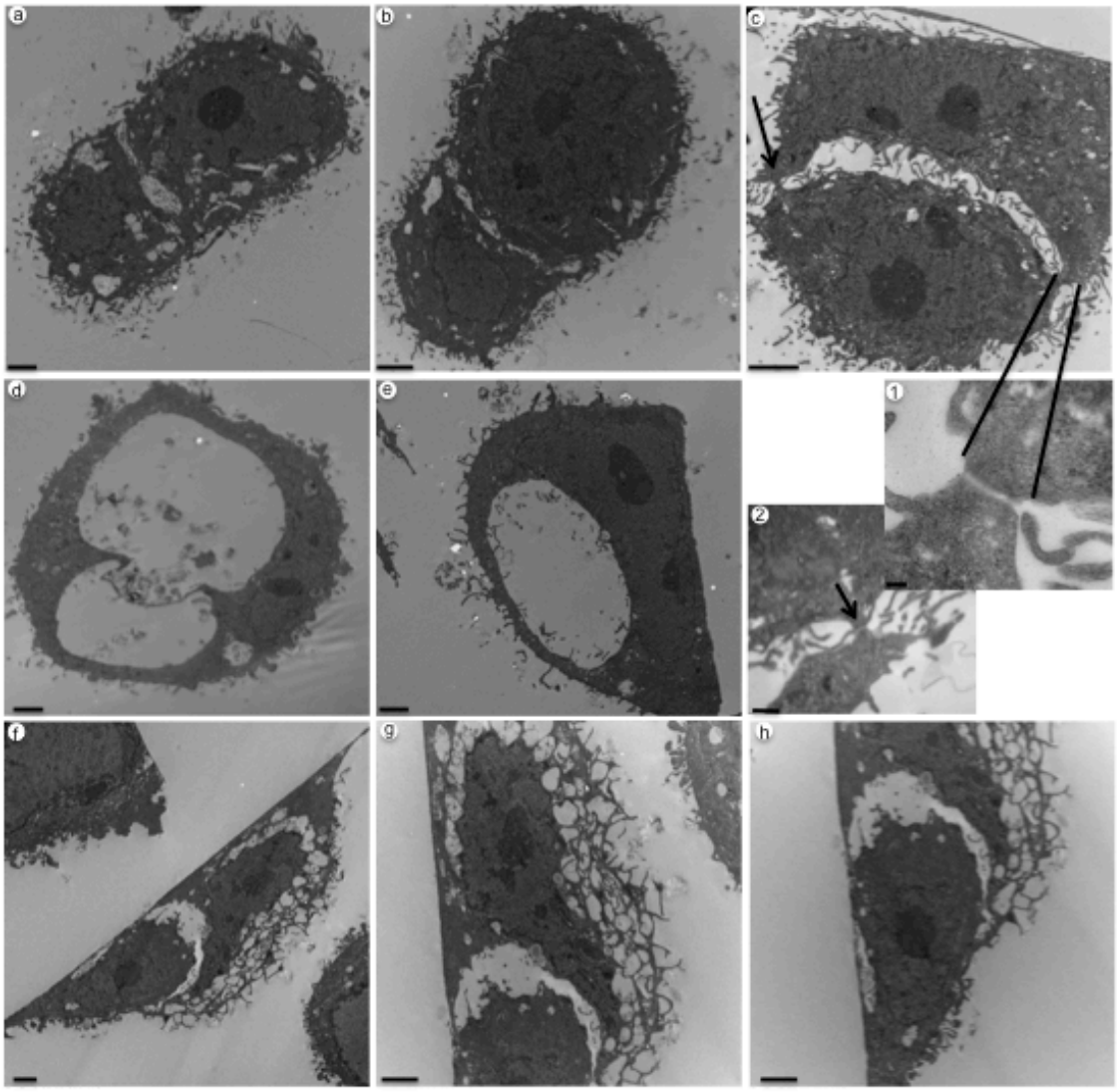

Figure 19. Ultrastructure analysis of LIP-mediated cell engulfment in MDA-MB-468 cells. Panels a-c, ultrastructure of engulfing intermediates at 48hrs post-infection; scale bar is 2μm. 1 and 2 indicate higher magnification of cell contacts present in panel c. Arrows indicate formation of cell contacts. Scale bar is 100nm and 500nm for panel 1 and 2, respectively. Panels d and e show LIP-expressing cells that have enormous vacuoles; scale bar is 2μm. Panels f-h illustrate an internalized cell at 72hrs post-infection; scale bar is 2μm. Panel g is a higher magnification to show the nucleus of engulfing (host) cell and the various projections typical of actively phagocytic cells. Panel h depicts the engulfed cell inside of the vacuole of the host cell.

Figure 19 panels g and h are magnified images that show the nuclei of both cells remain intact and the various projections typical of actively phagocytic cells. We had previously shown that LIP could stimulate autophagy in these cells. Therefore, it is reasonable to see the presence of highly vacuolated cells as those seen in Figure 19 panels d-h. Taken together, these images provide strong evidence that LIP expression leads to the engulfment of neighboring cells in the MDA-MB-468 breast cancer cell line.

Quantitation of LIP-mediated cell engulfment

In order to acquire quantitative data on the engulfment process, I employed FACS analysis. In these experiments, GFP positive LIP-expressing cells were mixed in a 1:3 ratio with control uninfected CellTracker-labeled cells. 24-48hrs post-mix cells were collected and analyzed by flow cytometry. We monitored green cells that were also positive for orange label. This population represents the LIP-expressing cells that have engulfed orange-labeled cells. As mentioned above, green LIP-expressing cells also engulf other green cells. However, by mixing the green cells with an excess of orange cells in a 1:3 ratio, it is more likely that a green cell will encounter an orange cell to engulf rather than another green cell. Nonetheless, the percent of LIP-expressing cells positive for orange label still underrepresents the number of LIP-expressing cells engaged in engulfing other cells. We detected a small percent (6%) of cell engulfment at 24hrs post-infection. However, as presented in Figure 20A panel a, nearly 25% of the Ad-LIP MDA-MB-468 cells engulf orange-labeled cells at 48hrs post-

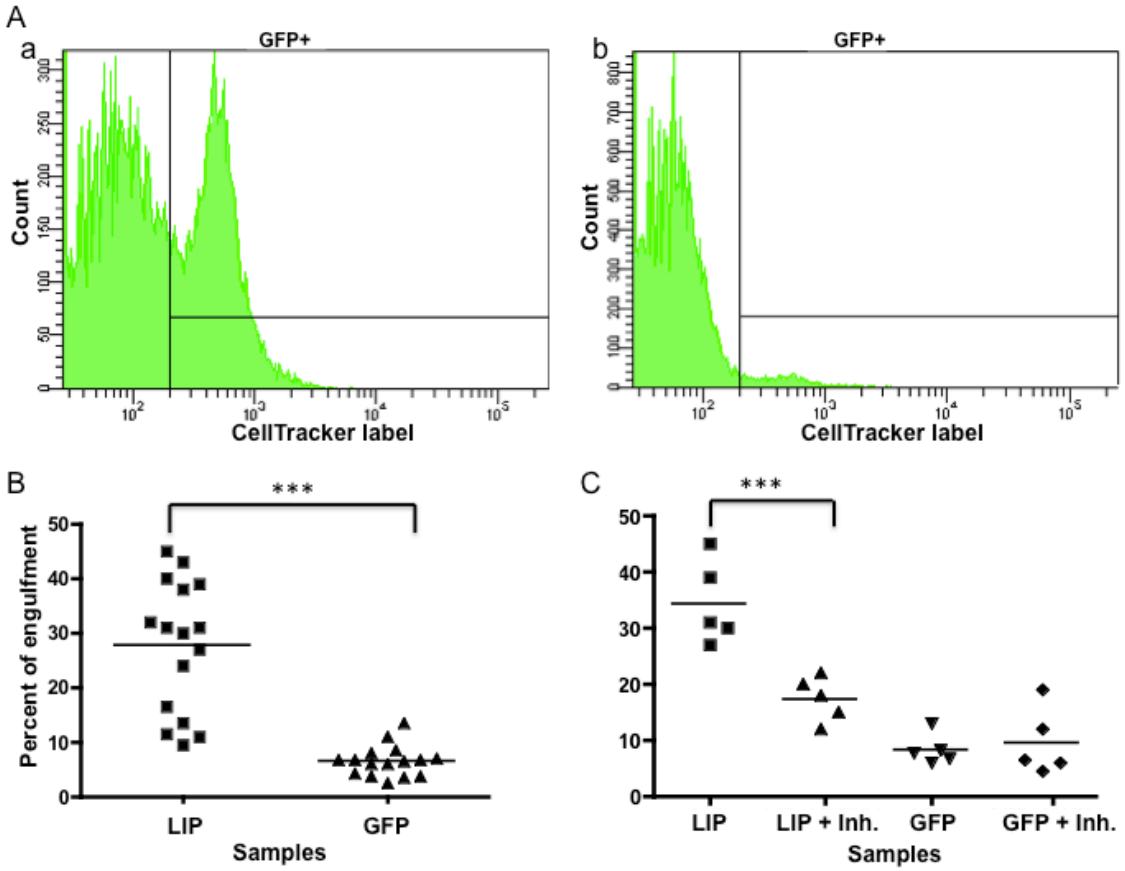

Figure 20. Quantification of LIP-mediated cell engulfment. A, Panel a shows the percent of Ad-LIP MDA-MB-468 cells that are double positive for GFP and CellTracker label. Panel b shows the percent of control Ad-GFP MDA-MB-468 cells that are double positive for GFP and CellTracker label. **B**, Quantification of the percent of GFP positive cells that have engulfed uninfected CellTracker labeled cells. Results are shown for 16 different experiments with a p-value of <0.0001 using paired t-test and Wilcoxon matched pairs test for statistical analysis. **C**, Quantification of the percent of GFP positive cells that have engulfed uninfected CellTracker labeled cells after treatment with 40μM of the ROCK inhibitor, Y-27632. Results are shown for 5 different experiments with a p-value of <0.0001 using ANOVA followed by the Student-Newman-Keuls multiple comparisons test.

mixing. Meanwhile, only a meager 1.8% of the control AD-GFP MDA-MB-468 cells engulf an orange-labeled cell (Figure 20A panel b). These experiments were repeated 16 different times and found on average 30% of the LIP-expressing cells engulf CellTracker-labeled cells (Figure 20B). This is significant relative to control GFP only cells with a p-value of <0.0001.

LIP-mediated cell engulfment requires Rho

Because the time-lapse photography of LIP-mediated cell engulfment shows considerable changes in the actin cytoskeleton occurring, I examined whether Rho signaling, which is a critical regulator of actin, plays a role in the engulfment process. Rho-associated protein kinase (ROCK) proteins, the downstream effectors of Rho GTPases, were inhibited with Y-27632. ROCK inhibition resulted in a significant decrease (p-value: <0.0001) of LIP-mediated cell engulfment as determined by quanititative FACS analysis of green LIP-expressing cells containing CellTracker-labeled cells (Figure 20C). The Rho-ROCK-actin pathway was previously found to be an important regulator during entosis (Overholtzer *et al*., 2007).

LIP does not appear to stimulate the "eat me" signal

As described in chapter 1 of this document, phospatidylserine translocation from the inner to outer leaflet of the plasma membrane is referred to as an "eat me" signal. PtdSer exposure marks the cell for recognition and engulfment by neighboring cells or macrophages. Since we observe LIP-expressing cells engulfing neighboring cells, we wanted to test whether expression of LIP in the MDA-MB-468 cells leads to an increase in PtdSer

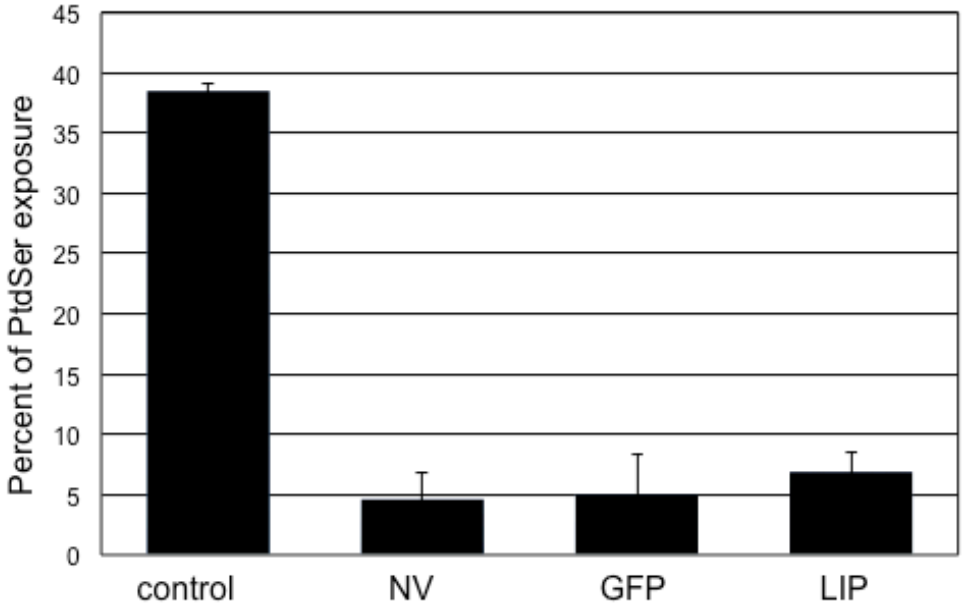

Figure 21. LIP does not appear to stimulate PtdSer exposure in MDA-MB-468 cells. Control MDA-MB-468 cells treated with cisplatin to induce apoptosis. MDA-MB-468 cells infected and collected and stained with Annexin V. Cell populations were analyzed by flow cytometry. Experiments were performed at 72hrs post-infection.

exposure. In comparison to the control cisplatin treated cells that show a high percentage of cells positive for Annexin V staining, PtdSer exposure of LIP-expressing cells does not increase at the 72hrs post-infection time point (Figure 21). This time point was chosen since it is when we detect changes in DNA content (Figure 17) as well as detect the highest percent of cell engulfment (Figure 20B). LIP-expression does not appear to stimulate “eat me” signals in comparison to the uninfected and Ad-GFP MDA-MB-468 cells.

LIP-mediated cell engulfment is not dependent on adenoviral infection

To address concerns regarding whether adenoviral infection is required for LIP-mediated cell engulfment, we transfected MDA-MB-468 cells with expression vectors for GFP and LIP, or GFP alone. Cells were observed via fluorescent microscopy beginning 48hrs after transfection. Although the transfection efficiency was low (approximately 5-10%), we were still able to monitor GFP positive cells. At days 4-6 post-transfection, cells were fixed and stained for beta-catenin (to better delineate cell boundaries) and nuclear DNA. Similar to our adenoviral studies, we were able to capture engulfing intermediates (Figure 22, panel a) and LIP-expressing cells that have engulfed anywhere from one to three neighboring cells (Figure 22, panels b-e). In addition, we observed LIP-expressing cells that had broken down into vesicles (Figure 22, panel f). Next, I imaged the engulfed cells using confocal microscopy in order to confirm that the LIP-expressing host cell had engulfed its neighboring target cell. Figure 23 depicts a series of images (z-stack) taken of a LIP-expressing cell that has a target cell within (also see movie 5). These studies corroborate the fact that it is

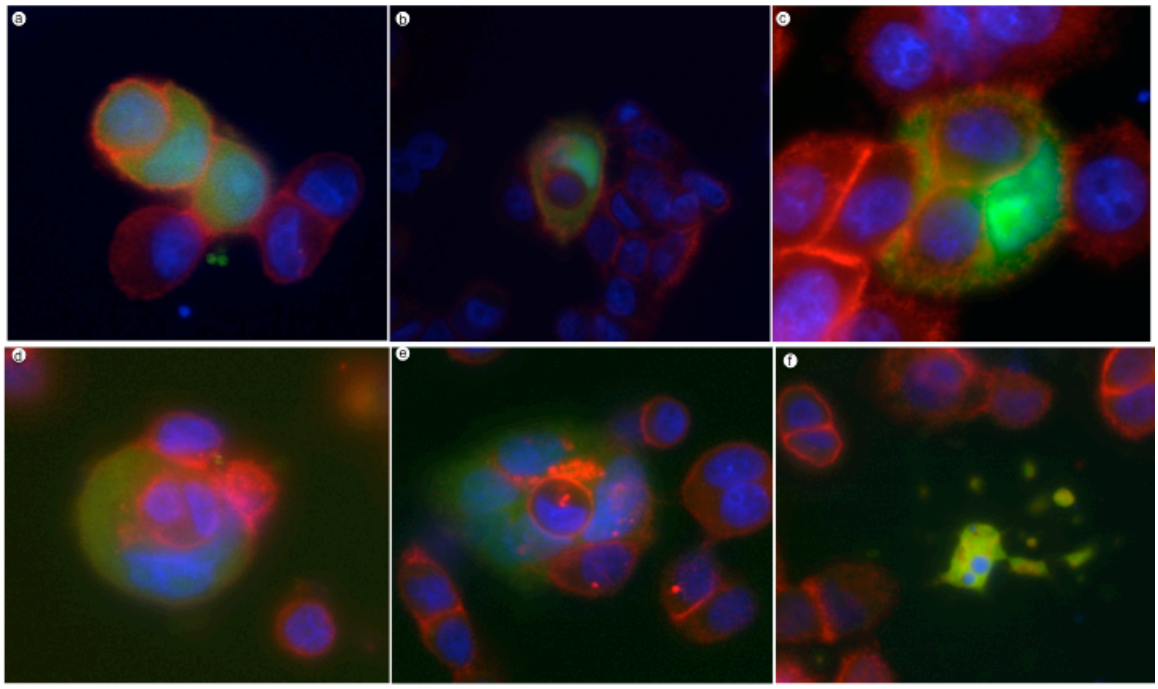

Figure 22. LIP-mediated cell engulfment is not dependent on adenoviral infection. MDA-MB-468 cells transfected with LIP and GFP expression vectors were stained with beta-catenin and Hoechst. Cells were imaged 4-6 days post-transfection.

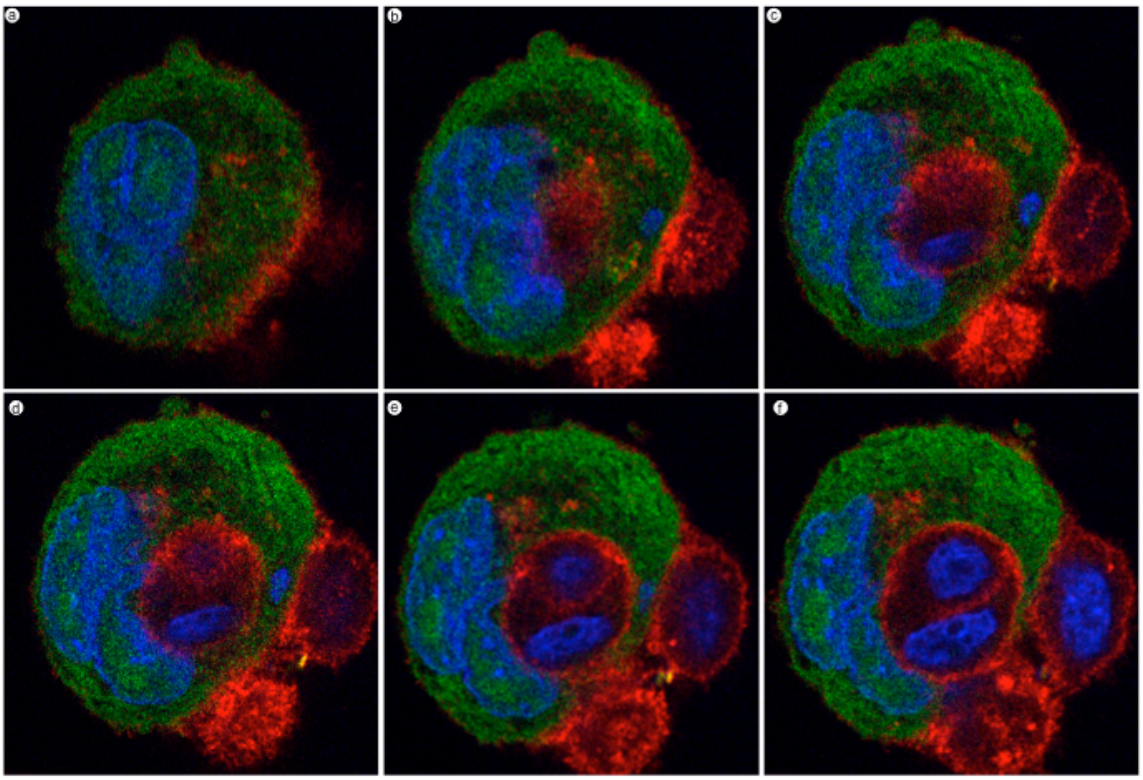

Figure 23. LIP engulfment of neighboring cells via confocal microscopy. LIP-expressing cells stained with beta-catenin and Hoechst DNA stain were imaged using confocal microscopy. Images represent a series of Z-stacks.

the overexpression of LIP that leads to this cell engulfment phenomena and not a side effect of using an adenoviral system to overexpress LIP.

LIP may play a physiological role during involution of the mammary gland.

Despite having few clues for the mechanism underlying LIP's ability to stimulate cell engulfment, we are nonetheless interested in considering possible physiological roles for this activity. C/EBPbeta is a well-established regulator of mammary gland development during puberty, pregnancy and involution (Grimm and Rosen, 2003). Involution of the mammary gland post-lactation is a physiological event that involves extensive cell death of the secretory epithelium (Monks *et al*., 2008). Studies have shown that neighboring mammary epithelial cells (MECs) can clear dying MECs in a process termed efferocytosis (Monks *et al*., 2008). In addition to apoptotic death, lysosomal pathways of cell death or autophagy have been implicated to occur during involution (Zarzynska and Motyl, 2008). Combining our observations that overexpression of LIP induces autophagy and leads to cell death with our observations that LIP overexpression leads to the engulfment of neighboring cells, we considered whether LIP may play a role in involution.

Mouse mammary glands were removed at various time points including pregnancy, early lactation, full lactation, early involution and late involution. Immunoblot analysis was carried out using a C/EBPbeta antibody that recognizes all three C/EBPbeta isoforms. As shown in Figure 24, we see a dramatic increase in LIP expression in the involuting mouse mammary glands at day 1 post-weaning in all three samples (lanes 5-7) isolated from separate mice.

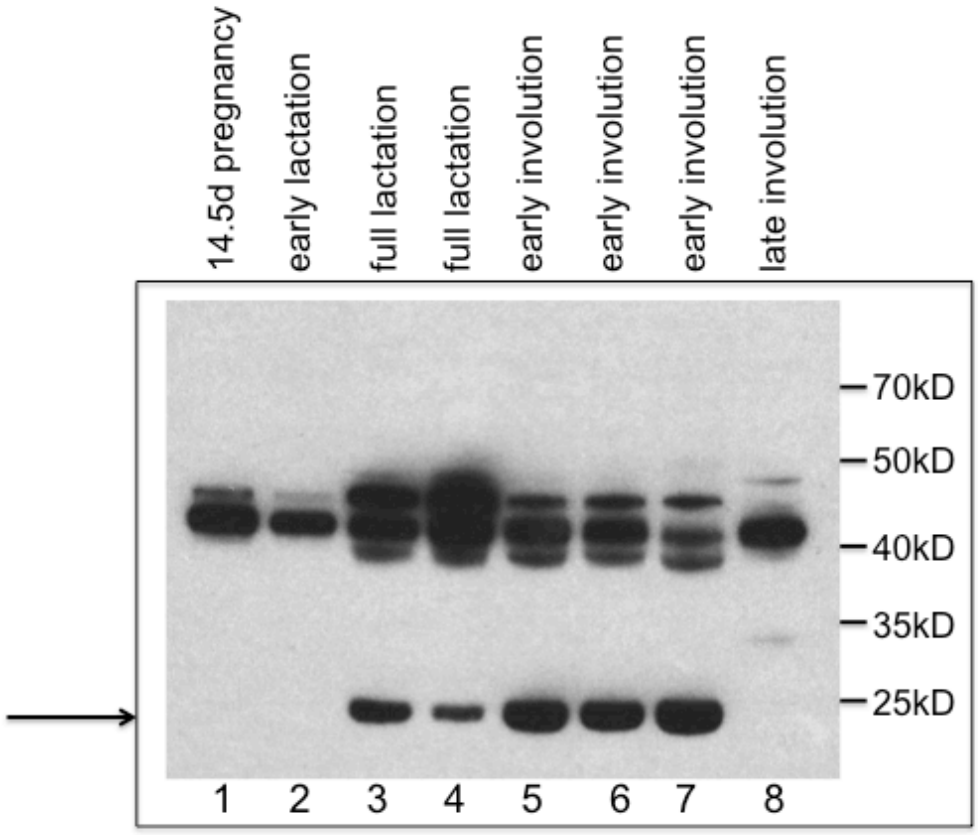

Figure 24. LIP expression in mouse mammary glands. Samples were analyzed by 10% SDS-PAGE. Immunoblot analysis was performed with an anti-C/EBPbeta antibody. Equal amounts of total protein were loaded in each lane as determined by Ponceau S staining. Lane 1, 14.5d pregnancy; Lane 2, early lactation; Lanes 3 and 4, full lactation; Lanes 5-7, early involution (day 1 post-wean); Lane 8, late involution (day 5 post-wean).

Interestingly, we do not detect LIP at late involution (day 5 post-weaning). LIP is not present in the samples from late pregnancy or early lactation, but is detectable during full lactation. Secretory cells are continually replenished during full lactation so there is likely to be some cell death during this period. Hence, LIP may play a role in the removal of these dying secretory epithelial cells. In any case, this preliminary data shows that LIP is elevated during early involution and suggests LIP may play a physiological role during mammary gland involution.

Discussion

In this chapter, I present data demonstrating exogenous expression of LIP in the human breast cancer epithelial cell line, MDA-MB-468, leads to the engulfment of neighboring epithelial cells. Cell cycle profiling studies show LIP-expressing cells have a dramatic increase in cells with more than 2n DNA content. In these studies, I was able to confirm that the increase in DNA content is due to the engulfment of neighboring cells by using fluorescent CellTracker dyes to monitor this cannibalistic process. Using a quantitative method to monitor cell engulfment, I was able to demonstrate on average approximately 30% of LIP-expressing cells have engulfed a target cell. Engulfment was significantly diminished upon treating with a ROCK inhibitor. LIP-mediated engulfment does not appear to depend on PtdSer exposure. When we performed ultrastructure analysis of LIP-expressing cells by TEM, we observe various engulfing intermediates as well as target cells that have been internalized

by LIP-expressing host cells. Cell engulfment was observed whether or not adenovirus was employed to overexpress LIP. Remarkably, I was able to show an increase in LIP protein levels in the early stages of involution of mouse mammary glands.

When we compare our findings to those published documenting entosis there are some similarities and major differences. Unlike the entosis process, which is described as a cell death mechanism that occurs due to loss of attachment to ECM, our studies were performed with matrix-attached cells. In our studies, we observe LIP cells engulfing the target cells and not an invasion process as described in entosis. Importantly, Overholtzer et al. examined a panel of human cell lines including the MDA-MB-468 human breast cancer cell line for possible entosis. Interestingly, they report that 0% of these cells underwent the entosis process (Overholtzer *et al*., 2007). However, similar to entosis, LIP expression leads to a nonapoptotic cell death process, live cells are engulfed, and this LIP mediated cannibalistic process requires ROCK activity.

Although our studies examined the response to exogenous LIP overexpression, the C/EBPbeta isoform, LIP, is elevated in a variety of processes such as endoplasmic reticulum (ER) stress and oncogenic signalling. As discussed in Chapter 2, increased LIP levels have been reported during the late phase of ER stress and this increase in LIP protein level is due to both increased synthesis as well as increased stability of the protein (Li *et al*., 2008). Also, ER stress induced by the proteasome inhibitor MG132 was shown to transiently increase C/EBPbeta mRNA levels and notably increased LIP protein levels

(Nakajima *et al*., 2011). Whether elevated LIP levels during ER stress could result in cell engulfment has yet to be determined.

Interestingly, there are also reports that couple oncogenic signaling pathways such as Epidermal Growth Factor Receptor (EGFR), Human Epidermal growth factor Receptor 2 (HER2/ErbB2), and Insulin-like growth factor I Receptor (IGF-IR) to increases in LIP protein levels. Baldwin et al. connect EGFR signaling in mammary epithelial cells to an increase in the LIP levels. They show that C/EBPbeta mRNA levels are unaffected by EGF stimulation and suggest that the increase in LIP expression is controlled posttranscriptionally and is partly due to the interaction of the translational regulatory factor CUG triplet repeat, RNA binding protein 1 (CUGBP1) with C/EBPbeta mRNA (Baldwin et al., 2004). In later studies by Arnal-Estapé et al., they report that hyperactivation of ErbB2 in patient-derived metastatic breast cancer samples leads to an increase in LIP. Similarly, ErbB2 signaling was shown to activate CUGBP1, a downstream effector of ErbB2/PI3K pathway. CUGBP1 appears to favor the production of LIP and inhibition of PI3K activity prevents LIP translation irrespectively of ErbB2 status (Arnal-Estapé *et al*., 2010). More recently, IGF-IR signaling has also been shown to increase LIP expression in an EGFR independent manner in mammary epithelial cells (Li *et al*., 2011). Li et al. conclude that Akt activity is an important regulator of IGF-IR induced LIP expression and that this elevation in LIP plays a significant role in regulating cellular survival via suppression of anoikis (Li *et al*., 2011). Cell-in-cell structures have long been noted in tumor samples, and thus it is possible that elevated LIP

levels consequent to oncogenic signaling could contribute to their formation by activating cell engulfment.

In regards to the clearance of live cells, studies in Drosophila have recently identified a new tumor-suppression mechanism that eliminates oncogenic imaginal epithelial cells (Ohsawa *et al*., 2011). Mutant epithelial cells that have lost their apicobasal polarity are actually engulfed and eliminated by surrounding normal epithelial cells. Engulfment is dependent on the activation of nonapoptotic JNK signaling in the normal imaginal cells in response to the emergence of neoplastic mutant cells (Ohsawa *et al*., 2011). Given that many components of the Drosophila antitumor cell engulfment pathway are conserved from flies to human, Ohsawa et al speculate that this is an evolutionarily conserved intrinsic tumor-suppression mechanism existing in normal epithelium (Ohsawa *et al*., 2011). Given that LIP can mediate live cell engulfment, it is interesting that C/EBPbeta is a downstream target of JNK signaling (Qiao *et al*., 2003).

Now that the potential for LIP-mediated engulfment of live cells is known, this may enable the possible recognition of this event during times when LIP levels are elevated, such as mammary gland involution (shown here) as well as ER stress or oncogenic signaling. Like entosis, it remains uncertain whether LIP-mediated engulfment serves a prosurvival role (such as a mechanism to escape immune surveillance) or a growth/tumor suppressor role (such as intrinsic epithelial surveillance and/or via inducing cell death). Specific inhibitors of the LIP-induced engulfment process will be necessary to address these questions.

Future studies aimed at characterizing the mechanism by which LIP induces engulfment will facilitate the development of inhibitors and thus a fuller understanding of its biological significance.

CHAPTER IV

C/EBPbeta3 (LIP) and transcriptional regulation

Introduction

As described in earlier chapters, exogenous expression of LIP in breast cancer cells leads to engulfment of neighboring cells, which is accompanied by autophagy, and ultimately leads to cell death. The ability of a transcription factor to stimulate cell engulfment has not, to our knowledge, previously been reported. In order to gain insight into the mechanism by which LIP expression leads to cell engulfment, autophagy, and the massive cell death that follows, we sought to identify some of the specific genes targeted by this transcription factor.

Previous studies have shown a role for C/EBPbeta in regulating transcription of a multitude of genes ranging from cyclooxygenase-2 (COX-2) (Wu *et al*., 2005), gluconeogenic phosphoenolpyruvate carboxykinase (PEPCK) (Jurado *et al*., 2002), receptor activator of nuclear factor kappa B ligand (RANKL) (Ng *et al*., 2010), and those encoding cytokines (IL-6, IL-1beta, TNF-alpha) to list a few (Yang *et al*., 2000; Russell *et al*., 2010; Bristol *et al*., 2009). We decided that a comprehensive and unbiased approach would be the best way to proceed and so we performed Affymetrix genomic profiling on control (NV or GFP) or LIP-expressing cells. We performed genomic profiling in both MDA-MB-231 and MDA-MB-468 breast cancer cells.

Despite the major phenotypic changes that result from LIP overexpression, there were surprisingly few changes in gene transcription using Affymetrix human genome U133 Plus 2.0 microarrays. The major difference was

an elevation of *HSPA1A* gene transcription, which we further characterized using qPCR. However, only a small increase in heat shock protein 70 (HSP70) cellular protein was detected. HSP70 has been shown to have different roles depending on its localization (Tytell, 2005). Intracellularly, HSPs function as molecular chaperones aiding in folding and transport of an assortment of polypeptides and proteins under normal physiological conditions and following stress stimuli (da Silva and Borges, 2011). HSPs localized extracellularly or plasma membrane-bound HSPs are known to provoke potent anti-cancer immune responses mediated either by the adaptive or innate immune system (van Noort *et al*., 2012). In addition, tumor cells can actively release HSP70s in lipid vesicles such as exosomes (van Noort *et al*., 2012).

In this chapter, I demonstrate that LIP expression leads to a substantial but transient increase in *HSPA1A* mRNA. This not only leads to a small increase in cellular HSP70 protein, but also an increase in HSP70-containing exosomes isolated from LIP-expressing cells. We address whether these exosomes are involved in cell engulfment via our quantitative cell engulfment assay using flow cytometry.

Materials and Methods

Cell Culture and adenoviral constructs

The human breast cancer cell lines MDA-MB-231 and MDA-MB-468 were obtained from the ATCC (Manassas, VA) and maintained as described in the

previous chapters. The adenoviral constructs used in these experiments were the same as discussed in the previous chapters. Cells were grown to subconfluency (60–70%) on 100mm dishes. Cells were either uninfected or adenovirally infected with Ad-GFP or Ad-LIP at a MOI: 5–10 for all experiments.

Genomic profiling

Total RNA was isolated 48hrs post-infection using the RNeasy Mini kit and RNase-Free DNase kit (Qiagen, Maryland, USA). RNA was submitted to the Vanderbilt Microarray Shared Resource for quality assurance. After confirming RNA quality, biotinylated complementary RNA was prepared, fragmented, and hybridized to Affymetrix GeneChip U133 PLUS 2.0 arrays. Three independent replicates were performed for the MDA-MB-231 cell line. Similar experiments were performed using the MDA-MB-468 cell line.

Real-time PCR

RNA was extracted as described above. cDNA was synthesized with the high capacity cDNA reverse transcription kit according to manufacturer's instructions (Applied Biosystems, Foster City, CA, USA). Next, Taqman real-time PCR was performed to determine the relative levels of targets. GAPDH was used as an internal control in these experiments. The HSPA1A probe used was Hs00359163_s1 (Applied Biosystems, Foster City, CA). Reactions were performed in a total volume of 20μL using a real-time PCR instrument (StepOnePlus, Applied Biosystems, Foster City, CA, USA).

Whole cell lysates and immunoblot analysis.

Whole cell extracts were prepared as described in chapter 2. Relative protein concentrations were determined using the Protein Assay Reagent (BioRad Laboratories, Hercules, CA, USA) as per manufacturer's instructions. After separation by electrophoresis the proteins were transferred to an Immobilon®-P filter and processed as previously described.

Exosome isolation

Exosomes were isolated from control MDA-MB-231 cells or MDA-MB-231 cells infected with Ad-GFP or Ad-LIP (Figure 25A). Normal growth media was removed 16hrs post-infection and replaced with serum-free Iscove's media. At 48hrs post-infection, media was collected from each cell population. We used two different methods to isolate exosomes. The first approach for exosome purification was through differential ultracentrifugation. After collecting media, the initial step is designed to eliminate large dead cells and large cell debris by centrifugations at a lower speed. Samples were kept on ice the entire duration of experiments and centrifugations were done at 4° C. The first spin was performed at 800 x *g* for 10 minutes. Supernatants were collected and transferred to new tubes. A second spin at 12,000 x *g* was performed for 30 minutes. The pellet for each population was collected in PBS (with addition of protease and phosphatase inhibitors). This fraction collected represents the microvesicles. Meanwhile, the supernatants were carefully removed and ultracentrifugation at 100,000 x *g* for 2hrs was performed. Following this spin, supernatant was

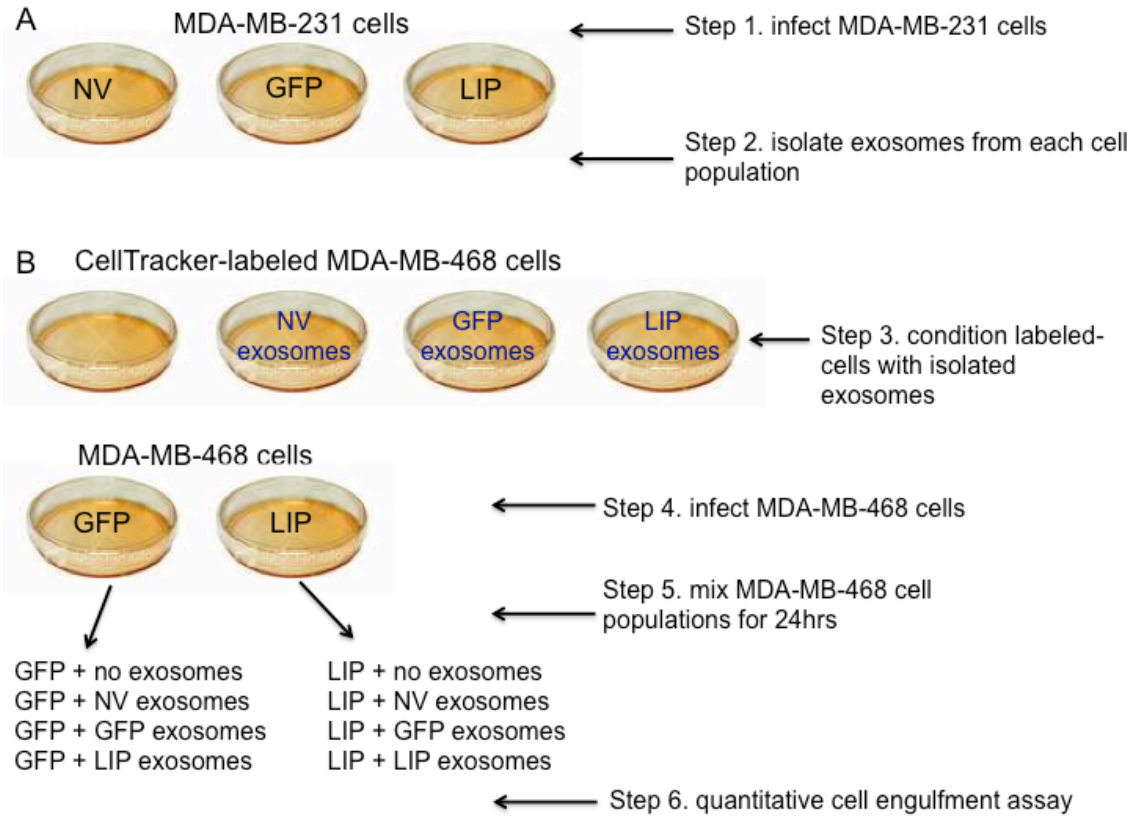

Figure 25. Schematic of experimental design.

removed and the pellet was resuspended in PBS (with addition of inhibitors) and this represents the exosomes fraction. The second approach was using the ExoQuick-TC^{TM} Exosome Precipitation Solution (Cat. # EXOTC50A-1, Systems Biosciences, Mountain View, CA). Exosomes were isolated as per manufacturer's instructions.

Quantitative cell engulfment assay using flow cytometry

In these assays, MDA-MB-468 cells were stained with CellTracker dye as per manufacturer's instructions (Figure 25B). Following the staining procedure, exosome pellets collected from control or (Ad-GFP or Ad-LIP) infected MDA-MB-231 cells were added to the labeled MDA-MB-468 cells. After 24hrs of conditioning with the exosomes, these MDA-MB-468 cells were mixed in a ratio of 3:1 with Ad-LIP or Ad-GFP MDA-468 cells as described in chapter 3. At 24hrs post-mixing, cells were trypsinized and collected in phenol-red free Iscove's media. Cells were collected for flow cytometry analysis using a 3-laser FACSCanto II instrument, (Becton-Dickinson, San Jose, CA) equipped with standard 5-2-2 filter configuration. FACSDiVa Software was used for data acquisition and analysis.

Results

Genomic profiling of LIP-expressing MDA-MB-231 cells

To characterize LIP regulation of gene expression in MDA-MB-231 cells, RNA was isolated from control (uninfected or Ad-GFP) and Ad-LIP MDA-MB-231

cells at 48hrs post-infection. Isolated RNA was hybridized to Affymetrix human genome U133 Plus 2.0 microarrays in what is now the Vanderbilt Genome Sciences Resource Core. A small number of genes, approximately 3% of the total represented on the U133 Plus 2.0 microarrays, showed minor alterations in expression in the LIP-expressing MDA-MB-231 cells 48hrs post-infection. In each set of experiments, we detect between 90-103 genes that were upregulated 1.5-fold or more in comparison to the control samples. The number of genes downregulated 1.5-fold or more was between from 80-110 genes. While we repeated these experiments three times, the only consistent result we obtained was increases in the HSPs as shown in Table 1. We were surprised when we did not detect significant changes in genes that are downregulated since LIP is a transcription repressor.

Affymetrix number	Gene symbol	Description	Fold increase
200799_at	HSPA1A	Heat shock 70kD protein 1A	7
200800_s_at	HSPA1A	Heat shock 20kD protein 1A	5.4
213418_at	HSPA6	Heat shock 70kD protein 6 (HSP70B')	6
117_at	HSPA6	Heat shock 70kD protein 6 (HSP70B')	3
202581_at	HSPA1B	Heat shock 70kD protein 1B	3.2

Table 1. LIP regulation of genes in MDA-MB-231 cells. Upregulated genes and their respective fold increase are depicted.

Genomic profiling of LIP-expressing MDA-MB-468 cells

During these studies, I tested a number of breast cancer cell lines as presented in Figures 6, 7, and 8 in chapter 2. We noticed that exogenous expression of LIP leads to cell death in all breast cancer cell lines tested. However, we do notice a difference in the time it takes for cells to die and the extent of cell death varies in the different breast cancer cell lines. After testing the MDA-MB-468 cell line, it was very apparent that LIP overexpression leads to cell death in a larger percent of cells in the population at a given time. Due to the fact that we saw small changes in the LIP-expressing MDA-MB-231 cells, that may have a small number of cells dying at any one time, we wanted to extend our studies and characterize LIP regulation of gene expression in MDA-MB-468 cells. RNA was isolated from control (uninfected or Ad-GFP) and Ad-LIP MDA-MB-468 cells at 48hrs post-infection. Isolated RNA was hybridized to Affymetrix human genome U133 Plus 2.0 microarrays in what is now the Vanderbilt Genome Sciences Resource Core. To our surprise, even though LIP overexpression leads to the presence of autophagy markers (chapter 2) and engulfment of neighboring cells (chapter 3) that together result in massive cell death, we did not detect any major changes at the transcription level. LIP expression in the MDA-MB-468 cell line leads to 222 genes that were upregulated more than 2-fold. Table 2 shows the top 10-upregulated genes and their respective fold changes. As mentioned LIP is thought to function as a transcriptional repressor, so it was even more surprising that we detect only 15 genes downregulated greater than 2–fold. This data is presented in table 2.

Affymetrix number	Gene symbol	Description	Fold change
1555436_a_at	AFF4	AF4/FMR2 family, member 4	3
235645_at	ESCO1	Establishment of cohesion 1 homolog 1	2.67
220407_s_at	*TGFB2	Transforming growth factor, beta 2	3.8
205017_s_at	MBNL2	Muscleblind-like 2	3.6
201730_s_at	TPR	Translocated promoter region {to activated MET oncogene}	3.3
222283_at	ZF	Zinc finger protein 480	2.35
221220_s_at	SCY1	SCY1-like 2	2.15
213286_at	ZFR	Zinc finger RNA binding protein	2
15700001_at	CASP8	Casp8 and FADD-like apoptosis regulator	1.7
218960_at	*TMPRSS4	transmembrane protease, serine 4	-3.44
227238_at	*MUC15	mucin 15, cell surface associated	-3
214829_at	AASS	aminoadipate-semialdehyde synthase	-2.75
235089_at	*FBXL20	F-box and leucine-rich repeat protein 20	-2.16
237493_at	*IL22RA2	interleukin 22 receptor, alpha 2	-2
202501_at	MAPRE2	(microtubule-associated protein, RP/EB family, member 2	-1.95
220907_at	*GPR110	G protein-coupled receptor 110	-1.8
222257_s_at	*ACE2	angiotensin I converting enzyme (peptidyl-dipeptidase A) 2	-1.5

Table 2. LIP regulation of genes in MDA-MB-468 cells. * denotes genes that contain C/EBPbeta site in promoter.

HSPA1A mRNA increase is transient

As mentioned above, heat shock protein genes exhibit the largest changes in gene expression in response to LIP expression, specifically in MDA-MB-231 cells. In order to confirm this genomic profiling data, I performed Real-Time PCR (qPCR). RNA was isolated from control (uninfected, Ad-GFP) and Ad-LIP MDA-MB-231 at various time (24-96hrs) points post-infection. We are able to confirm a transient increase in HSPA1A mRNA beginning at 48hrs post-infection in the LIP-expressing MDA-MB-231 cell line. In comparison to the microarray results where we detect on average a 7-fold increase, we detect up to a 50-fold increase in HSPA1A relative to control using qPCR. As shown in Figure 26, there are still elevated levels of HSPA1A mRNA at 72hrs post-infection. Yet, 96hrs post-infection HSPA1A mRNA levels are similar to those seen in control Ad-GFP.

Although we did not observe an increase in HSPA1A gene expression by microarray analysis in the MDA-MB-468 cells, we nonetheless performed qPCR with RNA from these cells over a similar time course. Interestingly, a similar transient increase in HSPA1A mRNA was observed in the LIP-expressing MDA-MB-468 cells (Figure 27). However, we detect only a 5-fold increase in HSPA1A transcript and this was observed 24hrs post-infection. This result explains why the increase in HSPA1A transcript was missed in the microarray analysis, because the RNA was analyzed at 48hrs post-infection. Nonetheless, our data suggest that increased *HSPA1A* transcription is a common response to LIP

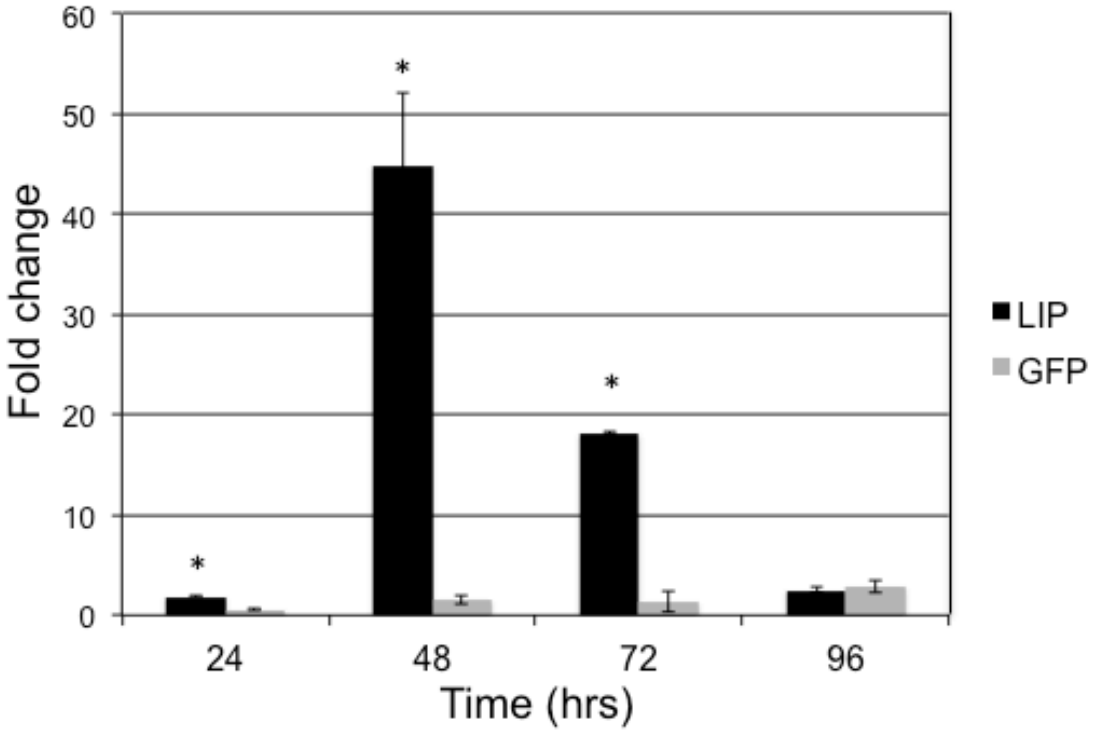

Figure 26. LIP induces HSPA1A expression in MDA-MB-231 cells. RNA was isolated from control uninfected as well as Ad-LIP and Ad-GFP MDA-MB-231 cells at different time points post-infection. cDNA was synthesized as described in Materials and Methods section. Results are presented as fold induction of HSPA1A compared to uninfected MDA-MB-231 cells. This assay was repeated three times and t-test analysis was performed. *p-value: <0.05

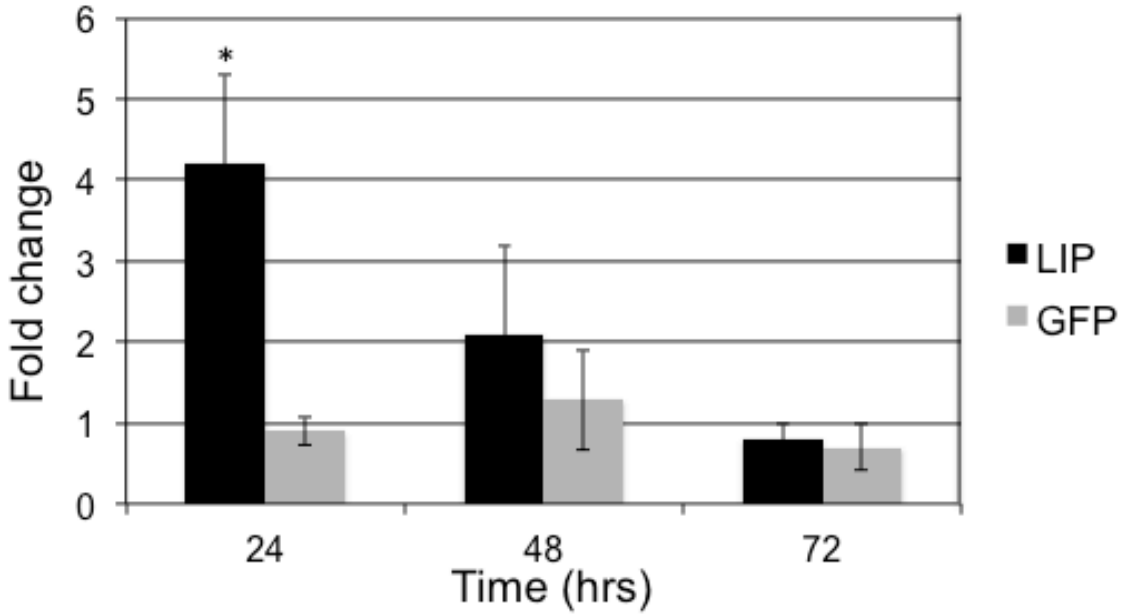

Figure 27. LIP induces HSPA1A expression in MDA-MB-468 cells. RNA was isolated from control uninfected as well as Ad-LIP and Ad-GFP MDA-MB-468 cells at different time points post-infection. cDNA was synthesized as described in Materials and Methods section. Results are presented as fold induction of HSPA1A compared to uninfected MDA-MB-468 cells. This assay was repeated three times and t-test analysis was performed. *p-value: <0.05

expression, although the specific time course and magnitude may vary by cell line.

HSP70 cellular protein levels do not correlate with HSPA1A mRNA increase

After observing such a dramatic increase in HSPA1A mRNA in MDA-MB-231 cells, we wanted to analyze cognate protein expression. Following adenoviral infection of MDA-MB-231 cells, whole cell lysates were prepared at days 2, 4, and 6 post-infection. Immunoblot analysis was carried out using an anti-HSP70 antibody. Figure 26A shows a small increase in cellular HSP70 protein at days 2 and 4 post-infection. However, this increase in protein does not correlate with the 50-fold increase of HSPA1A mRNA presented in Figure 26. In addition, I performed densitometric analysis of HSP70 protein levels (at days 2-5) relative to the control TFIID protein levels. As shown in Figure 28B, there is little difference between the cell population expressing LIP and control (NV and Ad-GFP) MDA-MB-231 cells.

LIP expression leads to increases in exosome secretion

In addition to its intracellular location, HSP70 is also known to be secreted from cells via a non-canonical pathway and the secreted HSP70 is a common component of exosomes (Tytell, 2005). Exosomes are 30- to 100-nm lipid bilayer vesicles that function to promote intercellular communication. Exosomes are derived from the fusion of multivesicular bodies with the plasma membrane and extracellular release of the intraluminal vesicles (Johnstone *et al*., 1987). Recent studies have focused on the biogenesis and composition of exosomes as well as regulation of exosome release (Schorey and Bhatnagar, 2008).

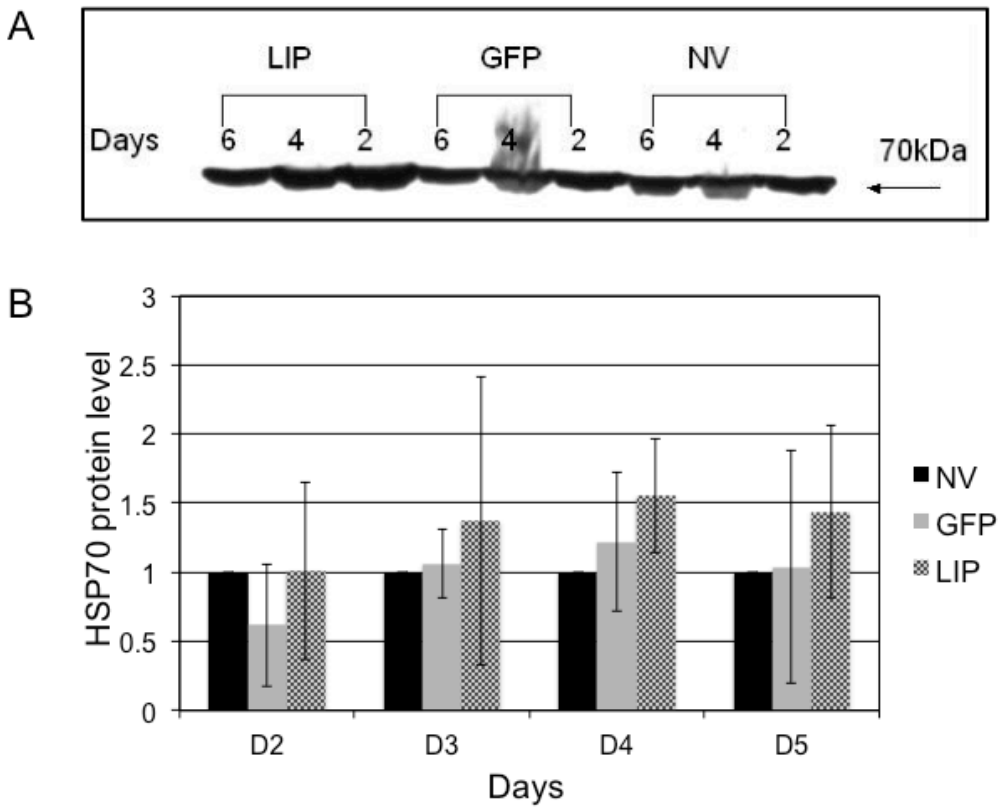

Figure 28. HSP70 protein levels in MDA-MB-231 cells. Whole cell lysates were prepared from Ad-LIP MDA-MB-231 cells, control Ad-GFP MDA-MB-231 cells, and control uninfected (NV) MDA-MB-231 cells at different time points (days 2–5) post-infection and analyzed by 10% SDS-PAGE. Immunoblot analysis with anti-HSP70 antibody is shown. **B**, Densitometric analysis of HSP70 in MDA-MB-231 cells using the ODYSSEY infrared imaging system. Data shown represents the mean ± SD. An anti-TFIID antibody was used as a loading control. Solid black bars represent the uninfected NV MDA-MB-231 cells; gray bars represent the Ad-GFP MDA-MB-231 cells, and the shaded bars represent the Ad-LIP MDA-MB-231 cells.

Various techniques including immunoblot analysis, immuno-EM, FACS, and mass spectrometry have been utilized to analyze the lipid and protein contents of exosomes. Exosome composition varies depending on the cell type of origin. Nevertheless, exosomes contain a number of common protein components for instance, Rabs, which promote exosome docking and the membrane fusion events; annexins, including annexin I, II, V and VI, which may regulate membrane cytoskeleton dynamics and membrane fusion events; several adhesion molecules (e.g. CD9, CD18, CD146, CD166) have also been identified in exosomal preparations (Schorey and Bhatnagar, 2008). Another characteristic feature of exosomes is the tetraspanins, which include CD9, CD63, CD81, and CD151 (Schorey and Bhatnagar, 2008; Simpson *et al*., 2008).

We detect a high level of HSPA1A mRNA, yet a small increase in cellular HSP70 protein levels. It is known that HSP70 can also function extracellularly and tumor cells secrete HSP70 in exosomes. We wanted to isolate exosomes from the MDA-MB-231 cell line since we see the most dramatic change in HSPA1A mRNA in this cell line. In this set of experiments, we analyzed both HSP70 and CD151 protein levels in control (uninfected, Ad-GFP) and Ad-LIP infected MDA-MB-231 cells. I used both the ultracentrifugation and/or kit method to isolate the exosomes. After collecting the conditioned media and performing ultracentrifugation or the kit method to isolate exosomes, samples were analyzed by western blot. Blots were probed with an anti-HSP antibody as well as anti-CD151 antibody. We detect an increase in HSP70 in the microvesicle (MV) fraction and the exosome fraction, of LIP-expressing MDA-MB-231 cells when we

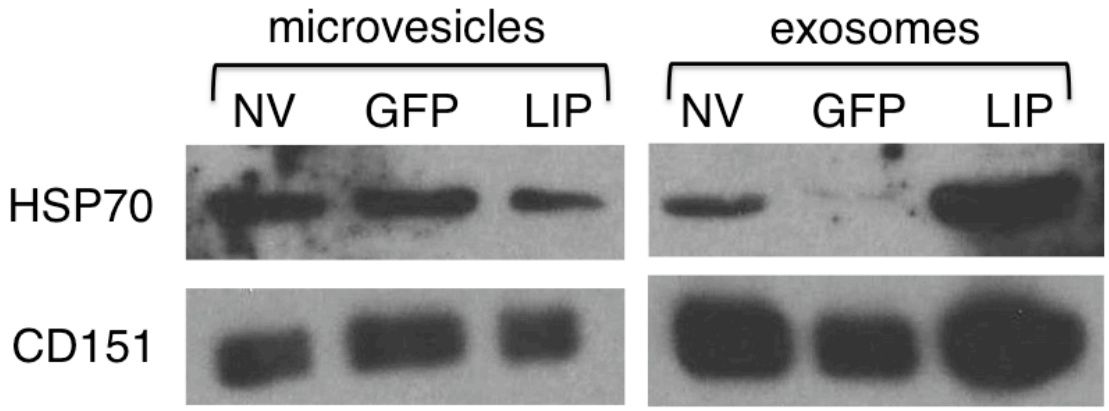

Figure 29. LIP expression leads to increased exosome secretion. Microvesicles and exosomes were isolated from control NV MDA-MB-231 cells, Ad-GFP, or Ad-LIP MDA-MB-231 cells. Samples were analyzed by western blot using anti-HSP70 and anti-CD151 antibodies.

perform the ultracentrifugation method (Figure 29). When the exosome kit method was utilized, we detect an increase in HSP70 protein levels in exosomes of LIP-expressing MDA-MB-231 cells. When using the kit method this procedure is devoid of collecting for microvesicles and the solution only isolates exosomes. In addition to increases in HSP70 protein levels, we also detect an increase in CD151 protein levels in exosomes isolated from LIP-expressing MDA-MB-231 cells. This suggests that we have more exosomes being secreted from LIP-expressing MDA-MB-231 cells, which could explain why there is more HSP70 in the exosome sample from LIP-expressing MDA-MB-231 cells.

LIP-derived exosomes are involved in cell engulfment

Throughout these studies, we were puzzled by the length of time it took to detect both signs of autophagy and engulfment. As shown in Figure 6, there are high levels of LIP at 48hrs post-infection, yet we see an increase in 2n DNA content at 72hrs post-infection as shown in Figure 17. In our cell engulfment experiments described in chapter 3, we show LIP-expression leads to approximately 30% engulfment of neighboring cells at 48hrs post-mixing. We were unable to detect significant levels of engulfment at 24hrs. This suggests that it takes a few days of chronic LIP expression for cell engulfment to occur.

As shown in Figure 29, it appears that LIP-expressing cells secrete more exosomes. It is known that exosomes function to promote intercellular communication. To determine if exosomes were involved in “sending messages” to neighboring cells to prepare them for cell engulfment, we used the MDA-MB-231 cell line. We chose to isolate the MDA-MB-231 exosomes since we had

observed high levels of HSPA1A mRNA at 48hrs post-infection in this cell line. In addition, we find HSP70 and CD151 protein levels increased in the exosomes isolated from LIP-expressing MDA-MB-231 cells. 16hrs post-infection, we replenished the different (NV, Ad-GFP, and Ad-LIP) cell populations with serum-free growth media. After an additional 24hrs, media was collected and following a series of centrifugation steps (Figure 25), isolated exosomes were added to CellTracker stained MDA-MB-468 cells. This conditioning period lasted 24hrs. Next, we used Ad-LIP and Ad-GFP infected MDA-MB-468 cells and mixed these cell populations with the exosome-treated fluorescent-labeled MDA-MB-468 cells in a 1:3 ratio as described previously for the quantitative cell engulfment assays. 24hrs post-mixing, the cell populations were analyzed by FACS to determine the extent of cell engulfment of neighboring cells. Conditioning of uninfected fluorescent-labeled MDA-MB-468 cells with exosomes isolated from LIP-expressing MDA-MB-231 cells leads to a dramatic increase in cell engulfment at 24hrs post-mixing. We detect approximately 33% of LIP-expressing cells engulfing their neighboring cells in comparison to the control (no exosomes) treatment where we only detect 11% cell engulfment 24hrs post-mix (Figure 30). Interestingly, conditioning of uninfected fluorescent-labeled MDA-MB-468 cells with exosomes isolated from LIP-expressing MDA-MB-231 cells marks these cells for engulfment.

We are able to show that GFP-expressing MDA-MB-468 cells can also engulf neighboring cells considerably once they have been conditioned with

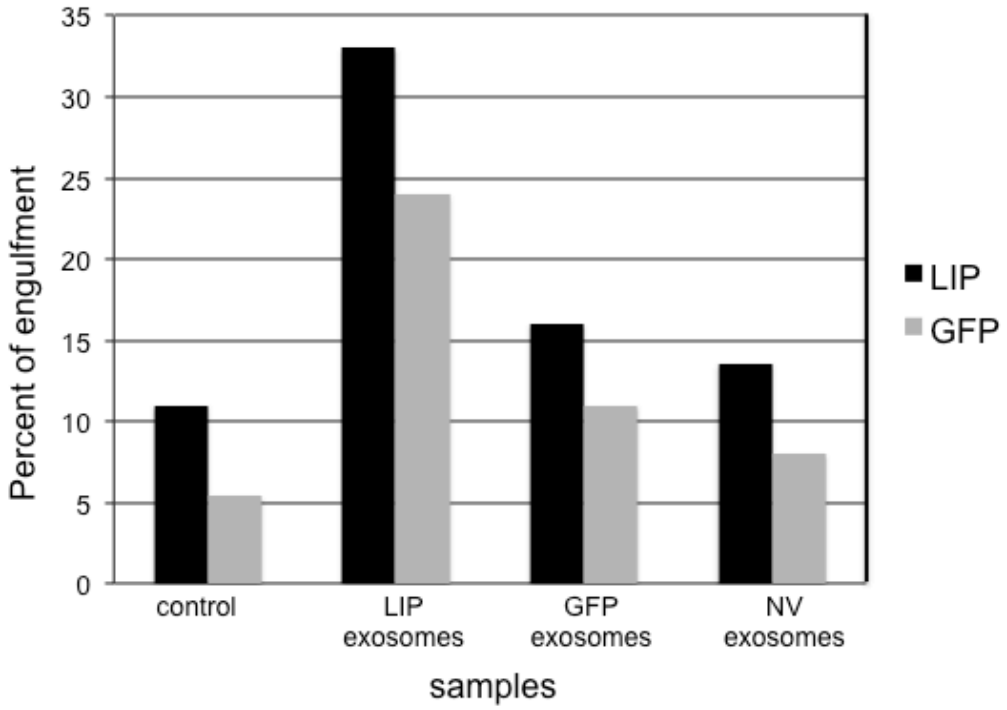

Figure 30. LIP-derived exosomes are involved in cell engulfment. Quantification of the percent of GFP positive cells that have engulfed uninfected CellTracker labeled cells at 24hrs post-mixing. Solid bars represent LIP-expressing MDA-MB-468 cells. Gray bars represent Ad-GFP control MDA-MB-468 cells. The following samples were either with no exosome treatment or with treated with exosomes isolated from the respective MDA-MB-231 cell line. Sample 1: no exosome treatment; Sample 2: LIP exosomes; Sample 3: Ad-GFP exosomes; Sample 4: uninfected (NV) exosomes.

exosomes isolated from LIP-expressing MDA-MB-231 cells. Without exosome treatment of target cells, cell engulfment with Ad-GFP cells was a meager 5% as shown in Figure 20 and Figure 30. However, conditioning of the target cells with LIP-derived exosomes leads to 25% cell engulfment. This suggests that exosomes derived from the LIP-expressing population may be involved in delivering messages to neighboring cells that marks them for cell engulfment. Conditioning with exosomes isolated from control Ad-GFP and NV MDA-MB-231 cells leads to a small increase of cell engulfment in comparison to target cells not exposed to exosomes. Nevertheless, a substantial increase in cell engulfment is observed in the cell populations that were conditioned with LIP-derived exosomes. We conclude from these studies that LIP may mediate cell engulfment by inducing the release of messages, in the form of exosomes, that in someway alter target cells to become “engulfable”.

Discussion

As discussed in previous chapters exogenous expression of the transcription factor LIP in breast cancer cells leads to engulfment of neighboring cells, which is accompanied by autophagy, and ultimately leads to cell death. In this chapter we set out to determine the genes that are regulated by LIP. To our surprise, the genomic profiling studies revealed very few changes in both the MDA-MB-231 and MDA-MB-468 cell lines at the 48hrs post-infection time point. LIP expression in the MDA-MB-231 cell line does lead to a striking increase in HSPA1A mRNA transcript. These results were further confirmed using qPCR.

Yet, for a 50-fold upregulation in transcript, we confirm only a small increase in cellular HSP70 protein levels. When we profiled the MDA-MB-468 cell line, we had expected to uncover genes that may be involved in the dramatic phenotype we illustrate in chapters 2 and 3. Yet, we were astonished to find that again very little changes were found at 48hrs post-infection. It is important to note that HSPs were not identified as an upregulated candidate in the microarrays performed with the MDA-MB-468 cells. However, as shown in Figure 2 that is due to the fact that we see upregulation of HSPA1A mRNA transcript 24hrs post-infection. We cannot conclude that LIP stimulation of autophagy and cell engulfment is not mediated through any transcriptional regulation, since we observe many changes are in fact transient. We know there is great heterogeneity in these cell populations and the autophagy and cell engulfment process is not synchronized, therefore it would be difficult to pinpoint the most appropriate window of time that could be used to study changes in gene expression due to LIP.

In our attempt to track down changes in HSP70 protein expression, we were able to document an increase in HSP70-containing exosomes in the culture medium of LIP-expressing MDA-MD-231 cells. Remarkably, the exosomes from LIP-expressing cells may contain message(s) that significantly increase the engulfability of target cells exposed to these exosomes. The fact that up to 25% of MDA-MB-468 cells only expressing GFP can engulf their neighbors, when conditioned by exosomes from LIP-expressing cells, suggest that engulfing other cells does not actually require elevated LIP expression. Rather it is the

conditioning of the target cells, conferring “engulfability” on them, that occurs upon LIP overexpression in neighboring cells. In other words, LIP does not convert cells into predators, so much as it alters cells into becoming prey. Exosomes appear to be one method for communicating with cells and converting them into “prey”. Our findings do not exclude, other, perhaps soluble factors from being involved as well. Exosomes are complex entities typically comprised of over 300 different proteins, as well as RNA, including microRNA and even DNA. The nature of the specific exosomal message(s) and how they convert an otherwise resilient target cell into an engulfable one, could be a complex task to identify. One interpretation of our data is that the lag between LIP overexpression and significant cell engulfment is due to the time required to convert a potential target cell into a engulfable one once exposed to exosomes secreted from LIP-expressing cells. Further research, in particular uncovering the nature of the messages exchanged exosomally, should help to determine if this interpretation is correct.

CHAPTER V

Summary and Discussion

The transcription factor C/EBPbeta is a critical player during mammary gland development. It plays a role in proliferation, differentiation, and cell death. As reported with other transcription factors (e.g., SNAIL, Twist) that are important during development, C/EBPbeta has been shown to affect tumor formation and progression in various organs including the mammary glands. Interestingly, the gene encoding C/EBPbeta (*CEBPB*) is not mutated in breast tumors. Little mutations have been identified in *CEBPB*, and those that do occur are not believed to promote epithelial cancers. *CEBPB* may, however, be amplified in a small subset of breast neoplasia. Alterations common to lobular carcinoma in situ of the breast include a gain at 20q13.13, which contains *CEBPB* (Mastracci *et al*., 2006).

When C/EBPbeta mRNA levels were queried with Oncomine 3.0 array, data analysis performed revealed that expression of C/EBPbeta mRNA is not altered in breast cancer cell lines or breast tumor tissue in comparison to normal breast tissue (Rhodes *et al*., 2005). Further gene expression studies have also shown that C/EBPbeta mRNA is unchanged and not altered in breast cancer upon stimuli such as oncogenic ErbB receptor activation. Still, differences in C/EBPbeta mRNA expression are observed among a few breast cancer subtypes. For instance, Oncomine analysis showed that a modest, but significant increase in C/EBPbeta mRNA is observed in estrogen-receptor-

negative breast cancers versus those tumors that are positive for the estrogen receptor. Also, an elevation in C/EBPbeta mRNA is associated with metastatic breast cancer, a high tumor grade, and an overall poorer prognosis (Milde-Langosch *et al*., 2003). While the data suggest that transcriptional control or regulation of mRNA stability may be a mechanism for CEBPbeta expression in more aggressive breast cancers, C/EBPbeta frequently goes under the radar in many genomic profiling studies. This is due to the fact that C/EBPbeta expression is significantly regulated at the translational level and multiple C/EBPbeta isoforms are produced. Translation of this intronless gene leads to the production of three protein isoforms, each with a distinct function in the mammary gland.

C/EBPbeta1 has been shown to play a role not only in differentiation, but our work demonstrates an important role for C/EBPbeta1 in oncogene-induced senescence (Atwood and Sealy, 2010). Our lab demonstrated a role for C/EBPbeta2 in proliferation, transformation, and epithelial-to-mesenchymal transition in culture (Bundy and Sealy, 2003). When we characterized C/EBPbeta in normal versus neoplastic mammary epithelial cells, we show an increase in C/EBPbeta2 protein levels in patient breast tumor samples. Contrary to others, we did not observe an increase in C/EBPbeta3 (LIP) in patient breast tumor samples; in fact LIP was undetectable (Eaton *et al*., 2001). In recent years, there has been progress in delineating the roles and differences between C/EBPbeta1 and C/EBPbeta2; yet the role of LIP is very unclear. In this work I set out to investigate the role of LIP in breast cancer. This thesis aims to

characterize the induction of autophagy as well as describe the ability to engulf neighboring cells which ultimately leads to cell death upon LIP expression in breast cancer cell lines.

Autophagy and Cancer

Autophagy is an intracellular process through which cytosolic components, ranging from lipids, proteins, carbohydrates and nucleotides to whole organelles and invading pathogens, are targeted for lysosomal degradation. Currently, our understanding of whether autophagy is an ally or enemy in breast cancer development, progression and treatment remains ambiguous. Interestingly, cancer was the first human pathology connected to autophagy through the discovery that Beclin1, a core component of the autophagosome nucleation complex, was monoallelically deleted in 40–75% of sporadic human breast, ovarian and prostate cancers. Reduction in autophagic activity in early stages of the oncogenic process favors malignant transformation, as the accumulation of certain molecules can activate signaling mechanisms that promote necrosis and inflammation. In addition, poor quality control as a result of diminished autophagy can result in accumulation of defective organelles (e.g. mitochondria), with the subsequent release of harmful molecules (cytochrome *c* and reactive oxygen species) that contribute to further altering genome maintenance. In later stages of tumor progression, activation of autophagy is observed in many oncogenic processes, in part to compensate for the poor nutritional supply associated with growing tumors and to defend cancer cells against damage induced by anti-oncogenic therapies. In addition, enhanced mitochondrial

degradation in this stage may contribute to the up-regulation of glycolysis to maintain the energetic balance (Warburg effect) characteristic of malignant cells. Effectors and modulators of autophagy have become attractive targets in the treatment of cancer.

Like many cellular processes, a fine balance in the autophagic process is essential. While autophagy may play dual roles, it seems that the status of the cell, whether normal or transformed, is of great importance. Additionally, it is critical to not only focus on the role of autophagy in epithelial cells, but the surrounding microenvironment is most likely also playing a role during tumor progression. The role of autophagy in stromal cells is a very poorly understood area that needs to be studied in greater detail. Complete inhibition of autophagy as that proposed by many investigators may lead to an initial decrease in tumor size or inhibition of cell survival in metastatic cells, but it may also lead to more aggressive tumors or the development of different death-causing diseases. Using genetically engineered mouse models for cancer where autophagy is inhibited, Eileen White's group recently demonstrated that inhibition of autophagy does not alter the survival rate of mice bearing lung tumors. Lung tumors of genetically engineered mice accumulate defective mitochondria, and while there is an induction of growth arrest, there is no effect on survival. They conclude that these mice have massive increases in the inflammatory response and this leads to a pneumonia-like death.

In general, whether the focus is on autophagy or other mechanisms, I believe it is essential to find ways to specifically target tumor cells. Clearly, this is

very challenging as tumor cells were basically normal cells until their regulatory systems were hijacked. Otherwise, general inhibition of any process, like the use of chemotherapy, is ultimately going to be an issue of weighing out the benefits over the detrimental effects.

C/EBPbeta3 (LIP) and Cancer

In a similar way, identifying the role of LIP in breast cancer development has been somewhat complicated. While Zahnow's group reported high levels of LIP protein expression in breast tumor samples, our own studies do not corroborate these results. In addition, Zahnow et al. report transgenic mice that overexpress LIP in the mammary gland develop focal and diffuse alveolar hyperplasia as well as small percent (9%) form non-invasive carcinomas (Zahnow *et al*., 2001). Unfortunately, because the LIP transgene was not epitope-tagged in these mice it is not possible to ascertain transgene expression distinguished from any endogenous LIP expression. Moreover, the level of LIP expression (transgene or endogenous) in the mammary tumors was not actually examined. On the other hand, work published by Meir et al. demonstrates a decrease in tumor size of LIP overexpressing mice. They conclude LIP augmented ER stress-triggered cell death whereas overexpression of C/EBPbeta2 (LAP) attenuated cell death (Meir *et al*., 2010). Hence, the puzzle of LIP's role in tumorigenesis remains to be solved.

C/EBPbeta3 (LIP) and autophagy: explaining the paradox?

The work in chapter 2 of this document describes the role of LIP in stimulating the self-cannibalization process of autophagy and inducing cell death

in breast cancer cell lines. I provide evidence for this by monitoring autophagy using various well-accepted methods (e.g. ultrastrucure analysis and autophagosome formation), performing cell proliferation assays, as well as colony formation assays. Figure 6 and figure 7 demonstrate that high levels of LIP attenuate proliferation and lead to cell death in the MDA-MB-468 and MDA-MB-231 cell lines. I also show that LIP overexpression does not lead to a cell cycle block or apoptotic (type I) or necrotic (type III) cell death. In addition, I provide evidence of autophagy in LIP-expressing cells by ultrastructure analysis of MDA-MB-231 cells. In these studies, I detect an increase in various different autophagic vesicles and lamellar structures found in later stages of autophagy. Using different biochemical methods we were able to confirm that LIP-expressing cells have an increase in acidic vesicles. Along those lines, we detect an increase in LC3-II protein levels in LIP-expressing cells indicative of autophagosome formation. Finally, I show that LIP expression leads to DOR shuttling from the nucleus to the cytoplasm.

This study is important because our finding that LIP expression is involved in the autophagic process may help resolve the paradox over whether LIP is pro- or anti-tumorigenic. This may be due to the fact that autophagy has dual roles in cancer as described above. We propose that at early stages of tumor development, LIP expression leads to attenuation of cell proliferation, induction of autophagy and cell death of damaged cells. Yet at later stages, expression of LIP may stimulate autophagy and lead to cell survival, playing a pro-tumorigenic role.

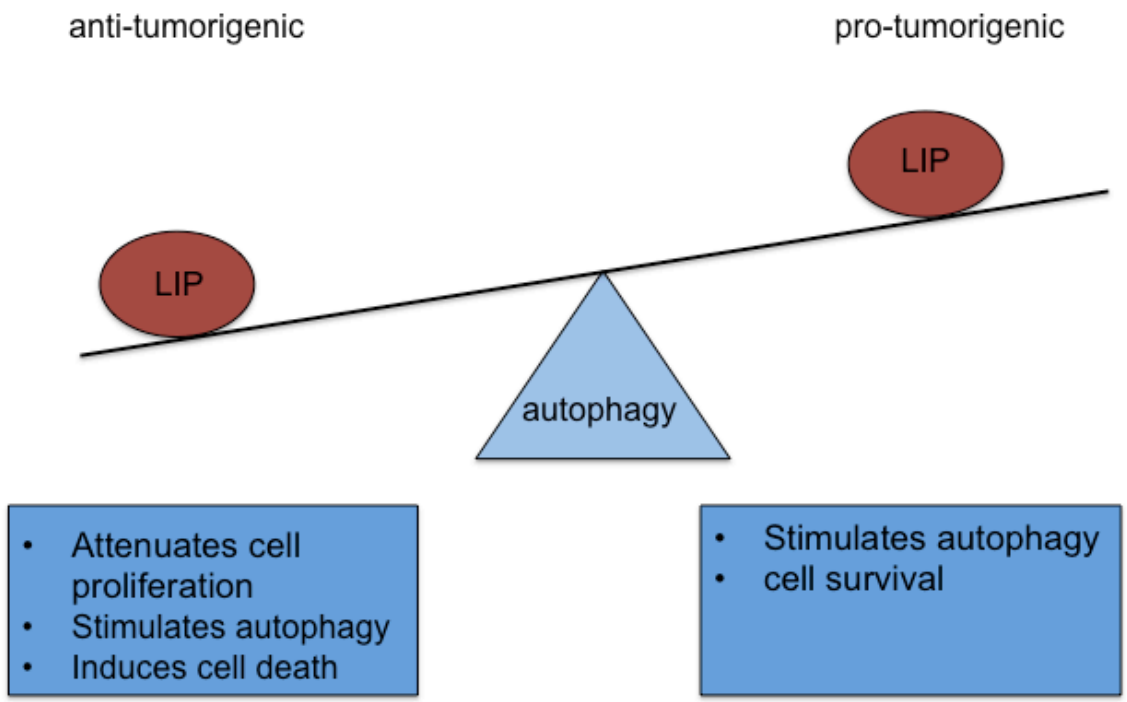

Figure 31. LIP may have dual roles in tumor development and progression. At early stages of tumor development, LIP may have anti-tumorigenic roles. LIP expression attenuates proliferation, stimulates autophagy that may lead to the demise of damaged cells. Later stages of tumor progression, LIP stimulation of autophagy may lead to cell survival providing a pro-tumorigenic role.

The intensely investigated process of autophagy continues to evolve. Interestingly, proposed increases in autophagy are based on the fact that levels of autophagy-related proteins are higher during certain drug treatments or stimulation by various factors. Yet, up-regulation of autophagy markers does not necessarily mean increased autophagic flux. In fact, evidence suggests that if autophagy is functioning properly, accumulation of autophagic compartments rarely occurs. Accordingly, it is possible that the observed increase in autophagic markers is actually a reflection of a compromise in the clearance of autophagic compartments, rather than in their formation. Accumulation of autophagolysosomes can contribute to cell toxicity and be detrimental for the affected cells. Remarkably, this toxic effect of the 'congestion' of the autophagic pathway is currently being explored for therapeutic purposes.

C/EBPbeta3 (LIP) and cell engulfment

While exogenous expression of LIP leads to the presence of autophagic markers it also leads to massive cell death. Low levels of LIP may stimulate autophagy and promote cell survival, but our data provides evidence that high levels of LIP leads to cell death. Yet, many of the original claims of "cell death by autophagy" have currently been revised and reformulated as "cell death with autophagy". These revisions led us to further query the literature for different types of cell death that do not involve apoptosis or necrosis. Through this literature mining, we came across entosis, a nonapoptotic cell death mechanism by cell-in-cell invasion. During this process, the internalized cells detected in suspended MCF10A and MCF7 cultures closely resemble commonly observed

cytological features referred to as cell-in-cell or cell cannibalism in clinical cancer specimens. These features are most frequently detected in metastatic tumor cells that grow in a partial state of suspension in fluid exudates, as those observed in the pleural space surrounding the lungs. During entosis, cells that are grown in suspension invade neighboring cells and this leads to the formation of cell-in-cell structures. This *in vitro* model mimics distinguishing features of the cell-in-cell phenomenon observed in human tumor cells in fluid exudates. In their studies, Overholtzer et al. suggest that entosis may have tumor suppressive roles, as the fate of many target cells is cell death. Additionally, they assayed MCF7 cells for anchorage-independent growth in soft agar. Inhibiting entosis leads to a 10-fold increase in colony formation implying that entosis could oppose proliferation to inhibit the number and size of soft agar colonies. Entosis, however, is not the only process described in the literature that leads to cell-in-cell structures. Many have described various homotypic and heterotypic cell interactions since the 1800's. Yet, the exact role of cell-in-cell structures is poorly understood. Interestingly, they are frequently associated with metastatic disease. To our knowledge, there are no reports of a transcription factor that may play a role in live cell engulfment.

In chapter 3 of this work, the data presented illustrates a role for LIP in mediating cell engulfment. Overexpression of LIP in breast cancer cell lines leads to cell death. It also leads to the appearance of very vacuolated cells and multinucleated cells. When we analyzed the DNA content of LIP-expressing cells, we were able to detect an increase in cells that had more than 2n DNA

content in this population. After this initial clue that LIP may be involved in cell engulfment, we used a number of tools to monitor this process. Taking advantage of fluorescent-labeled dyes and microscopy, we were able track the green LIP-expressing cells engulfing neighboring fluorescent-labeled cells as illustrated in Figure 18. We monitored this process by live cell imaging and found that engulfed cells can also be released. However, it is likely that the fate of the majority of engulfed cells is cell death. In addition, we were able to detect the disintegration of both host and target cells in our live cell imaging experiments. Ultrastructure analysis was performed and we found various engulfing intermediates and the presence of a target cell within the host cell's vacuole. I was able to develop a quantitative method to monitor cell engulfment and on average we detect 30% of LIP-expressing cells engulf target cells. Engulfment was significantly diminished upon treating with a ROCK inhibitor. Engulfment does not appear to require "eat me" signals (PtdSer exposure). Notably, cell engulfment was observed whether or not adenovirus was employed to overexpress LIP.

Engulfment can be pro- or anti- tumorigenic

The role of cell-in-cell structures, which is defined as a cell enclosing another cell within its cytoplasm, is becoming an important morphologic feature to distinguish benign from malignant lesions. There are various processes that have been described that lead to cell-in-cell structures. Ongoing research is focused on the nature and the significance of processes such as entosis and cell cannibalism in cancer. Entosis was shown to have tumor suppressive roles and

the majority of the live cells that invade into neighboring cells end up dying through lysosomal cell death. While LIP-expressing cells have similar characteristics to those described during the entosis process, LIP expression resembles more of a cell cannibalism process. In our case, LIP-expressing cells actively engulf the neighboring cells. As previously mentioned, cell-in-cell phenomenon have been observed in human tumor cells in fluid exudates. When Gomis et al. examined pleural effusion samples isolated from patients with metastatic breast cancer, this study found an elevation in LIP protein levels.

While the exact role of cell cannibalism is unknown one can speculate that it may be a feature of malignant cells to control tumor growth. It may be one of the last attempts to remove neighboring cells before they reach their metastatic site. In 1984, Brouwer et al. reported that in cell lines of human small cell carcinoma of the lung (SCCL), cells were observed which completely interiorized other cells leading to death of the target cells and many times to complete self-destruction of the cultures. They refer to this phenomenon as “cell cannibalism” and found it to be conserved in fresh tumor biopsies from SCCL patients. Cell cannibalism was absent in serum-free cultured cells but could be re-induced by serum exposure. Therefore they proposed that serum factors are responsible for the induction of cannibalism in cells. In different ultrastructural studies, lysosomal structures are noted to be scarce in cannibalistic host cells in comparison to the target cells. Therefore, it has been postulated that the target cells apparently die due to the lack of nutrition. If engulfment or cell cannibalism

leads to cell death of the target cell and many times both the target and host cell die, then cell cannibalism may play a role in tumor suppression (Figure 32).

In recent Drosophila studies, Ohsawa et al. have identified a new tumor-suppression mechanism that eliminates oncogenic imaginal epithelial cells (Ohsawa *et al*., 2011). Mutant epithelial cells that have lost their apicobasal polarity are actually engulfed and eliminated by surrounding normal epithelial cells. Engulfment is dependent on the activation of nonapoptotic JNK signaling in the normal imaginal cells in response to the emergence of neoplastic mutant cells (Ohsawa *et al*., 2011). Given that many components of the Drosophila antitumor cell engulfment pathway are conserved from flies to human, Ohsawa et al speculate that this is an evolutionarily conserved intrinsic tumor-suppression mechanism that may also exist in normal epithelium (Ohsawa *et al*., 2011). Inducing cell cannibalism that leads to this form of “neighborhood watch” and leads to cell death could be a valuable way of inducing alternative cell death programs in tumors that have defective apoptotic machinery.

There is an abundant amount of work published since the mid 1950’s that shows that tumor cells can engulf not only their siblings, but also a variety of cell types. Heterotypic interactions have been reported between tumor host cells and neutrophils, lymphocytes, natural killer (NK) cells, as well as erythrocytes to list a few (Overholtzer and Brugge, 2008). NK cell internalization has been shown to precede target tumor cell death and NK cell self-destruction, suggesting that this cell-in-cell pathway is a mechanism to kill tumor cells (Xia *et al*., 2008). On the other hand, there is data to suggest that tumor cells can engulf and kill

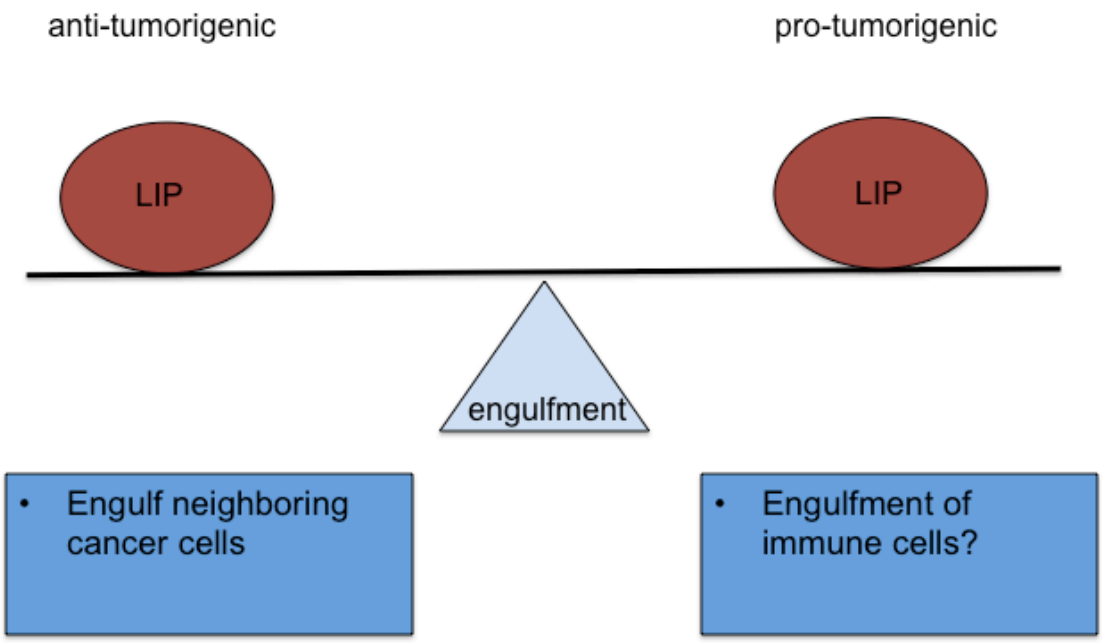

Figure 32. LIP may have dual roles in tumor progression. LIP stimulates engulfment of neighboring cells, which leads to the removal and death of these sibling tumor cells. Hence, LIP engulfment may have anti-tumorigenic roles. However, LIP may stimulate engulfment of immune cells, which leads to escape of immune surveillance providing a pro-tumorigenic role.

lymphocytes, neutrophils, and T cells that are involved in tumor immune response. Therefore, metastatic tumor cells may use cannibalism as mechanism to escape tumor immune surveillance. If tumor cells not only escape immune surveillance, but also cannibalize sibling cells to survive in adverse conditions such as those they encounter during metastasis this behavior favors a pro-tumorigenic role for cell cannibalism (Figure 32). Understanding the role of cell cannibalism in cancer is thus imperative as it can be utilized as an innovative pharmacological target in the clinical management of metastatic disease.

Using the quantitative cell engulfment assays described in this work would be a good method to address whether LIP-expressing cancer cells can engulf all cells including “normal” epithelial cells. As described by Ohsawa et al., mutant epithelial cells that have lost their apicobasal polarity become targeted for engulfment. These cells are eliminated by surrounding normal epithelial. Future studies could focus on cell polarity and its role in LIP-mediated cell engulfment. In addition, it is important to test whether overexpression of LIP in other breast cancer cell lines leads to this same phenomenon. Finally, it is of great interest to determine whether LIP-expressing cancer cells engulf immune cells, such as NK cells or macrophages.

C/EBPbeta3 (LIP) and transcriptional regulation

In order to gain insight into the mechanism by which LIP expression leads to cell engulfment, autophagy, and the massive cell death that follows, we sought to identify some of the specific genes targeted by this transcription factor. We were surprised when we detected such few changes in gene expression in both

cell lines tested. While large fold changes were absent at the 48hr post-infection time point, it is important to note that it could be the sum of all the small fold changes that are essential for the phenotype observed upon LIP expression. Nevertheless, we do detect a significant increase in HSPA1A mRNA levels in the MDA-MB-231 cells, which I confirmed with qPCR. While we detect a small increase in cellular HSP70 protein, I was able to show a substantial increase in HSP70 in exosomes isolated from LIP-expressing MDA-MB-231 cells.

Although LIP is thought to function as a transcription repressor, the most significant change we observed is an increase in HSPA1A transcripts. Hence, LIP may play other roles besides transcription repression in cells. We are unable to conclude at this time whether the transcriptional upregulation is through direct regulation via DNA binding or whether LIP indirectly regulates transcription through combinatorial control and its interactions with numerous factors in the nucleus. LIP may repress or through protein-protein interactions sequester factors including repressors that may be involved in regulating HSPA1A transcription.

C/EBPbeta3 (LIP) and exosome secretion

It is known that exosomes play a role in intercellular communications and we tested whether these exosomes are involved in cell engulfment. Conditioning of cells with LIP-derived exosomes lead to an increase in cell engulfment at 24hrs post-infection. This data suggest that LIP-derived exosomes are “carrying messages” to target cells to mark them for engulfment. While we were always puzzled by the length of time it took to observe changes in autophagy markers,

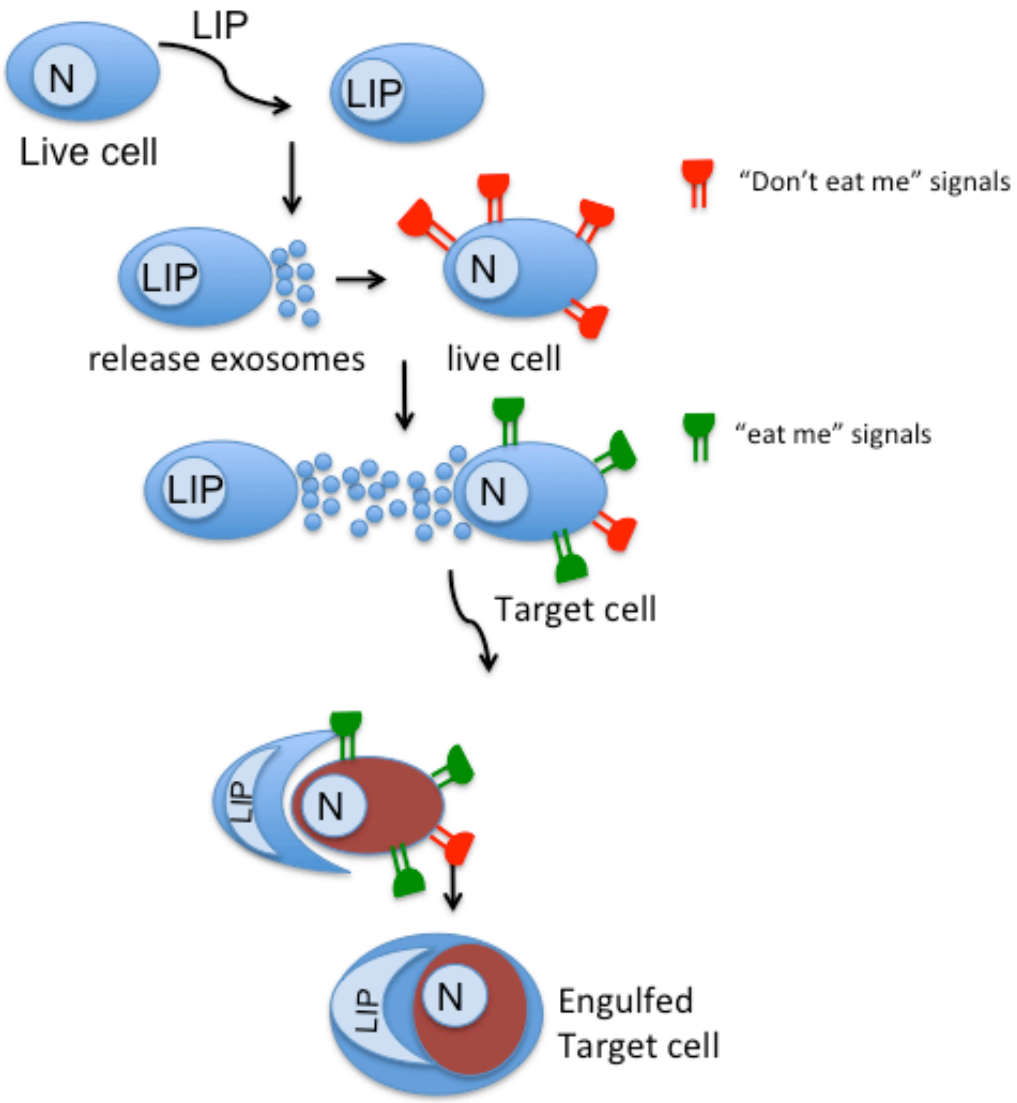

Figure 33. LIP-mediated cell engulfment. High levels of LIP lead to increases in exosome secretion. These exosomes deliver messages which condition neighboring cells and "marks" them as target cells for engulfment.

engulfment, and cell death upon LIP expression, one possibility for the lag between LIP overexpression and significant cell engulfment may be due to the time required to mark cells as potential targets. Once exposed to exosomes secreted from LIP-expressing cells, this marks the cell to be engulfed and destroyed (Figure 33).

What changes or marks these cells for engulfment is an area that needs to be further explored. It is known that exosomes contain between 300-500 proteins. mRNAs and even miRNAs are also components of exosomes. It would be interesting to compare exosomes isolated from control uninfected, Ad-GFP, and Ad-LIP MDA-MB-231 cells. Proteomic analysis, genomic profiling, as well as miRNA profiling would be very useful tools to gain information on the contents of LIP-derived exosomes. It is also known that different cells phagocytose exosomes based on specific molecules that may coat the outer surface of the exosomal membrane. While we do not detect changes in PtdSer exposure in LIP-expressing cells, it would be valuable to determine whether LIP-derived exosomes present different types of “eat me” signals including PtdSer exposure that can be recognized by the target cells.

Additionally, while there are many types of “eat me” signals described in the literature, there are new findings that also describe “don’t eat me” signals. Recent work shows that CD47 functions as a binding partner for thrombospondin-1 and as a ligand for the transmembrane signal regulatory protein (SIRP)-alpha. CD47 appears to function as a molecular switch from “don’t eat me signal” to “eat me” signals depending on its conformational change

and interaction partners. Expression of the glycoprotein CD31 has also been shown to be function as a “don’t eat me” signal. Thus, characterizing the cell surface expression of these proteins in the control uninfected, Ad-GFP, and Ad-LIP MDA-MB-468 cells is of great interest.

LIP expression may lead to many cell fates

Our data provides strong evidence that exogenous expression of LIP leads to cell death. However, our time-lapse microscopy and conditioning with LIP-derived exosomes allows us to speculate on the many cell fates that can occur due to LIP overexpression (Figure 34). As the time-lapse movies show, engulfed cells can be released. Whether these cells that escape stay alive and are somewhat more aggressive, sustaining harsh conditions while in the lysosome of the host cell and staying alive, is a possibility that cannot be ruled out and an area for further investigations. As shown in movie 4, cells that have been engulfed appear to disintegrate along with the host cells. We also detect LIP-expressing cells that have engulfed two or more cells. This hyperphagic behavior may also lead to cell death due to oxidative imbalances in the cell. In fact, Tinari et al., propose that large amounts of toxic species derived from the over-ingestion of oxidized components and organelles from cannibalized cells, could provoke cell death (Tinari et al., 2008). LIP overexpression may also lead to overconsumption of itself with the continuous stimulation of autophagy. In these studies, we did not perform autophagic flux experiments. It may very well be that LIP overexpression blocks the completion of autophagy and hence this leads to increases in toxic substances leading to the demise of the cell. Finally, we show

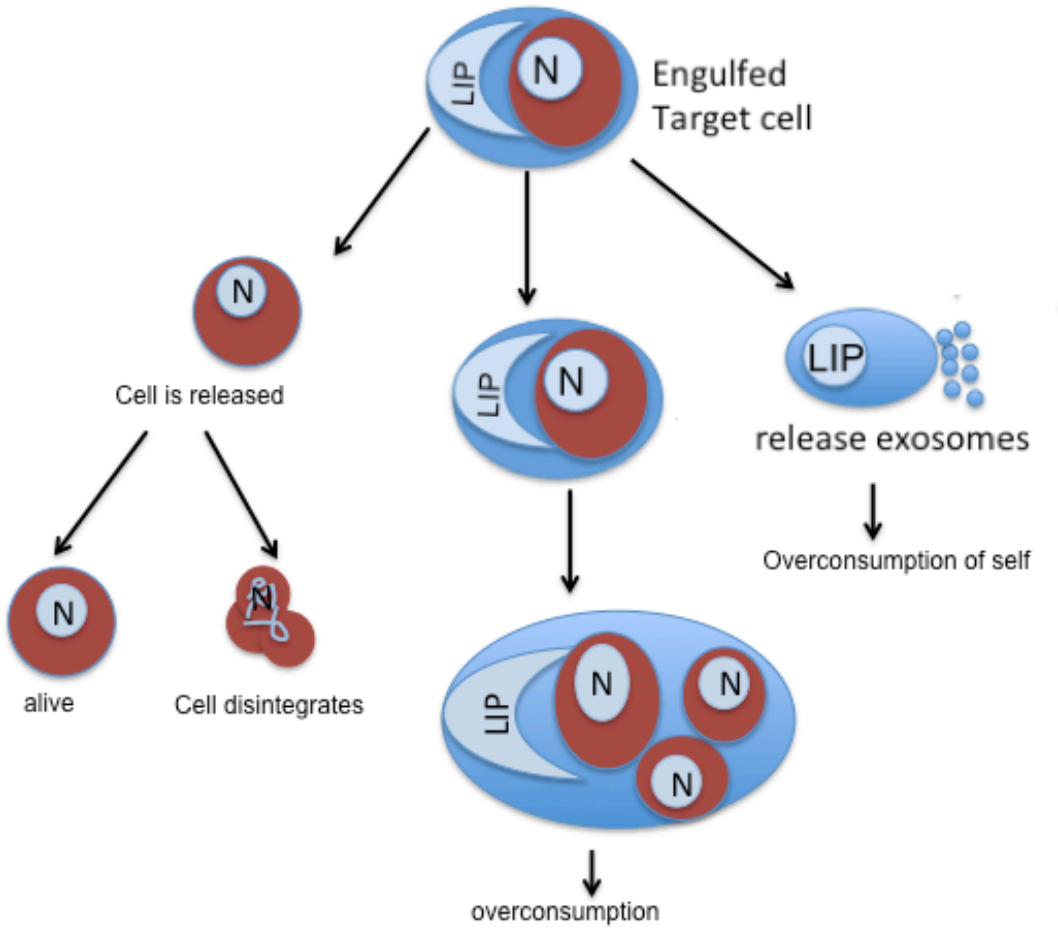

Figure 34. The many cell fates of LIP-expressing cells. LIP expression can result in cell being released and possibly staying alive or disintegrating. LIP overexpression may lead to cell death due to hyperphagia or overconsumption of other cells or itself.

preliminary data that LIP-derived exosomes mark neighboring cells as prey. Neighboring cells that are not overexpressing LIP can then engulf these target cells. Uncovering the mechanism(s) by which LIP overexpression marks cells as prey for cell engulfment and ultimately leads to cell death is an area that merits future investigation. This may lead to a greater understanding of not only how cells communicate in the tumor microenvironment, but help find ways to deliver messages of self-destruction to tumor cells or even stromal cells that may be feeding the tumor cells.

A possible physiological role for LIP-mediated cell engulfment

The mammary gland undergoes cycles of growth, differentiation, milk secretion, regression, and remodeling. C/EBPbeta is critical for normal mammary gland development. Each C/EBPbeta isoform may play a role at different stages of mammary gland development. Our studies provide strong evidence that exogenous expression of LIP leads to cell engulfment of neighboring cells. In an attempt to uncover a physiological role for LIP-mediated cell engulfment, we analyzed LIP protein levels during involution. Involution begins with the cessation of milk secretion. During this process, the mammary gland resorbs the elaborate milk-producing lobuloalveoli generated during pregnancy and returns to its rudimentary, ductal state. Phagocytes and neighboring living epithelial cells engulf dying cells to prevent inflammation and autoimmune response against intracellular antigens. Interestingly, when we analyzed LIP protein levels at different stages of the mammary gland (pregnancy, lactation, to involution), we were able to show that LIP protein levels increase in mouse mammary glands

during the involution process.

It is well known that key mechanisms involved in normal mammary gland development are hijacked, bypassed or corrupted during the development and progression of breast cancer. From our data, we can speculate that LIP levels are increased in the involuting gland in order to engulf and remove dying cells. Remarkably, exosomes are present and function at the different stages of mammary gland development (Hendrix and Hume, 2011). For instance, breast milk has been shown to contain exosomes with the capacity to influence immune responses in infants. Also, exosome-secreted milk fat globule EGF factor 8 (MFG-E8) is involved in the recognition and clearance of apoptotic mammary epithelial cells during mammary involution (Hendrix and Hume, 2011). Since we observe an increase in LIP levels during involution and we show LIP-derived exosomes may mark cells for engulfment, it would be fitting to examine the expression levels of MFG-E8 or factors similar to it that are involved in the recognition and targeting of neighboring tumor cells in the MDA-MB-468 cells.

Remodeling of the mammary gland during involution is associated with an influx of immune cells, MMP-dependent ECM reorganization and loss of basement membrane functions with subsequent release of growth factors and bioactive fibronectin fragments. For this reason, it is proposed that the involution process supports metastasis. Additionally, some suggest that exosomes released during involution communicate to regional lymph nodes or distant organs, inducing a favorable niche for cancer cells. However, it would be beneficial to find a way to hijack the early steps of this normal physiological

process during cancer and cause the engulfment of neighboring tumor cells, which ultimately leads to cell death.

In conclusion, this work demonstrates a role for C/EBPbeta3 (LIP) in stimulating autophagy and cell engulfment in breast cancer cells. Exogenous expression of LIP leads to an increase in exosome secretion, which appear to communicate with target cells and mark them for engulfment. High levels of LIP ultimately lead to cell death in breast cancer cell lines. A normal physiological role for these processes induced by LIP may occur during involution of the mammary gland postlactation.

REFERENCES

Aderem A, Underhill DM (1999) Mechanisms of phagocytosis in macrophages. *Annu Rev Immunol* **17**:593-623.

Akira S, Isshiki H, Sugita H, Tanabe O, Kinoshita S, Nishio Y, *et al*. (1990) A nuclear factor for IL-6 expression (NF-IL6) is a member of a C/EBP family. *EMBO J* **9**: 1897–1906.

Arnal-Estapé A, Tarragona M, Morales M, Guiu M, Nadal C, Massagué J, Gomis RR (2010) HER2 silences tumor suppression in breast cancer cells by switching expression of C/EBPbeta isoforms. *Cancer Res* **70**(23): 9927-9936.

Atwood AA, Sealy L (2010) Regulation of C/EBPbeta1 by Ras in mammary epithelial cells and the role of C/EBPbeta1 in oncogene-induced senescence. *Oncogene* **29**(45): 6004-6015.

Atwood AA, Jerrell R, Sealy L (2011) Negative regulation of C/EBPbeta1 by sumoylation in breast cancer cells. *PLoS One* **6**(9): e25205.

Baer M, Johnson PF (2000) Generation of truncated C/EBPbeta isoforms by in vitro proteolysis. *J Biol Chem* **275**(34): 26582-26590.

Baldwin BR, Timchenko NA, Zahnow CA (2004) Epidermal growth factor receptor stimulation activates the RNA binding protein CUG-BP1 and increases expression of C/EBPbeta-LIP in mammary epithelial cells. *Mol Cell Biol* **24**(9): 3682-3691.

Balogh GA, Heulings R, Mailo DA, Russo PA, Sheriff F, Russo IH, *et al*. (2006) Genomic signature induced by pregnancy in the human breast. *Int J Oncol* **28**(2): 399–410.

Barros, LF, Hermosilla T, and Castro J (2001) Necrotic volume increase and the early physiology of necrosis. *Comp Biochem Physiol A Mol Integr Physiol* **130**: 401–409.

Baumgartner BG, Orpinell M, Duran J, Ribas V, Burghardt HE, Bach D, *et al*. (2007) Identification of a novel modulator of thyroid hormone receptor-mediated action. *PLoS One* **2**(11): e1183.

Bratton DL, Fadok VA, Richter DA, Kailey JM, Guthrie LA, Henson PM (1997) Appearance of phosphatidylserine on apoptotic cells requires calcium-mediated nonspecific flip-flop and is enhanced by loss of the aminophospholipid translocase. *J Biol Chem* **272**(42): 26159-26165.

Bristol JA, Morrison TE, Kenney SC (2009) CCAAT/enhancer binding proteins alpha and beta regulate the tumor necrosis factor receptor 1 gene promoter. *Mol Immunol* **46**(13): 2706-2713.

Brody LC, Biesecker BB (1998) Breast cancer susceptibility genes. BRCA1 and BRCA2. *Medicine* (Baltimore) **77**(3): 208-226.

Brouwer M, de Ley L, Feltkamp CA, Elema J, Jongsma AP (1984) Serum-dependent "cannibalism" and autodestruction in cultures of human small cell carcinoma of the lung. *Cancer Res* **44**(7): 2947-2951.

Bundy LM, Sealy L (2003) CCAAT/enhancer binding protein beta (C/EBPbeta)-2 transforms normal mammary epithelial cells and induces epithelial to mesenchymal transition in culture. *Oncogene* **22**(6):869-883.

Bundy L, Wells S, Sealy L (2005) C/EBPbeta-2 confers EGF-independent growth and disrupts the normal acinar architecture of human mammary epithelial cells. *Mol Cancer* **4**:43.

Bursch W (2001) The autophagosomal-lysosomal compartment in programmed cell death. *Cell Death Differ* **8**: 569–581.

Calkhoven CF, Müller C, Leutz A (2000) Translational control of C/EBPalpha and C/EBPbeta isoform expression *Genes D*ev **14**(15): 1920-1932.

Cao Z, Umek RM, McKnight SL (1991) Regulated expression of three C/EBP isoforms during adipose conversion of 3T3-L1 cells. *Genes Dev* **5**(9): 1538-1552.

Chautan M, Chazal G, Cecconi F, Gruss P, Golstein P (1999) Interdigital cell death can occur through a necrotic and caspase-independent pathway. *Curr Biol* **9**(17): 967-970.

Christofferson DE, Yuan J (2010) Necroptosis as an alternative form of programmed cell death. *Curr Opin Cell Biol* **22**(2): 263-268.

Clarke PG (1990) Developmental cell death: morphological diversity and multiple mechanisms *Anat Embryol* (Berl.) **181**:195–213.

Cohen GM (1997) Caspases: the executioners of apoptosis. *Biochem J* **326** (Pt1): 1–16.

Connelly L, Robinson-Benion C, Chont M, Saint-Jean L, Li H, Polosukhin VV, et al. (2007) A transgenic model reveals important roles for the NF-kappa B alternative pathway (p100/p52) in mammary development and links to tumorigenesis. *J Biol Chem* **282**(13): 10028-10035.

Coombs NJ, Cronin KA, Taylor RJ, Freedman AN, Boyages J (2010) The impact of changes in hormone therapy on breast cancer incidence in the US population. *Cancer Causes Control* **21**(1): 83-90.

Copetti T, Bertoli C, Dalla E, Demarchi F, Schneider C (2009) p65/RelA modulates BECN1 transcription and autophagy. *Mol Cell Biol*. **29**:2594–2608.

Crighton D, Wilkinson S, O'Prey J, Syed N, Smith P, Harrison PR, *et al*. (2006) DRAM, a p53-induced modulator of autophagy, is critical for apoptosis. *Cell* **126**: 121–134.

da Silva KP, Borges JC (2011) The molecular chaperone Hsp70 family members function by a bidirectional heterotrophic allosteric mechanism. *Protein Pept Lett* **18**(2): 132-142.

D'Cruz CM, Moody SE, Master SR, Hartman JL, Keiper EA, Imielinski MB, *et al*. (2002) Persistent parity-induced changes in growth factors, TGF-beta3, and differentiation in the rodent mammary gland. *Mol Endocrinol* **16**(9): 2034–2051.

Dearth LR, Hutt J, Sattler A, Gigliotti A, and DeWille J (2001). Expression and function of CCAAT/enhancer bind- ing proteinbeta (C/EBPbeta) LAP and LIP isoforms in mouse mammary gland, tumors and cultured mammary epithelial cells. *J Cell Biochem* **82**:357–370.

Debnath J, Brugge JS (2005) Modelling glandular epithelial cancers in three-dimensional cultures. *Nat Rev Cancer* **5**(9): 675-688.

Degenhardt K, Mathew R, Beaudoin B, Bray K, Anderson D, Chen G, *et al*. (2006) Autophagy promotes tumor cell survival and restricts necrosis, inflammation, and tumorigenesis. *Cancer Cell* **10**:51–64.

Degryse B, Bonaldi T, Scaffidi P, Muller S, Resnati M, Sanvito F, *et al*. (2001) The High Mobility Group (HMB) Boxes of the Nuclear Protein HMG1 induce chemotaxis and cytoskeleton reorganization in rat smooth muscle cells. *Journal of Cell Biology* **152**: 1197–1206.

Degterev A, Huang Z, Boyce M, Li Y, Jagtap P, Mizushima N, et al (2005) Chemical inhibitor of nonapoptotic cell death with therapeutic potential for ischemic brain injury. *Nat Chem Biol* **1**(2): 112-119.

Descombes P, Chojkier M, Lichtsteiner S, Falvey E, and Schibler U (1990) LAP, a novel member of the C/EBP gene family, encodes a liver-enriched transcriptional activator protein. *Genes Dev* **4**: 1541–1551.

Descombes P, Schibler U (1991) A liver-enriched transcriptional activator protein, LAP, and a transcriptional inhibitory protein, LIP, are translated from the same mRNA. *Cell* **67**:569–579.

Duong DT, Waltner-Law ME, Sears R, Sealy L, Granner DK (2002) Insulin inhibits hepatocellular glucose production by utilizing liver-enriched transcriptional inhibitory protein to disrupt the association of CREB-binding protein and RNA polymerase II with the phosphoenolpyruvate carboxykinase gene promoter. *J Biol Chem* **277**: 32234–32242.

Eaton EM, Hanlon M, Bundy L, Sealy L. (2001) Characterization of C/EBPbeta isoforms in normal versus neoplastic mammary epithelial cells. *J Cell Physiol* **189**(1): 91-105.

Eaton EM, Sealy L (2003) Modification of CCAAT/enhancer-binding protein-beta by the small ubiquitin-like modifier (SUMO) family members, SUMO-2 and SUMO-3. *J Biol Chem* **278**(35): 33416-33421.

Ellisen LW, Haber DA (1998) Hereditary breast cancer. *Annu Rev Med* **49**: 425-36.

Elmore S (2007) Apoptosis: a review of programmed cell death. *Toxicol Pathol* **35**(4): 495-516.

Fadok VA, de Cathelineau A, Daleke DL, Henson PM, Bratton DL (2001) Loss of phospholipid asymmetry and surface exposure of phosphatidylserine is required for phagocytosis of apoptotic cells by macrophages and fibroblasts. *J Biol Chem* **276**(2): 1071-1077.

Fadok VA, Voelker DR, Campbell PA, Cohen JJ, Bratton DL, Henson PM (1992) Exposure of phosphatidylserine on the surface of apoptotic lymphocytes triggers specific recognition and removal by macrophages. *J Immunol* **148**(7): 2207-2216.

Festjens N, Vanden Berghe T, Vandenabeele P (2006) Necrosis, a well-orchestrated form of cell demise: signalling cascades, important mediators and concomitant immune response. *Biochim Biophys Acta* **1757**(9-10): 1371-1387.

Florey O, Kim SE, Sandoval CP, Haynes CM, Overholtzer M (2011) Autophagy machinery mediates macroendocytic processing and entotic cell death by targeting single membranes. *Nat Cell Biol* **13**(11): 1335-1343.

Frank DA (2009) Targeting transcription factors for cancer therapy. *IDrugs* **12**(1): 29-33.

Fuchs Y, Steller H (2011) Programmed cell death in animal development and disease. *Cell* **147**(4): 742-758.

Gardai SJ, Bratton DL, Ogden CA, Henson PM (2006) Recognition ligands on apoptotic cells: a perspective. *J Leukoc Biol* **79**(5): 896-903.

Geiss-Friedlander R, Melchior F (2007) Concepts in sumoylation: a decade on. *Nat Rev Mol Cell Biol* **8**(12): 947-956.

Geng J, Klionsky DJ (2008) The Atg8 and Atg12 ubiquitin-like conjugation systems in macroautophagy. 'Protein modifications: beyond the usual suspects' review series. *EMBO Rep* **9**:859–864.

Glinskii AB, Glinsky GV, Lin HY, Tang HY, Sun M, Davis FB et al. (2009). Modification of survival pathway gene expression in human breast cancer cells by tetraiodothyroacetic acid (tetrac). *Cell Cycle* **8**: 3554–3562.

Golstein P, Kroemer G (2007) Cell death by necrosis: towards a molecular definition. *Trends Biochem Sci* **32**(1): 37-43.

Gomis RR, et al. C/EBPbeta at the core of the TGFbeta cytostatic response and its evasion in metastatic breast cancer cells. Cancer Cell. 2006;10:203–214.

Gozuacik D, Kimchi A (2004) Autophagy as a cell death and tumor suppressor mechanism. *Oncogene* **23**(16): 2891-2906.

Greenbaum LE, Li W, Cressman DE, Peng Y, Ciliberto G, Poli V, Taub R (1998) CCAAT enhancer- binding protein beta is required for normal hepatocyte proliferation in mice after partial hepatectomy. *J Clin Invest* **102**(5): 996-1007.

Grimm SL, Rosen JM (2003) The role of C/EBPbeta in mammary gland development and breast cancer. *J Mammary Gland Biol Neoplasia* **8**(2): 191-204.

Hanahan D, Weinberg RA (2000) The hallmarks of cancer. *Cell* **100**(1): 57-70.

Hendrix A, Hume AN (2011) Exosome signaling in mammary gland development and cancer. *Int J Dev Biol* **55**(7-9): 879-887.

Hennighausen L, Robinson GW (2005) Information networks in the mammary gland. *Nat Rev Mol Cell Biol* **6**(9): 715-725.

Hippert MM, O'Toole PS, Thorburn A (2006) Autophagy in cancer: good, bad, or both? *Cancer Res* **66**:9349–9351.

Hirsch T, Marchetti P, Susin SA, Dallaporta B, Zamzami N, Marzo I, Geuskens M, Kroemer G (1997) The apoptosis-necrosis paradox. Apoptogenic proteases activated after mitochondrial permeability transition determine the mode of cell death. *Oncogene* **15**:1573–1581.

Horvitz HR (1999) Genetic control of programmed cell death in the nematode *Caenorhabditis elegans*. *Cancer Res* **59**:1701s–1706s.

Høyer-Hansen M, Jäättelä M (2007) Connecting endoplasmic reticulum stress to autophagy by unfolded protein response and calcium. *Cell Death Differ* **14**:1576–1582.

Humble JG, Jayne WH, Pulvertaft RJ (1956) Biological interaction between lymphocytes and other cells. *Br J Haematol* **2**: 283–294.

Igney FH, Krammer PH (2002) Death and anti-death: tumour resistance to apoptosis. *Nat Rev Cancer* **2**(4): 277-288.

Johnson, PF and McKnight SL (1989) Eukaryotic transcriptional regulatory proteins. *Annu Rev Biochem* **58**: 799–839.

Johnstone RM, Adam M, Hammond JR, Orr L, Turbide C (1987) Vesicle formation during reticulocyte maturation. Association of plasma membrane activities with released vesicles (exosomes) *J Biol Chem* **262**: 9412‑9420.

Jurado LA, Song S, Roesler WJ, Park EA (2002) Conserved amino acids within CCAAT enhancer-binding proteins (C/EBP(alpha) and beta) regulate phosphoenolpyruvate carboxykinase (PEPCK) gene expression. *J Biol Chem* **277**(31): 27606-27612.

Kabeya Y, Mizushima N, Ueno T, Yamamoto A, Kirisako T, Noda T, *et al*. (2000) LC3, a mammalian homologue of yeast Apg8p, is localized in autophagosome membranes after processing. *EMBO J* **19**(21): 5720-5728.

Kanduc D, Mittelman A, Serpico R, Sinigaglia E, Sinha AA, Natale C, et al. (2002) Cell death: apoptosis versus necrosis. *Int J Oncol* **21**(1): 165-170.

Karamouzis MV, Gorgoulis VG, Papavassiliou AG (2002) Transcription factors and neoplasia: vistas in novel drug design. *Clin Cancer Res* **8**(5): 949-961.

Kerr, JF, Wyllie AH, and Currie AR (1972) Apoptosis: a basic biological phenomenon with wide-ranging implications in tissue kinetics. *Br J Cancer* **26**: 239–257.

Klionsky DJ, Emr SD (2000) Autophagy as a regulated pathway of cellular degradation. *Science* **290**:1717–1721.

Klionsky DJ, Cuervo AM, Seglen PO (2007) Methods for monitoring autophagy from yeast to human. *Autophagy* **3**:181–206.

Klionsky DJ (2007) Autophagy: from phenomenology to molecular understanding in less than a decade. *Nature Rev Mol Cell Biol* **8**: 931–937.

Klionsky DJ, Abeliovich H, Agostinis P, Agrawal DK, Aliev G, Askew DS, et al. (2008) Guidelines for the use and interpretation of assays for monitoring autophagy in higher eukaryotes. Autophagy **4**(2): 151-175.

Koslowski M, Türeci O, Biesterfeld S, Seitz G, Huber C, Sahin U (2009) Selective activation of trophoblast-specific PLAC1 in breast cancer by CCAAT/enhancer-binding protein beta (C/EBPbeta) isoform 2. *J Biol Chem* **284**(42): 28607-28615.

Kowenz-Leutz E, Leutz A (1999) A C/EBP beta isoform recruits the SWI/SNF complex to activate myeloid genes. *Mol Cell* **4**(5): 735-743.

Krick R, Bremer S, Welter E, Eskelinen EL, Thumm M (2011) Cheating on ubiquitin with Atg8. *Autophagy* **7**(2): 250-251.

Kurosaka K, Takahashi M, Watanabe N, Kobayashi Y (2003) Silent cleanup of very early apoptotic cells by macrophages. *J Immunol* **171**(9): 4672-4679.

Landschulz WH, Johnson PF, Adashi EY, Graves BJ, McKnight SL (1988) Isolation of a recombinant copy of the gene encoding C/EBP. *Genes Dev* **2**(7): 786-800.

Lauber K, Blumenthal SG, Waibel M, Wesselborg S (2004) Clearance of apoptotic cells: getting rid of the corpses. *Mol Cell* **14**(3): 277-287.

La Vecchia C, Giordano SH, Hortobagyi GN, Chabner B (2011) Overweight, obesity, diabetes, and risk of breast cancer: interlocking pieces of the puzzle. *Oncologist*. **16**(6): 726-729.

Lekstrom-Himes J, Xanthopoulos KG (1998) Biological role of the CCAAT/enhancer-binding protein family of transcription factors. *J Biol Chem* **273**(44): 28545-28548.

Levine B, Klionsky DJ (2004) Development by self-digestion: molecular mechanisms and biological functions of autophagy. *Dev Cell* **6**: 463–477.

Levine B, Yuan J (2005) Autophagy in cell death: an innocent convict? *J Clin Invest* **115**(10): 2679-2688.

Li Y, Bevilacqua E, Chiribau CB, Majumder M, Wang C, Croniger CM, *et al*. (2008) Differential control of the CCAAT/enhancer-binding protein beta (C/EBPbeta) products liver-enriched transcriptional activating protein (LAP) and liver-enriched transcriptional inhibitory protein (LIP) and the regulation of gene expression during the response to endoplasmic reticulum stress. *J Biol Chem* **283**(33): 22443-22456.

Li DD, Wang LL, Deng R, Tang J, Shen Y, Guo JF, *et al*. (2009) The pivotal role of c-Jun NH2-terminal kinase-mediated Beclin 1 expression during anticancer agents-induced autophagy in cancer cells. *Oncogene* **28**:886–898.

Li H, Baldwin BR, Zahnow CA (2011) LIP expression is regulated by IGF-1R signaling and participates in suppression of anoikis. *Mol Cancer* **10**: 100.

Liang XH, Jackson S, Seaman M, Brown K, Kempkes B, Hibshoosh H (1999) Induction of autophagy and inhibition of tumorigenesis by beclin 1. *Nature* **402**: 672–676.

Lin HY, Tang HY, Shih A, Keating T, Cao G, Davis PJ et al. (2007). Thyroid hormone is a MAPK-dependent growth factor for thyroid cancer cells and is anti-apoptotic. *Steroids* **72**: 180–187.

Lin HY, Sun M, Tang HY, Lin C, Luidens MK, Mousa SA et al. (2009). L-Thyroxine vs 3,5,3′-triiodo-L-thyronine and cell proliferation: activation of mitogen-activated protein kinase and phosphatidylinositol 3-kinase. *Am J Physiol Cell Physiol* **296**: C980–C991.

Lincoln AJ, Monczak Y, Williams SC, Johnson PF (1998) Inhibition of CCAAT/enhancer-binding protein alpha and beta translation by upstream open reading frames. *J Biol Chem* **273**(16): 9552-9560.

Madigan MP, Ziegler RG, Benichou J, Byrne C, Hoover RN (1995) Proportion of breast cancer cases in the United States explained by well-established risk factors. *J Natl Cancer Inst* **87**(22): 1681–1685.

Mailleux AA, Overholtzer M, Schmelzle T, Bouillet P, Strasser A, Brugge JS (2007) BIM regulates apoptosis during mammary ductal morphogenesis, and its absence reveals alternative cell death mechanisms. *Dev Cell* **12**(2): 221-234.

Mariño G, Salvador-Montoliu N, Fueyo A, Knecht E, Mizushima N, López-Otín C (2007) Tissue-specific autophagy alterations and increased tumorigenesis in mice deficient in Atg4C/autophagin-3. *J Biol Chem* **282**:18573–18583.

Mastracci TL, Shadeo A, Colby SM, Tuck AB, O'Malley FP, Bull SB et al. (2006) Genomic alterations in lobular neoplasia: a microarray comparative genomic hybridization signature for early neoplastic proliferationin the breast. *Genes Chromosomes Cancer* **45**(11): 1007-1017.

Mathew R, Kongara S, Beaudoin B, Karp CM, Bray K, Degenhardt K, *et al*. (2007) Autophagy suppresses tumor progression by limiting chromosomal instability. *Genes Dev* **21**: 1367–1381.

Mauvezin C, Orpinell M, Francis VA, Mansilla F, Duran J, Ribas V *et al*. (2010) The nuclear cofactor DOR regulates autophagy in mammalian and Drosophila cells. *EMBO Rep* **11**(1): 37-44.

McCormack VA, dos Santos Silva (2006) Breast density and parenchymal patterns as markers of breast cancer risk: a meta-analysis. *Cancer Epidemiol Biomarkers Prev* **15**:1159-1169.

Meijer AJ, Codogno P (2004) Regulation and role of autophagy in mammalian cells. *Int J Biochem Cell Biol* **36**: 2445–2462.

Meir O, Dvash E, Werman A, Rubinstein M (2010) C/EBP-beta regulates endoplasmic reticulum stress-triggered cell death in mouse and human models. *PLoS ONE* **5**:e9516.

Miki Y, Swensen J, Shattuck-Eidens D, Futreal PA, Harshman K, Tavtigian S, *et al*. (1994) A strong candidate for the breast and ovarian cancer susceptibility gene BRCA1. *Science* **266** (5182): 66-71.

Milde-Langosch K, Loning T, Bamberger AM (2003) Expression of the CCAAT/enhancer-binding proteins C/EBPalpha, C/EBPbeta and C/EBPdelta in breast cancer: correlations with clinicopathologic parameters and cell-cycle regulatory proteins. *Breast Cancer Research and Treatment* **79**:175–185.

Miura M, Zhu H, Rotello R, Hartwieg EA and Yuan J (1993) Induction of apoptosis in fibroblasts by IL-1 beta-converting enzyme, a mammalian homolog of the *C. elegans* cell death gene *ced-3*. *Cell* **75**, 653–660.

Monks J, Smith-Steinhart C, Kruk ER, Fadok VA, Henson PM (2008) Epithelial cells remove apoptotic epithelial cells during post-lactation involution of the mouse mammary gland. *Biol Reprod* **78**(4):586-594.

Moynahan ME, Chiu JW, Roller BH, Jasin M (1999) Brcal controls homology-directed DNA repair. *Mol Cell* **4**: 511–518.

Muppidi J, Porter M, Siegel RM (2004) Measurement of apoptosis and other forms of cell death. *Curr Protoc Immunol* Chapter 3:Unit 3.17.

Nakajima S, Kato H, Takahashi S, Johno H, Kitamura M. (2011) Inhibition of NF-κB by MG132 through ER stress-mediated induction of LAP and LIP. *FEBS Lett* **585**(14): 2249-2254.

Nakatogawa H, Suzuki K, Kamada Y, Ohsumi Y (2009) Dynamics and diversity in autophagy mechanisms: lessons from yeast. *Nat Rev Mol Cell Biol* **10**(7): 458-467.

Ng PK, Tsui SK, Lau CP, Wong CH, Wong WH, Huang L, Kumta SM (2010) CCAAT/enhancer binding protein beta is up-regulated in giant cell tumor of bone and regulates RANKL expression. *J Cell Biochem* **110**(2): 438-446.

Ohsawa S, Sugimura K, Takino K, Xu T, Miyawaki A, Igaki T (2011) Elimination of oncogenic neighbors by JNK-mediated engulfment in Drosophila. *Dev Cell* **20**: 315-328.

Overholtzer M, Mailleux AA, Mouneimne G, Normand G, Schnitt SJ, King RW, et al. (2007) A nonapoptotic cell death process, entosis, that occurs by cell-in-cell invasion. *Cell* **131**(5): 966-979.

Overholtzer M, Brugge JS (2008) The cell biology of cell-in-cell structures. *Nat Rev Mol Cell Biol* **9**(10): 796-809.

Paglin S, Hollister T, Delohery T, Hackett N, McMahill M, Sphicas E, *et al*. (2001) A novel response of cancer cells to radiation involves autophagy and formation of acidic vesicles. *Cancer Res* **61**:439–444.

Pelucchi C, Tramacere I, Boffetta P, Negri E, La Vecchia C (2011) Alcohol consumption and cancer risk. *Nutr Cancer* **63**(7): 983-990.

Polager S, Ofir M, Ginsberg D (2008) E2F1 regulates autophagy and the transcription of autophagy genes. *Oncogene* **27**:4860–4864.

Proskuryakov SY, Konoplyannikov AG, Gabai VL (2003) Necrosis: a specific form of programmed cell death? *Exp Cell Res* **283**:1–16.

Qiao L, Han SI, Fang Y, Park JS, Gupta S, Gilfor D, Amorino G, Valerie K, Sealy L, Engelhardt JF, Grant S, Hylemon PB, Dent P (2003) Bile acid regulation of C/EBPbeta, CREB, and c-Jun function, via the extracellular signal-regulated kinase and c-Jun NH2-terminal kinase pathways, modulates the apoptotic response of hepatocytes. *Mol Cell Biol* **23**: 3052-66.

Qu X, Yu J, Bhagat G, Furuya N, Hibshoosh H, Troxel A, *et al*. (2003) Promotion of tumorigenesis by heterozygous disruption of the beclin 1 autophagy gene. *J Clin Invest* **112**: 1809–1820.

Ramji DP, Foka P (2002) CCAAT/enhancer-binding proteins: structure, function and regulation. *Biochem J* **365**(Pt 3): 561-575.

Rask K, Thörn M, Pontén F, Kraaz W, Sundfeldt K, Hedin L, Enerbäck S. (2000) Increased expression of the transcription factors CCAAT-enhancer binding protein-beta (C/EBBeta) and C/EBzeta (CHOP) correlate with invasiveness of human colorectal cancer. *Int J Cancer* **86**(3): 337-343.

Raught B, Gingras AC, James A, Medina D, Sonenberg N, Rosen JM (1996) Expression of a translationally regulated, dominant-negative CCAAT/enhancer-binding protein beta isoform and up-regulation of the eukaryotic translation initiation factor 2alpha are correlated with neoplastic transformation of mammary epithelial cells. *Cancer Res* **56**(19): 4382-4286.

Ravdin PM, Cronin KA, Howlader N, Berg CD, Chlebowski RT, Feuer EJ, *et al*. (2007) The decrease in breast-cancer incidence in 2003 in the United States. *N Engl J Med* **356**(16): 1670-1674.

Rhodes DR, Yu J, Shanker K, Deshpande N, Varambally R, Ghosh D, et al. (2004) ONCOMINE: a cancer microarray database and integrated data-mining platform. *Neoplasia* **6**(1):1-6.

Robinson GW, Johnson PF, Hennighausen L, Sterneck E (1998) The C/EBPbeta transcription factor regulates epithelial cell proliferation and differentiation in the mammary gland. *Genes Dev* **12**(12): 1907-1916.

Roy R, Chun J, Powell SN (2011) BRCA1 and BRCA2: different roles in a common pathway of genome protection. *Nat Rev Cancer* **12**(1): 68-78.

Russell A, Boone B, Jiang A, Sealy L (2010) Genomic profiling of C/EBPbeta2 transformed mammary epithelial cells: a role for nuclear interleukin-1beta. *Cancer Biol Ther* **10**(5): 509-519.

Sakorafas GH, Tsiotou AG (2000) Ductal carcinoma in situ (DCIS) of the breast: evolving perspectives. *Cancer Treat Rev* **26**(2): 103-125.

Sauter B, Albert, ML, Francisco L, Larsson M, Somersan S, and Bhardwaj N (2000) Consequences of cell death: exposure to necrotic tumor cells, but not primary tissue cells or apoptotic cells, induces the maturation of immunostimulatory dendritic cells. *J Exp Med* **191**: 423–434.

Savill J, Fadok V (2000) Corpse clearance defines the meaning of cell death. *Nature* **407**:784–788.

Schorey JS, Bhatnagar S (2008) Exosome function: from tumor immunology to pathogen biology. *Traffic* **9**(6): 871-881.

Seagroves TN, Krnacik S, Raught B, Gay J, Burgess-Beusse B, Darlington GJ, Rosen JM (1998) C/EBPbeta, but not C/EBPalpha, is essential for ductal morphogenesis, lobuloalveolar proliferation, and functional differentiation in the mouse mammary gland. *Genes Dev* **12**(12): 1917-1928.

Sengupta A, Molkentin JD, Yutzey KE (2009) FoxO transcription factors promote autophagy in cardiomyocytes. *J Biol Chem* **284**(41): 28319-28331.

Sharma N, Dey P. (2011) Cell cannibalism and cancer. *Diagn Cytopathol* **39**: 229-233.

Siegel R, Ward E, Brawley O, Jemal A (2011) Cancer statistics, 2011: the impact of eliminating socioeconomic and racial disparities on premature cancer deaths. *CA Cancer J Clin* **61**(4): 212-36.

Simpson RJ, Jensen SS, Lim JW (2008) Proteomic profiling of exosomes: current perspectives. *Proteomics* **8**(19): 4083-4099.

Staiger J, Lueben MJ, Berrigan D, Malik R, Perkins SN, Hursting SD, Johnson PF (2009) C/EBPbeta regulates body composition, energy balance-related hormones and tumor growth. *Carcinogenesis* **30**(5):832-840.

Sterneck E, Tessarollo L, Johnson PF (1997) An essential role for C/EBPbeta in female reproduction. *Genes Dev* **11**(17): 2153-2162.

Sternlicht MD, Kouros-Mehr H, Lu P, Werb Z (2006) Hormonal and local control of mammary branching morphogenesis. *Differentiation* **74**(7): 365-381.

Sundfeldt K, Ivarsson K, Carlsson M, Enerbäck S, Janson PO, Brännström M, Hedin L (1999) The expression of CCAAT/enhancer binding protein (C/EBP) in the human ovary *in vivo*: specific increase in C/EBPbeta during epithelial tumour progression. *Br J Cancer* **79**(7-8):1240-1248.

Tasdemir E, Maiuri MC, Orhon I, Kepp O, Morselli E, Criollo A, Kroemer G (2008) p53 represses autophagy in a cell cycle-dependent fashion. *Cell Cycle* **7**: 3006–3011.

Thompson CB (1995) Apoptosis in the pathogenesis and treatment of disease. *Science*. 267(5203): 1456-1462.

Timchenko NA, Welm AL, Lu X, Timchenko LT (1999) CUG repeat binding protein (CUGBP1) interacts with the 5' region of C/EBPbeta mRNA and regulates translation of C/EBPbeta isoforms. *Nucleic Acids Res* **27**(22): 4517-4525.

Timchenko LT, Iakova P, Welm AL, Cai ZJ, Timchenko NA (2002) Calreticulin interacts with C/EBPalpha and C/EBPbeta mRNAs and represses translation of C/EBP proteins. *Mol Cell Biol* **22**(20): 7242-7257.

Timchenko LT, Salisbury E, Wang GL, Nguyen H, Albrecht JH, Hershey JW, Timchenko NA (2006) Age-specific CUGBP1-eIF2 complex increases translation of CCAAT/enhancer-binding protein beta in old liver. *J Biol Chem* **281**(43):32806-32819.

Tinari A, Matarrese P, Minetti M, Malorni W (2008) Hyperphagia by self- and xeno-cannibalism: cell death by indigestion?: a reminiscence of the Phedrus Fabula "Rana Rupta et Bos"? Autophagy **4**(1): 128-130.

Tsukada J, Yoshida Y, Kominato Y, Auron PE (2011) The CCAAT/enhancer (C/EBP) family of basic-leucine zipper (bZIP) transcription factors is a multifaceted highly-regulated system for gene regulation. *Cytokine* **54**(1): 6-19.

Tytell M (2005) Release of heat shock proteins (Hsps) and the effects of extracellular Hsps on neural cells and tissues. *Int J Hyperthermia* **21**(5): 445-455.

van Noort JM, Bsibsi M, Nacken P, Gerritsen WH, Amor S (2012) The link between small heat shock proteins and the immune system. *Int J Biochem Cell Biol*

Verga Falzacappa C, Petrucci E, Patriarca V, Michienzi S, Stigliano A, Brunetti E et al. (2007). Thyroid hormone receptor TRbeta1 mediates Akt activation by T3 in pancreatic beta cells. *J Mol Endocrinol* **38**: 221–233.

Wang CW, Klionsky DJ (2003) The molecular mechanism of autophagy. *Mol Med* **9**: 65–76.

Watson CJ, Khaled WT (2008) Mammary development in the embryo and adult: a journey of morphogenesis and commitment. *Development* **135**(6): 995-1003.

Welm AL, Mackey SL, Timchenko LT, Darlington GJ, Timchenko NA (2000) Translational induction of liver-enriched transcriptional inhibitory protein during acute phase response leads to repression of CCAAT/enhancer binding protein alpha mRNA. *J Biol Chem* **275**(35): 27406-27413.

Wethmar K, Smink JJ, Leutz A (2010) Upstream open reading frames: molecular switches in (patho)physiology. *Bioessays* **32**(10):885-893.

Williams A, Jahreiss L, Sarkar S, Saiki S, Menzies FM, Ravikumar B, Rubinsztein

DC (2006) Aggregate-prone proteins are cleared from the cytosol by autophagy: therapeutic implications. *Curr Top Dev Biol* **76**: 89–101.

Wu KK, Liou JY, Cieslik K (2005) Transcriptional Control of COX-2 via C/EBPbeta. *Arterioscler Thromb Vasc Biol* **25**(4): 679-685.

Xia P, Wang S, Guo Z, Yao X (2008) Emperipolesis, entosis and beyond: Dance with fate. *Cell Research* **18**: 705–707.

Yang Z, Wara-Aswapati N, Chen C, Tsukada J, Auron PE (2000) NF-IL6 (C/EBPbeta) vigorously activates il1b gene expression via a Spi-1 (PU.1) protein-protein tether. *J Biol Chem* **275**(28): 21272-21277.

Yoshida K, Miki Y (2004) Role of BRCA1 and BRCA2 as regulators of DNA repair, transcription, and cell cycle in response to DNA damage. *Cancer Sci* **95**(11): 866-871.

Yoshimori T, Noda T (2008) Toward unraveling membrane biogenesis in mammalian autophagy. *Curr Opin Cell Biol* **20**(4): 401-407.

Yuan J, Shaham S, Ledoux S, Ellis HM and Horvitz HR (1993) The C. elegans cell death gene ced-3 encodes a protein similar to mammalian interleukin-1 beta-converting enzyme. *Cell* **75**, 641–652.

Yuan J, Kroemer G (2010) Alternative cell death mechanisms in development and beyond. *Genes Dev* **24**(23): 2592-2602.

Zahnow CA, Younes P, Laucirica R, Rosen JM (1997) Overexpression of C/EBPbeta-LIP, a naturally occurring, dominant-negative transcription factor, in human breast cancer. *J Natl Cancer Inst* **89**(24):1887-1891.

Zahnow CA, Cardiff RD, Laucirica R, Medina D, Rosen JM (2001) A role for CCAAT/enhancer binding protein beta-liver-enriched inhibitory protein in mammary epithelial cell proliferation. *Cancer Res* **61**(1):261-269.

Zarzynska J, Motyl T (2008) Apoptosis and autophagy in involuting bovine mammary gland. *J Physiol Pharmacol* 59 Suppl **9**:275-288.

Zeiss CJ (2003) The apoptosis-necrosis continuum: insights from genetically altered mice. *Vet Pathol* **40**:481–95